[redacted]

NASA TECHNICAL MEMORANDUM

NASA TM X-2808

NASA TM X-2808



# WIND-TUNNEL DEVELOPMENT OF UNDERWING LEADING-EDGE VORTEX GENERATORS ON AN NASA SUPERCRITICAL-WING RESEARCH AIRPLANE CONFIGURATION

*by Dennis W. Bartlett, Charles D. Harris, and Thomas C. Kelly*

*Langley Research Center*
*Hampton, Va. 23665*

NATIONAL AERONAUTICS AND SPACE ADMINISTRATION • WASHINGTON, D. C. • NOVEMBER 1973

[redacted]

# WIND-TUNNEL DEVELOPMENT OF UNDERWING LEADING-EDGE VORTEX GENERATORS ON AN NASA SUPERCRITICAL-WING RESEARCH AIRPLANE CONFIGURATION*

By Dennis W. Bartlett, Charles D. Harris, and Thomas C. Kelly
Langley Research Center

## SUMMARY

A program for the wind-tunnel development of underwing leading-edge vortex generators on an NASA supercritical-wing research airplane configuration has been conducted in the Langley 8-foot transonic pressure tunnel at Mach numbers from 0.25 to 0.99. The addition of the vortex generators to the clean wing (one per wing panel) delayed pitch-up to significantly higher angles of attack, and in the region where the angle of attack at pitch-up was extended, there were significant increases in lift and reductions in drag.

The effect of the vortex generators on the longitudinal aerodynamic characteristics was found to be sensitive to relatively small changes in the orientation of the vortex generators with respect to the wing (i.e., distance from wing leading edge, leading-edge sweep angle, toe-in angle, and small changes in the wing semispan location). However, during the investigation the span of the vortex generators was reduced 33 percent without degrading their favorable effect on the pitching-moment characteristics. For a sideslip angle of approximately $5^{\circ}$, the vortex generators had only small effects on the lateral-directional aerodynamic characteristics of the model.

Limited data obtained on a wing upper-surface fence (one per wing panel) located near the trailing edge indicated that the fence delayed pitch-up but not to as high an angle of attack as the vortex generator, and when pitch-up occurred with the fences on the wing, it appeared even more abrupt than for the clean wing configuration.

## INTRODUCTION

Early wind-tunnel tests (refs. 1 and 2) of a research airplane incorporating an NASA supercritical wing of relatively high aspect ratio and sweep indicated the occurrence of a longitudinal instability (pitch-up) at moderate angles of attack (approximately $6^{\circ}$ to $12^{\circ}$) for Mach numbers of 1.02 and below. Longitudinal instabilities of this nature on sweptback

*Title, Unclassified.

wings are associated with the boundary-layer-separation phenomenon over the outer wing panels and are typical for wings of such planform. Although the unstable pitching-moment variations occurred at lift coefficients (approximately 0.70 to 1.00) well beyond those for level-flight cruise (0.40), simulator studies conducted by the NASA Flight Research Center indicated that stability augmentation would be necessary in the interest of flight safety to permit exploration of the airplane buffet boundaries.

In view of the long-recognized effectiveness of vortices in boundary-layer control (ref. 3, for example) and the evidence of significant effects that wing pylons have on pitch-up (refs. 4 and 5), it was anticipated that an underwing leading-edge vortex generator might alleviate the pitch-up problem. Consequently, an investigation was conducted in the Langley 8-foot transonic pressure tunnel to assess the effectiveness of such a vortex generator in delaying or eliminating pitch-up. The test program, however, was directed toward the alleviation of a particular problem rather than a general study and, as a consequence, is somewhat limited in scope. Included, however, are the effects of vortex-generator wing semispan location, distance from wing leading edge, leading-edge sweep angle, toe-in angle, and span. A limited amount of data was also obtained on a wing upper-surface, partial-chord fence.

In general, data were obtained for Mach numbers from 0.25 to 0.99 and at angles of attack associated with the unstable pitching-moment region. In addition, data were also obtained at sideslip angles up to about $5^{\circ}$ to determine the influence of the underwing leading-edge vortex generators on the lateral-directional aerodynamic characteristics of the model.

The effects of the final vortex-generator configuration on the longitudinal aerodynamic characteristics and the wing pressure distributions of an area-ruled version of the TF-8A supercritical-wing research airplane at Mach numbers from 0.80 to 1.00 have been reported in reference 6, in which the flow mechanism involved was qualitatively described. The present paper is, in a sense, supplemental to reference 6 and is concerned primarily with the experimental development of the underwing leading-edge vortex generator described in reference 6.

## SYMBOLS

Results presented herein are referred to the stability-axis system for the longitudinal aerodynamic characteristics and to the body-axis system for the lateral and directional aerodynamic characteristics. Force and moment data have been reduced to conventional coefficient form based on the geometry of the basic wing planform, that is, the planform produced by extending the straight leading and trailing edges of the outboard sections of the wing to the fuselage center line. (See fig. 1(a).) Moments are referenced

to the quarter-chord point of the mean geometric chord of the basic wing panel, which is located at model station 99.45 cm (39.155 in.). All dimensional values are given in both SI and U.S. Customary Units; however, measurements and calculations were made in U.S. Customary Units.

Coefficients and symbols used herein are defined as follows:

$b$ wing span, 114.30 cm (45.000 in.)

$C_D$ drag coefficient, $\frac{\text{Drag}}{qS}$

$C_L$ lift coefficient, $\frac{\text{Lift}}{qS}$

$C_l$ rolling-moment coefficient, $\frac{\text{Rolling moment}}{qSb}$

$C_m$ pitching-moment coefficient, $\frac{\text{Pitching moment}}{qS\bar{c}}$

$C_n$ yawing-moment coefficient, $\frac{\text{Yawing moment}}{qSb}$

$C_Y$ side-force coefficient, $\frac{\text{Side force}}{qS}$

$c$ streamwise chord of basic wing panel

$\bar{c}$ mean geometric chord of basic wing panel, $\frac{2}{S}\int_0^{1.0} c^2 d\left(\frac{y}{b/2}\right)$, 18.09 cm (7.121 in.)

$c'$ streamwise chord of total wing planform including leading-edge glove and trailing-edge extension

$M$ free-stream Mach number

$q$ free-stream dynamic pressure, $N/m^2$ ($lb/ft^2$)

$S$ area of basic wing planform including fuselage intercept, 0.193 $m^2$ (2.075 $ft^2$)

$y$ spanwise distance measured normal to plane of symmetry

$\alpha$ angle of attack, referred to a fuselage water line, deg

$\beta$ angle of sideslip, referred to fuselage center line (positive when nose is left), deg

## APPARATUS AND PROCEDURES

### Model

Wing characteristics.- Results reported herein were obtained with two wings, geometrically identical but with different aeroelastic characteristics. One wing, instrumented with static-pressure orifices and used in the investigations reported in references 1, 2, and 6, was constructed of a steel core with plastic fill in which steel pressure tubing was embedded. The second wing was made of aluminum and was used for control effectiveness studies. Static loadings of the two wings indicated that the steel wing was approximately 65 percent as flexible as the aluminum wing. Tests were conducted during this investigation for Mach numbers of 0.80, 0.90, and 0.95 at dynamic pressures scaled according to this percentage in order to maintain the same aeroelastic deformation for the two wings. (See table I.)

Measured deflections of the steel wing (determined by static loadings) associated with an actual aerodynamic load distribution at near-cruise conditions are given in references 1 and 2, along with the basic or unloaded wing coordinates for several streamwise sections.

The model wing was mounted with respect to the fuselage at a root-chord incidence angle of $1.5^{\circ}$ and has approximately $5^{\circ}$ of twist (washout) from root to tip in the unloaded condition. The basic wing planform has a taper ratio of 0.36, an aspect ratio of 6.8, and $42.24^{\circ}$ of sweepback at the quarter-chord line. The area of the basic wing planform including the fuselage intercept is 0.193 $m^2$ (2.075 $ft^2$), and the mean geometric chord of the basic wing panel is 18.09 cm (7.121 in.).

Complete model.- Geometric characteristics of the 0.087-scale research airplane model are presented in figure 1, and photographs of the model are presented as figure 2. The basic fuselage and tails are scaled versions of those utilized on the test-bed airplane (TF-8A). The fuselage was equipped with flow-through ducts which discharge at the base of the model on either side of the flat-sided model support sting. The aft section of the flow-through ducts used in the present investigation had smaller exit areas than ducts used in wind-tunnel tests previously reported (refs. 1, 2, and 6), and as a result, absolute drag level cannot be directly compared. The use of smaller ducts was necessitated by a slightly wider model support sting employed in the present investigation to allow tests in sideslip.

Midway through the test program, aileron hinge fairings (figs. 1(f) and (g)) were added to the lower surface of the steel wing to simulate the full-scale airplane configuration more accurately. These aileron hinge fairings were required when structural design dictated a hinge point below the wing lower surface. It should be noted, however, that the aileron hinge fairings were not included on the aluminum wing for this investigation.

Vortex generator and wing upper-surface, partial-chord fence. - Details of the underwing leading-edge vortex generator, from the initial to the final configuration, are presented in figures 1(c), (d), and (e). The vortex generators were 10-percent-thick Clark Y airfoils with the flat lower surface facing inboard, each wing panel having a single vortex generator. Vortex-generator configurations after the initial configuration (fig. 1(c)) were designated, for convenience, as numbered modifications (fig. 1(d)). The various vortex-generator configurations are outlined in table II, and a brief description of each modification is given as follows:

Modification 1. - The initial vortex generator was moved to the wing leading edge from 0.16 cm (0.063 in.) aft of the wing leading edge.

Modification 2. - The vortex-generator leading-edge sweep angle was increased from $40^{\circ}$ to $42^{\circ}$.

Modification 3. - The vortex generator was moved 0.16 cm (0.063 in.) ahead of the wing leading edge to allow the leading edge of the vortex generator to fair in tangent to the wing upper surface.

Modification 4. - The vortex-generator toe-in angle (table II and fig. 1(c)) was reduced from $5^{\circ}$ to $0^{\circ}$.

Modification 5. - The vortex-generator span was reduced by 0.318 cm (0.125 in.) (from 1.90 to 1.59 cm (0.75 to 0.625 in.)).

Modification 6. - The vortex-generator span was reduced an additional 0.318 cm (0.125 in.) (from 1.59 to 1.27 cm (0.625 to 0.50 in.)), and the root chord was increased by 0.305 cm (0.120 in.).

Modification 6 (fig. 1(e)) is also referred to as the final configuration since it was installed on the full-scale airplane.

It might be noted that the aileron hinge fairings were added to the steel wing after modification 4.

The wing upper-surface fences (one per wing panel) were located at the 60-percent-wing-semispan station and were oriented with respect to the wing as shown in figure 1(b). The wing upper-surface fences were composed of flat-plate sections approximately 0.127 cm (0.05 in.) thick with sharp leading edges.

## Test Facility

The Langley 8-foot transonic pressure tunnel (ref. 7) is a single-return, continuous-flow, rectangular, slotted-throat wind tunnel with controls that allow for the independent variation of Mach number, stagnation pressure, temperature, and dewpoint. The stagnation temperature of the tunnel air was automatically maintained at approximately 322 K

($120^{\circ}$ F), and the air was dried until the dewpoint in the test section was reduced sufficiently to avoid significant condensation effects (ref. 8). The upper and lower test-section walls are axially slotted to permit testing through the transonic speed range. The regular tunnel slots, which produce an average open ratio per wall of approximately 0.06, were replaced for the present investigation by slots which increased the open ratio to 0.22 (open ratio is the ratio of total slot width to the width of the wall). These latter slots were designed on the basis of reference 9 to permit testing of the relatively large model with minimum effects of blockage.

## Measurements and Test Conditions

Measurements of overall forces and moments on the model were obtained from a six-component, electrical strain-gage balance housed within the fuselage cavity. Differential pressure transducers referenced to free-stream static pressure were used to measure the pressure in the fuselage balance chamber and at the model base.

Since the investigation was exploratory and developmental in nature, the range of Mach numbers and angles of attack for which results were obtained varied between configurations. For the intermediate vortex-generator configurations, results were generally obtained only in the immediate angle-of-attack region of pitch-up at selected Mach numbers to determine whether the effects of the modification on pitch-up were favorable or unfavorable. For the final configuration (modification 6), data were obtained at Mach numbers from 0.25 to 0.95 over a relatively extensive angle-of-attack range. Results were also obtained at a sideslip angle of approximately $5^{\circ}$ over a Mach number range from 0.25 to 0.98 for the model with the modification 6 configuration to determine whether the vortex generators had any adverse effect on the lateral-directional aerodynamic characteristics.

Specific tunnel conditions for the present investigation are presented in table I. The horizontal tail was deflected $-2.5^{\circ}$ (leading edge down) for all tests.

Boundary-layer-trip arrangements for the wing are shown in figure 3 and discussed in reference 1. To reduce tunnel testing time during the early phases of the investigation (through modification 4), the rearward location of the wing upper-surface boundary-layer trips, normally used for Mach numbers 0.95 to 0.99, was also used at Mach numbers 0.80 and 0.90 since incremental effects were of primary interest. Configurations after modification 4 were tested with the appropriate wing upper-surface boundary-layer-trip arrangement as shown in figure 3 (rearward for $M = 0.95$ to 0.99 and forward for $M = 0.25$ to 0.90). It should be noted, however, that modification 4 was also tested with the forward boundary-layer-trip arrangement at Mach numbers of 0.80 and 0.90 to allow a direct comparison at these Mach numbers with modification 5.

No. 120 carborundum grains were located on the horizontal and vertical tails at 5 percent of the local streamwise chords and were also applied 2.54 cm (1.00 in.) aft of the model nose. All boundary-layer trips were applied to the model in bands that were 0.127 cm (0.05 in.) wide and which were located by measurements taken in the streamwise direction.

## Corrections

Drag coefficients contained herein have been adjusted to correspond to a condition of free-stream static pressure acting in the balance chamber and at the model base (excluding the duct exit area). No adjustments have been made, however, for internal duct drag.

Corrections have been made to the measured angles of attack to account for deflection of the model balance and sting support system under aerodynamic load, for tunnel airflow angularity, and for the first-order boundary-induced lift-interference effects as calculated from the theory of reference 10. This last correction amounts to a reduction in the measured angle of attack of 0.24 multiplied by the normal-force coefficient.

## PRESENTATION OF RESULTS

The results of this investigation are presented in the following figures:


| | Figure |
|---|---|
| Oil-flow photographs of wing upper surface at a Mach number of 0.95; $\beta = 0^{o}$ . . . | 4 |
| Longitudinal aerodynamic characteristics ($\beta = 0^{o}$): | |
| Effect of wing upper-surface fences and initial underwing vortex generators located at 60-percent-semispan station; steel wing . . . . . | 5 |
| Effect of wing semispan location of initial underwing vortex generators; steel wing . . . . . | 6 |
| Effect of vortex-generator modifications 1, 2, and 3; steel wing . . . . . | 7 |
| Effect of vortex-generator toe-in angle; steel wing . . . . . | 8 |
| Effect of wing upper-surface boundary-layer-trip location at Mach numbers of 0.80 and 0.90; steel wing, vortex-generator modification 4 . . . . . | 9 |
| Effect of aileron hinge fairings at Mach numbers of 0.95 and 0.99; steel wing, vortex-generator modification 4 . . . . . | 10 |
| Effect of vortex-generator span; steel wing, aileron hinge fairings on . . . . . | 11 |
| Effect of vortex-generator span; aluminum wing . . . . . | 12 |
| Effect of final vortex-generator configuration (modification 6); aluminum wing . . | 13 |
| Lift and pitching-moment characteristics of model with final vortex-generator configuration (modification 6) at extended angles of attack; aluminum wing . . . | 14 |

Figure

Lateral-directional aerodynamic characteristics:
Effect of final vortex-generator configuration (modification 6) for $\beta \approx 5^{o}$; steel wing, aileron hinge fairings on . . . . . 15
Effect of sideslip angle for model with final vortex-generator configuration (modification 6); steel wing, aileron hinge fairings on . . . . . 16

## DISCUSSION

The investigation and the results reported herein can be essentially divided into three phases: first, assessment of the relative effectiveness of the underwing leading-edge vortex generator and the wing upper-surface fence in reducing off-design pitch-up tendencies; second, refinement or development of the vortex generator into a final configuration; and third, determination of the influence of the vortex generators on the lateral-directional aerodynamic characteristics.

### Comparison of Initial Vortex Generator and Upper-Surface Fence

The 60-percent-wing-semispan location for the initial vortex generator and upper-surface fence was selected primarily on the basis of oil-flow observations on the clean wing configuration, which indicated that at pitch-up most of the separated flow occurred outboard of this station with considerable spanwise flow over the wing inboard of this station. Both the initial vortex-generator and the upper-surface fence configurations had significant effects on the longitudinal aerodynamic characteristics of the model. (See fig. 5.)

Initial vortex generator.- As described in reference 6, the vortex generators produce vortices over the upper surface of the wing which rotate in a direction such that they act as an aerodynamic barrier to the spanwise boundary-layer flow. The vortices also transport higher momentum air to the lower levels of the boundary layer – thereby, separation and the associated pitch-up are delayed to significantly higher angles of attack. The vortices are created as a result of the interference between the vortex generators and the wing leading-edge cross flow and are stronger at the relatively higher angles of attack because of increased cross-flow interference as the stagnation point moves farther onto the lower surface of the wing. At the relatively lower angles of attack, near those at which the cruise lift coefficient of 0.40 occurs, the vortex generators have little influence on the behavior of the wing (also discussed in ref. 6).

Because of the abbreviated angle-of-attack range, the initial vortex generators do not appear to have much effect on the pitching-moment break at $M = 0.90$ in figure 5; however, the results of figure 13(d) for the aluminum-wing configuration do show a beneficial effect on the pitching-moment curve at angles of attack beyond the initial pitch break.

Two additional wing semispan locations were investigated with the initial vortex-generator configuration. The results (fig. 6) show that although relatively small effects resulted from spanwise movement, the 60-percent-semispan location did appear to be somewhat more favorable than the other two locations. Accordingly, the 60-percent-semispan station was selected for the remainder of the investigation.

Upper-surface fence.- The upper-surface fence had a larger favorable effect on the longitudinal aerodynamic characteristics at the relatively lower angles of attack ($\alpha \approx 4.5^{\circ}$ to $7.5^{\circ}$) than did the initial vortex generator; however, the vortex generator was more beneficial at angles of attack above $7.5^{\circ}$. (See figs. 5(c) and (d).) This is a probable result of the proximity of the fence to the trailing edge (fig. 1(b)) and the fact that at the lower angles of attack the vortices shed from the vortex generators are relatively weak. The favorable effect of the upper-surface fence on the longitudinal aerodynamic characteristics is probably related to the retardation of spanwise boundary-layer flow near the trailing edge with an attendant reduction in separation over the outer wing panels. Oil-flow photographs (fig. 4) show that for the lower angles of attack (less than $7.5^{\circ}$), trailing-edge separation is confined behind the leading edge of the upper-surface fence. With increasing angle of attack, however, the amount of trailing-edge separation also increases until it completely envelops the fence and spills around the fence leading edge (fig. 4). This rapidly increases the amount of separation outboard of the fence and results in the abrupt decrease in lift-curve slope and the unstable pitching-moment breaks shown in figure 5 for the upper-surface fence configuration. Although pitch-up was delayed by the upper-surface fence, the delay was not maintained to as high an angle of attack as provided by the initial vortex generator (fig. 5(d)), and when pitch-up occurred with the fences on the wing, it appeared even more abrupt than for the clean wing configuration.

## Development of Vortex Generators

The oil-flow photographs of figure 4 suggest that a longer upper-surface fence would probably further delay pitch-up, and that it may also be possible to obtain more improvements in the longitudinal stability characteristics by utilizing a combination of underwing leading-edge vortex generators and upper-surface fences since each appeared more effective for a different segment of the angle-of-attack range. However, since a primary goal of the investigation was not to degrade the cruise performance of the airplane, it was considered necessary to minimize both the number and size of any "add-on" devices and their associated aerodynamic loads. For these reasons, the vortex generators, which had demonstrated the ability to improve the longitudinal stability characteristics of the model over a relatively large angle-of-attack range while adding only a small cruise-drag penalty, were selected for further refinement and investigation and inclusion on the full-scale research airplane.

After phase one, therefore, successive modifications were made to the geometry and orientation of the initial vortex generators in an attempt to enhance their effectiveness and to minimize any drag penalty associated with them. (See table II and fig. 1(d).)

Modifications 1 and 2.- Modifications 1 and 2 were intended to project the vortex generators more into the wing leading-edge cross flow. The results (fig. 7) show that moving the vortex generators to the wing leading edge (modification 1) resulted in modest improvements in the pitching-moment characteristics for Mach numbers of 0.90 and above with little effect at a Mach number of 0.80. Increasing the forward sweep of the vortex generators by $2^{\circ}$ (modification 2) had only minor additional effects (fig. 7).

Modification 3.- The vortex generators were then moved 0.16 cm (0.063 in.) ahead of the wing leading edge (fig. 1(d)). This allowed the leading edge of the vortex generators to fair in tangent to the wing upper surface; thus, the discontinuity at the juncture of the wing and the vortex-generator leading edge was removed. Modification 3 resulted in significant improvements in the lift, drag, and pitching-moment characteristics at Mach numbers of 0.95 and 0.99 (fig. 7). As with modifications 1 and 2, these improvements are believed to result from the vortex generators being projected more into the wing leading-edge cross flow.

Modification 4.- The vortex generators were then alined with the free-stream direction in an effort to reduce the drag at cruise conditions $(M = 0.99, \quad C_L = 0.40)$. As indicated in figure 8, small drag improvements were obtained at the lower lift coefficients for Mach numbers of 0.95 and 0.99, and no detrimental effects are noted in the pitching-moment characteristics at the Mach numbers for which data are presented. The initial $5^{\circ}$ of tow-in angle relative to the free-stream direction (utilized for the initial vortex-generator configuration through modification 3) had been selected somewhat arbitrarily but was intended to aline the vortex generators with the local flow at cruise conditions. Recent unpublished wind-tunnel results for a low-wing advanced transport model with a similar supercritical wing have indicated that the lowest cruise-drag penalty can be achieved if the vortex generators are canted slightly inboard, approximately $2^{\circ}$, instead of being alined with the free stream.

Wing upper-surface boundary-layer-trip location.- For Mach numbers of 0.90 and below, it was found necessary in earlier tests (refs. 1 and 2) to move the wing upper-surface boundary-layer trips (fig. 3) forward (to 0.05c') to prevent laminar separation near the wing leading edge at high angles of attack, particularly at a Mach number of 0.90. Such separation was considered unnatural in the sense that it would not be expected at the Reynolds numbers associated with full-scale conditions. As previously discussed, the rearward trip arrangement for the wing upper surface (fig. 3) was employed at Mach numbers of 0.80 to 0.99 through modification 4 as an expediency in testing; however, for the remainder of the investigation, the forward trip arrangement (fig. 3) was used only at

Mach numbers of 0.90 and below. An illustration of the effects of wing upper-surface boundary-layer-trip location on the longitudinal aerodynamic characteristics is presented in figure 9 at Mach numbers of 0.80 and 0.90 for modification 4. This particular configuration was tested with both the fore and aft trip arrangements at Mach numbers of 0.80 and 0.90 to allow a direct comparison at these two Mach numbers with modification 5 (fig. 11).

Although the rearward trip arrangement is believed to produce performance results closer to what would be obtained at full-scale Reynolds numbers (ref. 11), its use is not feasible when the laminar flow ahead of the trips is separated.

Aileron hinge fairings.- After modification 4, aileron hinge fairings (figs. 1(f) and (g)) were added to the underside of the steel wing to simulate the full-scale research airplane configuration more accurately. Figure 10 presents the effects of these aileron hinge fairings on the longitudinal aerodynamic characteristics at Mach numbers of 0.95 and 0.99. The aileron hinge fairings did cause a small increase in drag but generally had only small effects on the lift and pitching-moment characteristics at these Mach numbers. Although the aileron hinge fairings were included on the steel wing for tests after modification 4, they were not added to the aluminum wing (figs. 12 to 14).

Modifications 5 and 6.- Since no hard points had been provided on the wing for "add-on" devices, these last two modifications were undertaken to minimize the stress at the attachment points resulting from the aerodynamic loads on the vortex generators. Data presented in figures 11 (effect of modification 5) and 12 (effect of modification 6) indicate that the span of the vortex generators could be reduced by approximately 33 percent (from 1.90 to 1.27 cm (0.75 to 0.50 in.)) before significantly compromising their effectiveness. Modification 6, in addition to further reducing the span by 0.318 cm (0.125 in.), increased the root chord by 0.305 cm (0.120 in.).

Results for final vortex-generator configuration.- The longitudinal aerodynamic characteristics for the model with the aluminum wing with and without the final vortex-generator configuration (modification 6) are presented over a fairly large angle-of-attack range for Mach numbers of 0.25 to 0.95 in figure 13. The longitudinal aerodynamic characteristics for an extended angle-of-attack range are also presented in figure 14 for the model with the aluminum wing and the final vortex-generator configuration. The higher angle-of-attack data of figure 14 were obtained with the offset sting arrangement shown in figure 1(h), and the interference effects associated with this particular model support system account for the misalinement with the lower angle-of-attack results which were obtained with a straight sting arrangement.

Several distinctive features are evident in the pitching-moment curves of figures 13 and 14. Pitch-up is delayed to significantly higher angles of attack and lift coefficients as a result of the vortex generators (fig. 13), and although pitch-up does occur eventually

with the vortex generators on the model, the aircraft becomes stable again at a higher angle of attack (fig. 14). In the region where the angle of attack at pitch-up has been extended, there are significant increases in lift and reductions in drag which are associated with the vortex generators (fig. 13). These improvements in the lift and drag characteristics result from a reduction in the extent of separated flow on the wing.

It should be pointed out, however, that part of the effect on the pitching-moment characteristics results from a change in aerodynamic load on the horizontal tail (discussed in ref. 6). This change in horizontal-tail lift, due directly or indirectly to the influence of the vortex generators, results in the pitching-moment-coefficient increments as indicated in reference 6.

### Effect of Vortex Generators on the Lateral-Directional Aerodynamic Characteristics

The effect of the final vortex generators on the lateral-directional aerodynamic characteristics is presented in figure 15 for a sideslip angle of approximately $5^{\circ}$, and also, the lateral-directional aerodynamic characteristics for the model with the final vortex generators are presented in figure 16 for sideslip angles from approximately $-6^{\circ}$ to $6^{\circ}$. Generally, the vortex generators have only small effects on the lateral-directional aerodynamic characteristics, as shown in figure 15. Additional lateral-directional data for the model without vortex generators are presented in reference 1.

## SUMMARY OF RESULTS

A program for the wind-tunnel development of underwing leading-edge vortex generators on an NASA supercritical-wing research airplane configuration has shown the following results:

1. The addition of vortex generators to the wing (one per wing panel) delayed pitch-up to significantly higher angles of attack, and in the region where the angle of attack at pitch-up was extended, there were significant increases in lift and reductions in drag.

2. Effectiveness of the vortex generators in extending the angle of attack at which pitch-up occurs was not significantly degraded by a 33-percent reduction in the vortex-generator span (from 1.90 to 1.27 cm (0.75 to 0.50 in.)).

3. Effect of the vortex generators on the longitudinal aerodynamic characteristics was sensitive to relatively small changes in their orientation with respect to the wing (i.e., distance from wing leading edge, leading-edge sweep angle, toe-in angle, and small changes in the wing semispan location).

4. For a sideslip angle of approximately $5^{o}$, the vortex generators had only small effects on the lateral-directional aerodynamic characteristics of the model.

5. Limited data obtained on a wing upper-surface fence (one per wing panel) located near the trailing edge indicated that the fence delayed pitch-up but not to as high an angle of attack as the vortex generator, and when pitch-up occurred with the fences on the wing, it appeared even more abrupt than for the clean wing configuration.

Langley Research Center,
National Aeronautics and Space Administration,
Hampton, Va., June 20, 1973.

REFERENCES

1. Bartlett, Dennis W.; and Re, Richard J.: Wind-Tunnel Investigation of Basic Aerodynamic Characteristics of a Supercritical-Wing Research Airplane Configuration. NASA TM X-2470, 1972.

2. Harris, Charles D.: Wind-Tunnel Measurements of Aerodynamic Load Distribution on an NASA Supercritical-Wing Research Airplane Configuration. NASA TM X-2469, 1972.

3. Pearcey, H. H.: Shock-Induced Separation and Its Prevention by Design and Boundary Layer Control. Boundary Layer and Flow Control, Vol. 2, G. V. Lachmann, ed., Pergamon Press, 1961, pp. 1166-1344.

4. Carmel, Melvin M.; and Fischetti, Thomas L.: A Transonic Wind-Tunnel Investigation of the Effects of Nacelles on the Aerodynamic Characteristics of a Complete Model Configuration. NACA RM L53F22a, 1953.

5. Kelly, Thomas C.: Transonic Wind-Tunnel Investigation of the Effects of External Stores and Store Position on the Aerodynamic Characteristics of a 1/16-Scale Model of the Douglas D-558-II Research Airplane. NACA RM L55I07, 1955.

6. Harris, Charles D.; and Bartlett, Dennis W.: Wind-Tunnel Investigation of Effects of Underwing Leading-Edge Vortex Generators on a Supercritical-Wing Research Airplane Configuration. NASA TM X-2471, 1972.

7. Schaefer, William T., Jr.: Characteristics of Major Active Wind Tunnels at the Langley Research Center. NASA TM X-1130, 1965.

8. Jordan, Frank L., Jr.: Investigation at Near-Sonic Speed of Some Effects of Humidity on the Longitudinal Aerodynamic Characteristics of an NASA Supercritical Wing Research Airplane Model. NASA TM X-2618, 1972.

9. Davis, Don D., Jr.; and Moore, Dewey: Analytical Study of Blockage- and Lift-Interference Corrections for Slotted Tunnels Obtained by the Substitution of an Equivalent Homogeneous Boundary for the Discrete Slots. NACA RM L53E07b, 1953.

10. Wright, Ray H.; and Barger, Raymond L.: Wind-Tunnel Lift Interference on Swept-back Wings in Rectangular Test Sections With Slotted Top and Bottom Walls. NASA TR R-241, 1966.

11. Blackwell, James A., Jr.: Preliminary Study of Effects of Reynolds Number and Boundary-Layer Transition Location on Shock-Induced Separation. NASA TN D-5003, 1969.

TABLE I.- TUNNEL TEST CONDITIONS

| Mach number | Dynamic pressure | | | | Reynolds number | | | |
|---|---|---|---|---|---|---|---|---|
| | Steel wing | | Aluminum wing | | Steel wing | | Aluminum wing | |
| | $N/m^2$ | $lb/ft^2$ | $N/m^2$ | $lb/ft^2$ | per m | per ft | per m | per ft |
| 0.25 | 8 523 | 178 | 8 523 | 178 | $10.2 \times 10^6$ | $3.1 \times 10^6$ | $10.2 \times 10^6$ | $3.1 \times 10^6$ |
| .50 | 23 940 | 500 | 23 940 | 500 | 14.4 | 4.4 | 14.4 | 4.4 |
| .80 | 47 880 | 1000 | 31 122 | 650 | 20.0 | 6.1 | 13.1 | 4.0 |
| .90 | 47 880 | 1000 | 31 122 | 650 | 18.4 | 5.6 | 12.1 | 3.7 |
| .95 | 44 193 | 923 | 28 728 | 600 | 16.4 | 5.0 | 10.8 | 3.3 |
| .98 | 44 193 | 923 | ----- | --- | 16.1 | 4.9 | --------- | -------- |
| .99 | 44 193 | 923 | ----- | --- | 16.1 | 4.9 | --------- | -------- |

TABLE II.- VORTEX-GENERATOR CONFIGURATIONS

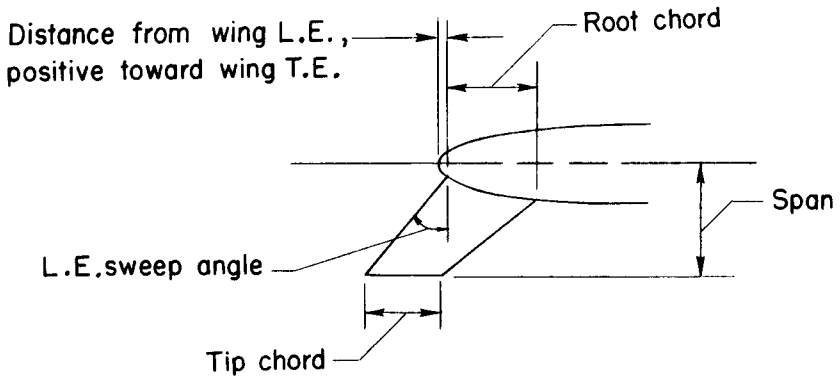


| Vortex generator | Wing semispan location, $\frac{y}{b/2}$ | Span | | Leading-edge sweep angle, deg | Root chord | | Tip chord | | Distance from wing L.E. | | Toe-in angle, deg (a) |
|---|---|---|---|---|---|---|---|---|---|---|---|
| | | cm | in. | | cm | in. | cm | in. | cm | in. | |
| Initial | 0.56 | 1.90 | 0.75 | 40 | 1.52 | 0.60 | 1.27 | 0.500 | 0.16 | 0.063 | 5 |
| | .60 | 1.90 | .75 | 40 | 1.52 | .60 | 1.27 | .500 | .16 | .063 | 5 |
| | .65 | 1.90 | .75 | 40 | 1.52 | .60 | 1.27 | .500 | .16 | .063 | 5 |
| Modification 1 | .60 | 1.90 | .75 | 40 | 1.52 | .60 | 1.27 | .500 | 0 | 0 | 5 |
| Modification 2 | .60 | 1.90 | .75 | 42 | 1.52 | .60 | 1.27 | .500 | 0 | 0 | 5 |
| Modification 3 | .60 | 1.90 | .75 | 42 | 1.52 | .60 | 1.27 | .500 | -.16 | -.063 | 5 |
| Modification 4 | .60 | 1.90 | .75 | 42 | 1.52 | .60 | 1.27 | .500 | -.16 | -.063 | 0 |
| Modification 5 | .60 | 1.59 | .625 | 42 | 1.52 | .60 | 1.33 | .525 | -.16 | -.063 | 0 |
| Modification 6 | .60 | 1.27 | .50 | 42 | 1.83 | .72 | 1.33 | .525 | -.16 | -.063 | 0 |

[a] See figure 1(c).

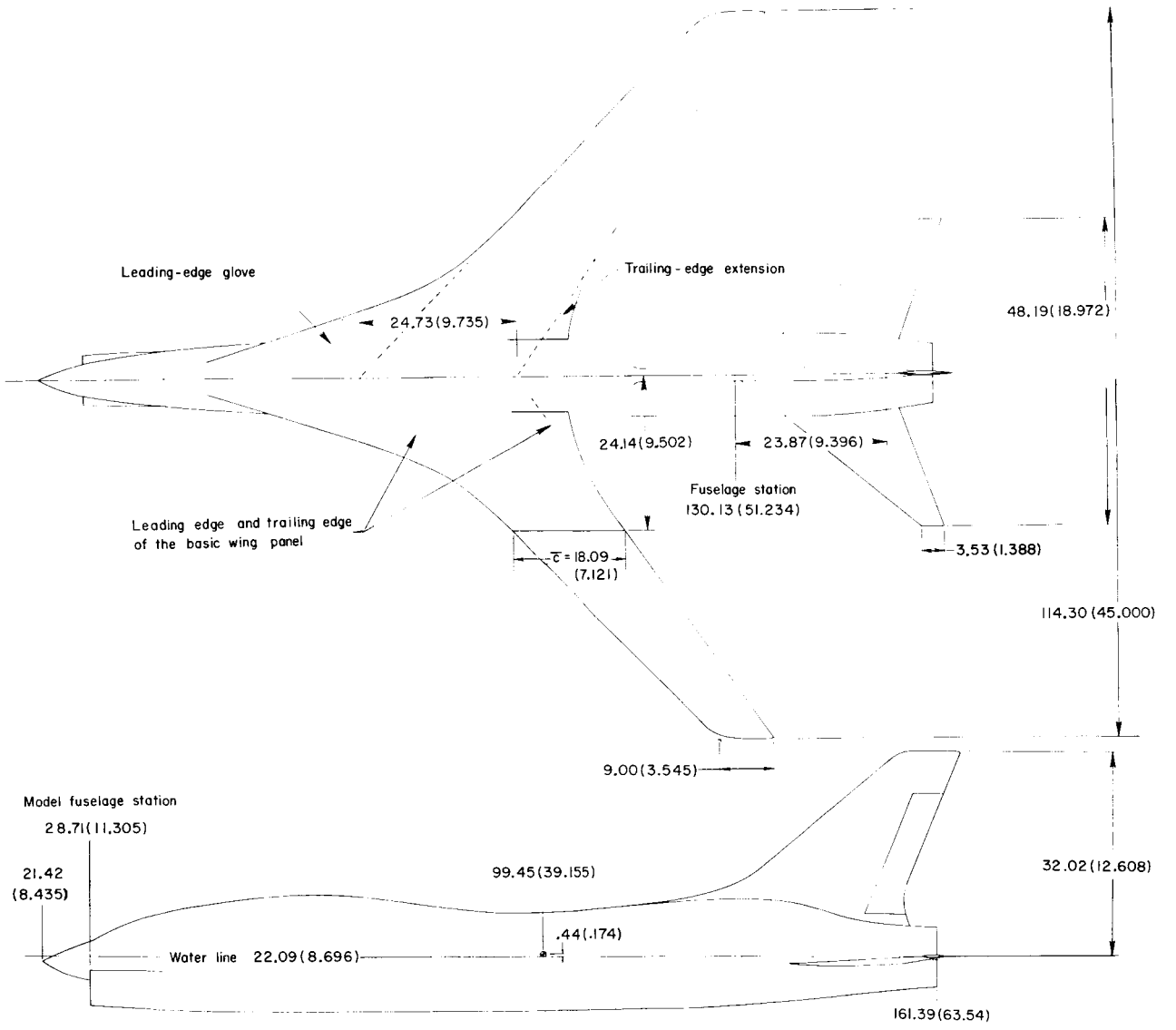


(a) General arrangement of 0.087-scale model.

Figure 1.- Model details. Dimensions are given in centimeters (inches).

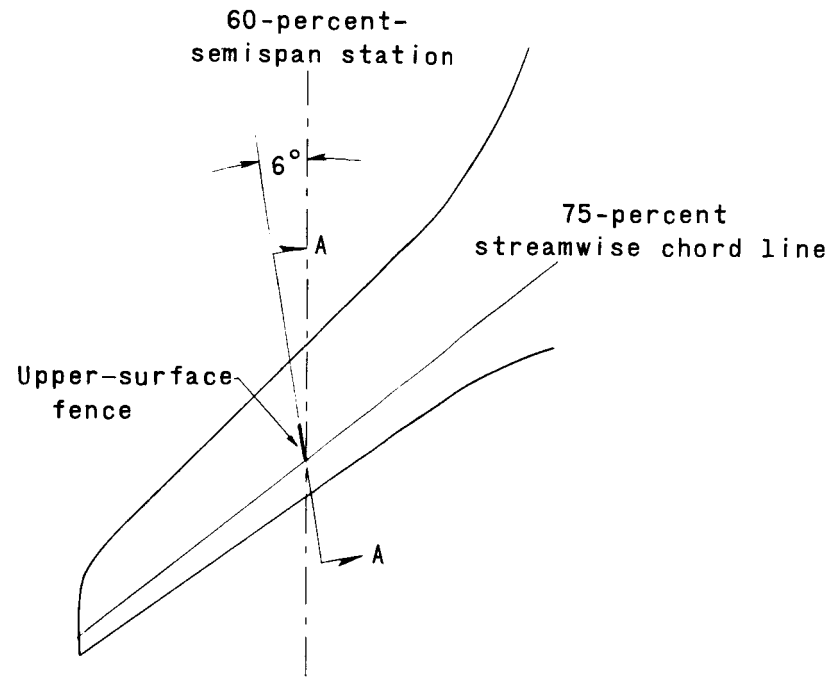


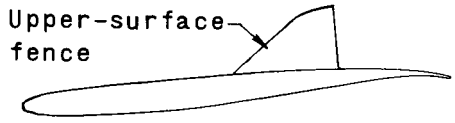


Sketch of section A-A

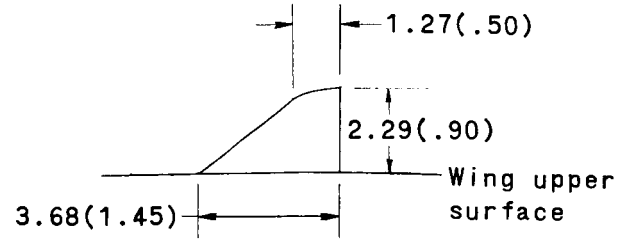


Details of upper-surface fence

(b) Upper-surface fence.

Figure 1.- Continued.

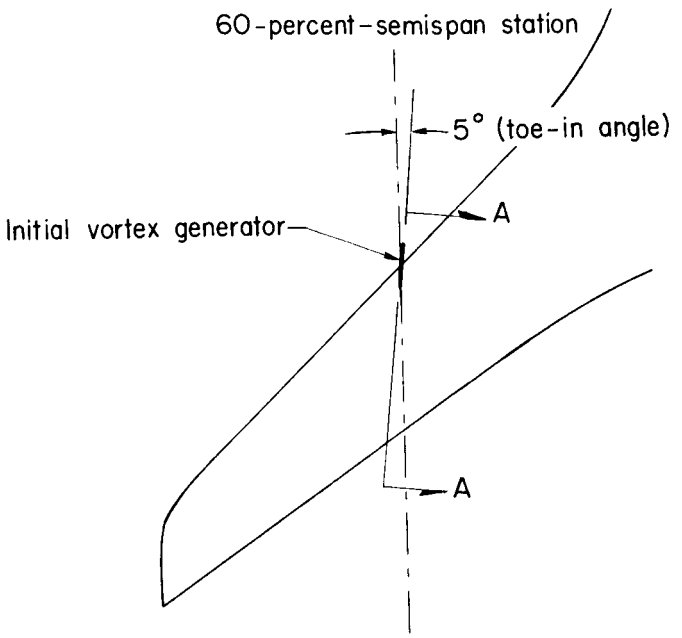


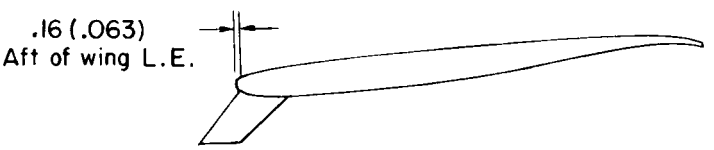


Sketch of section A–A

(10-percent-thick Clark Y airfoil, flat surface facing inboard)

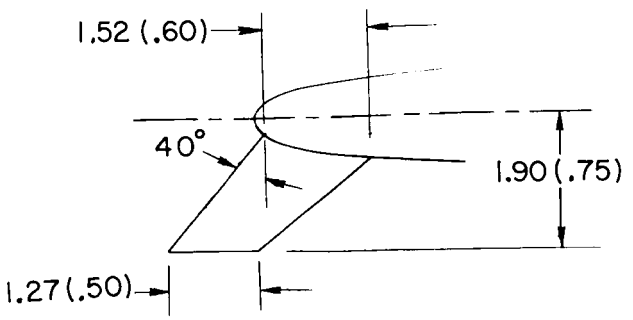


Details of initial vortex generator

(c) Initial vortex generator.

Figure 1.- Continued.

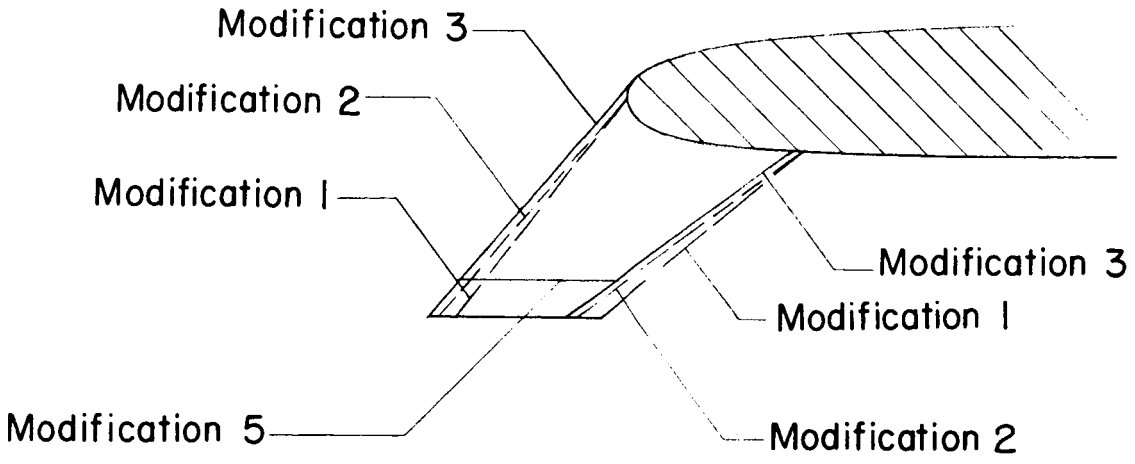


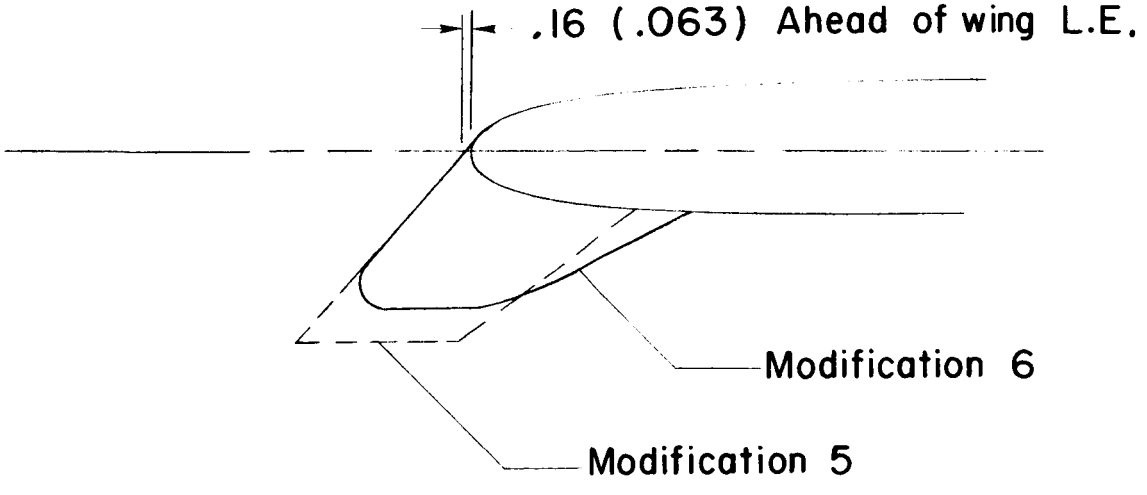


(d) Vortex-generator modifications.

Figure 1.- Continued.

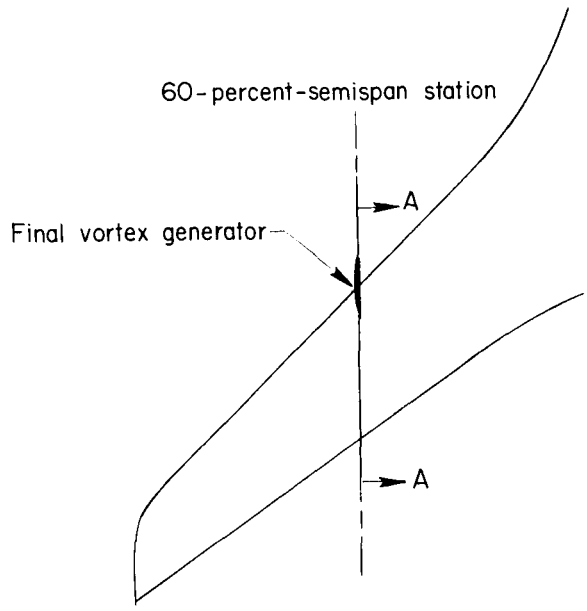


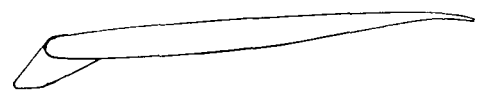

Sketch of section A–A

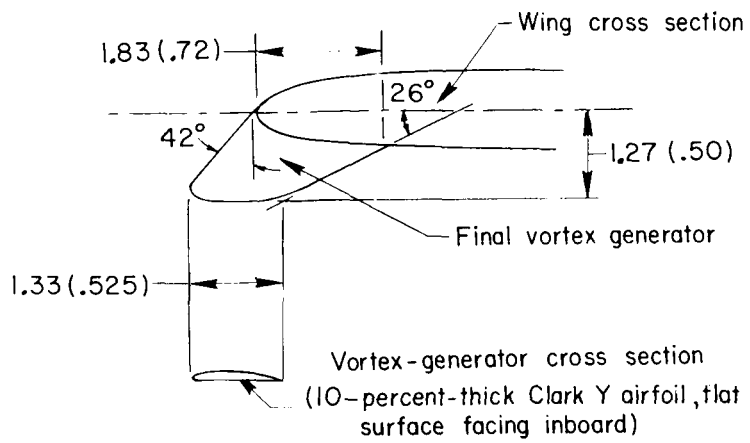


Details of final vortex generator (modification 6)

(e) Final vortex generator (modification 6).

Figure 1.- Continued.

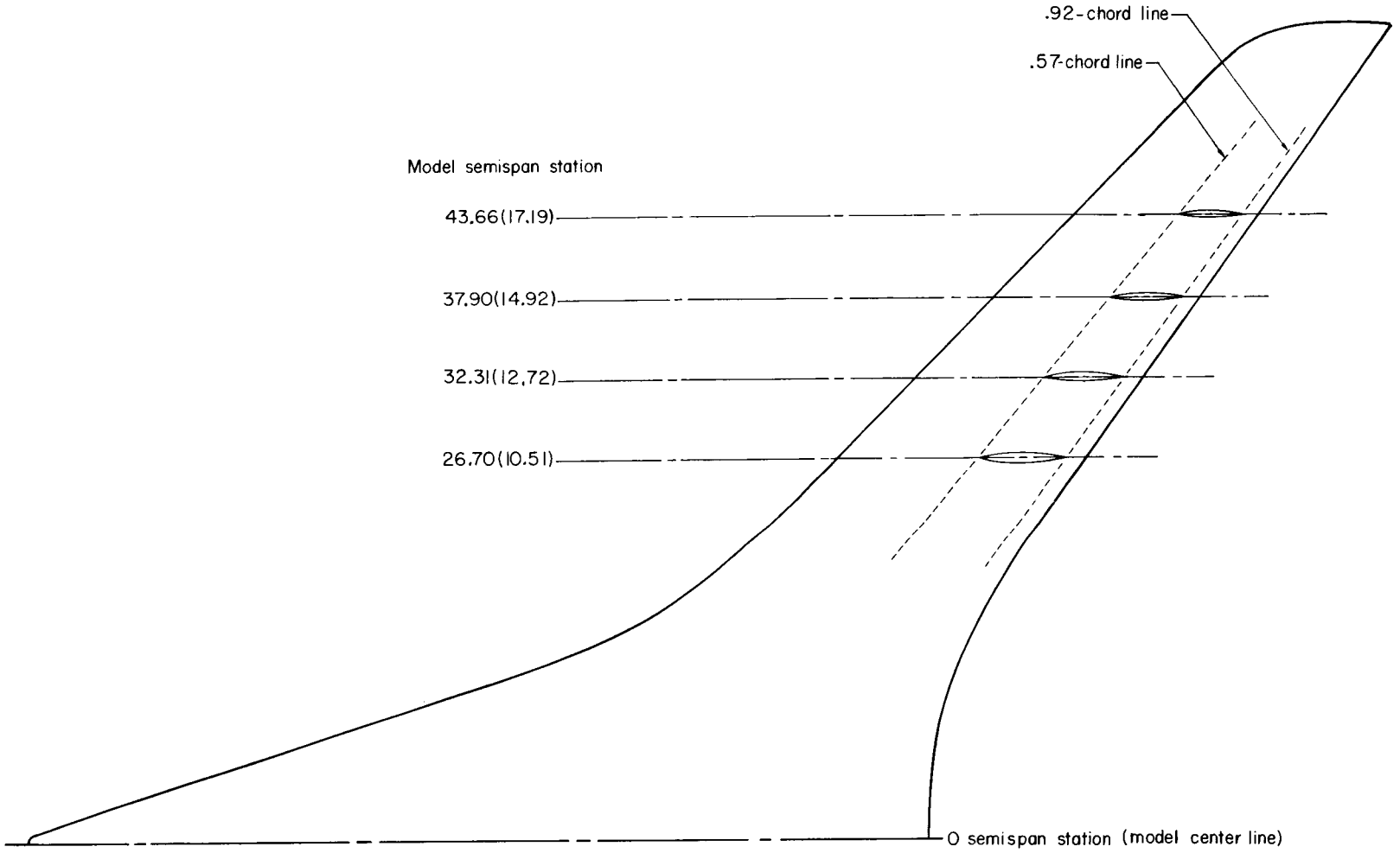


(f) Location of aileron hinge fairings.

Figure 1.- Continued.

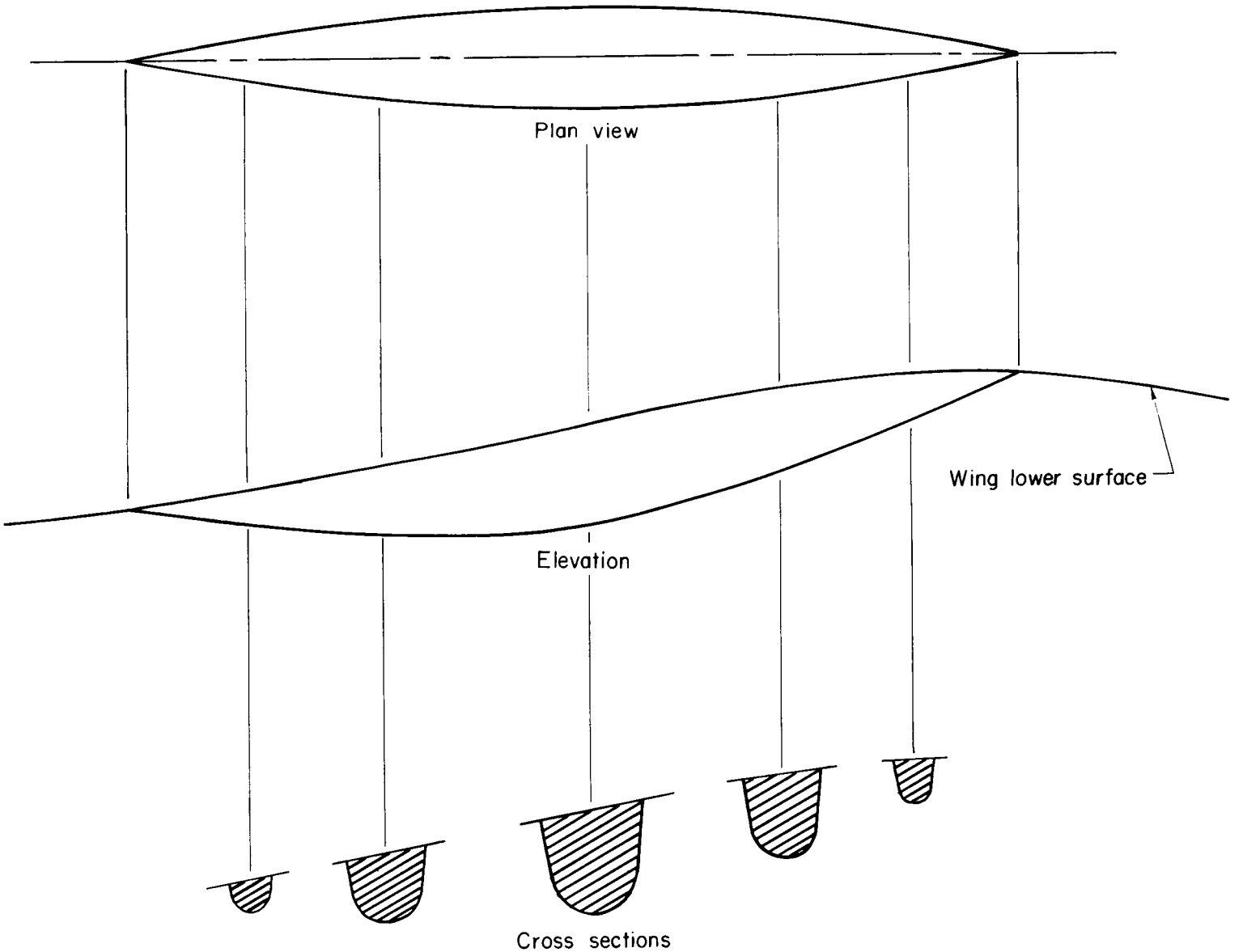


(g) Sketch of typical aileron hinge fairing.

Figure 1.- Continued.

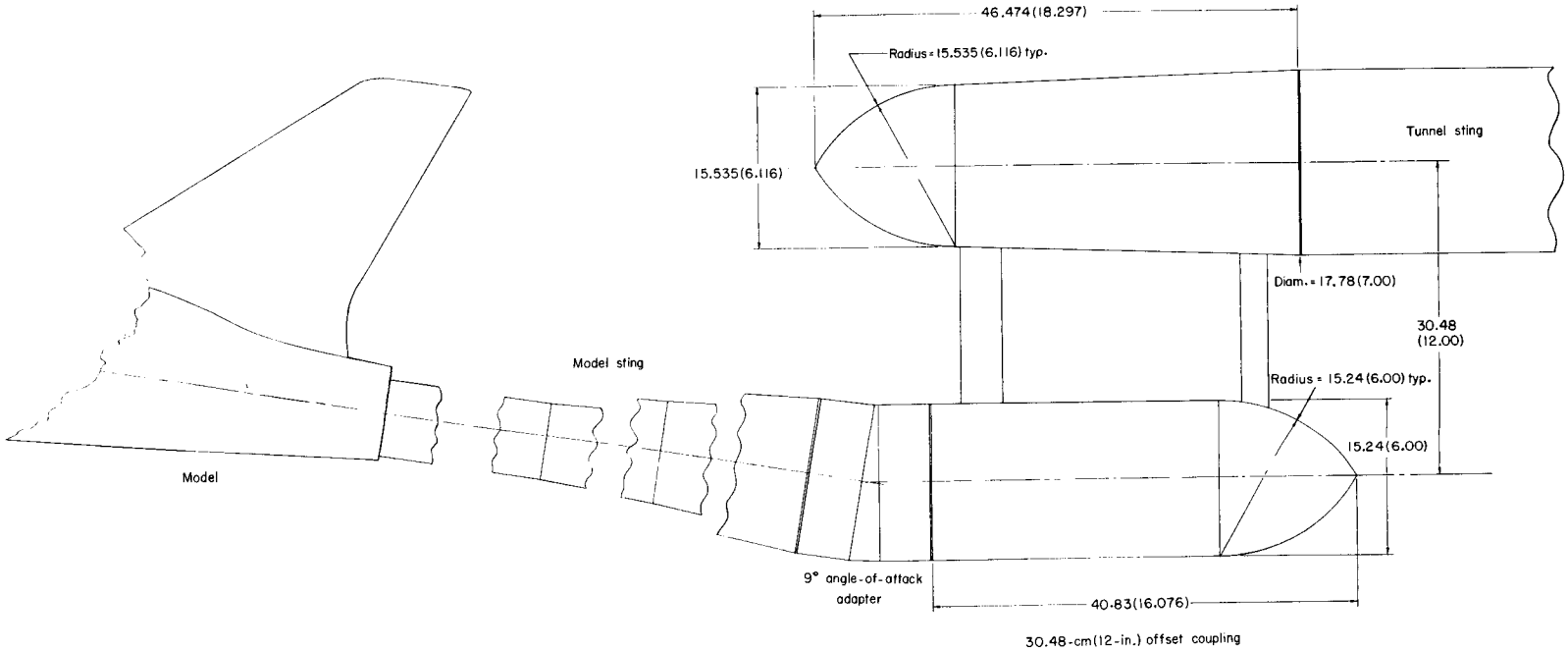


(h) Offset sting arrangement.

Figure 1.- Concluded.

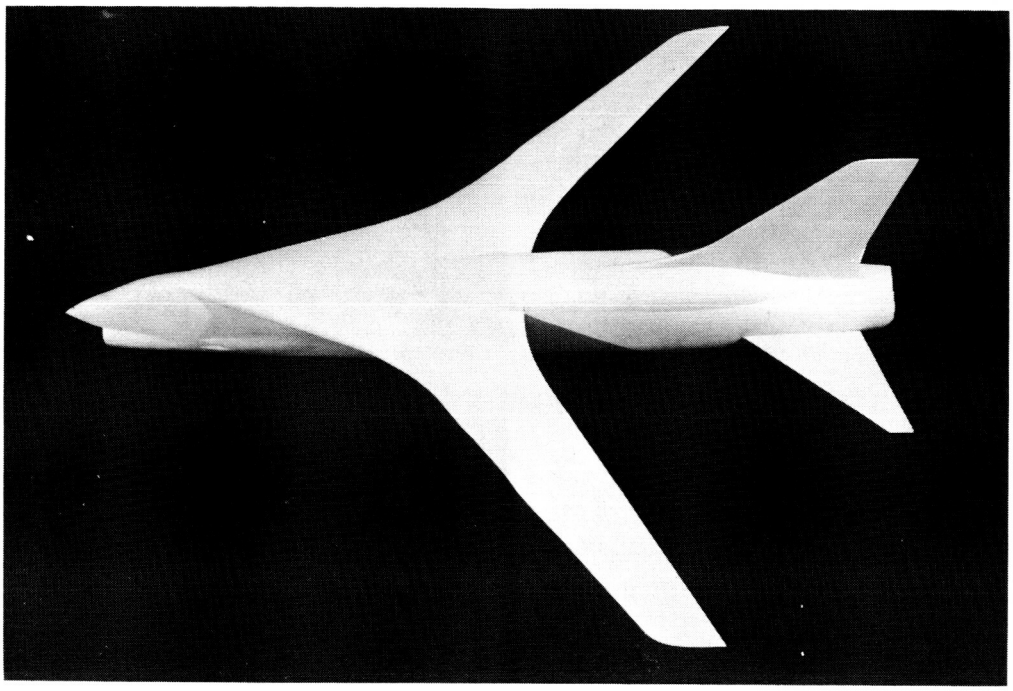

L-69-6086

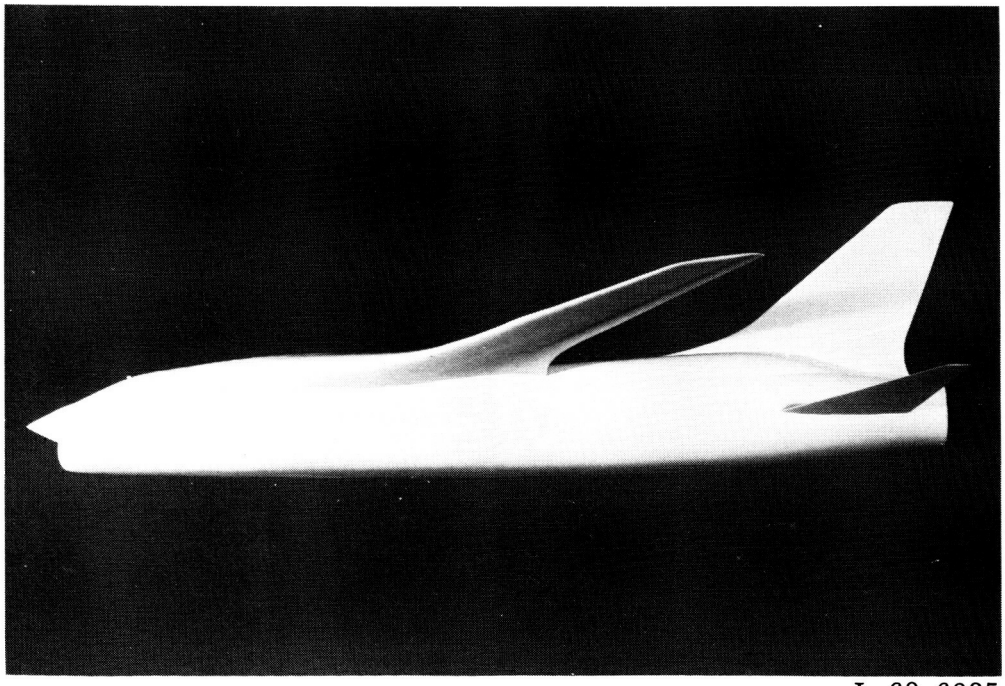

L-69-6085

Figure 2.- 0.087-scale wind-tunnel model.

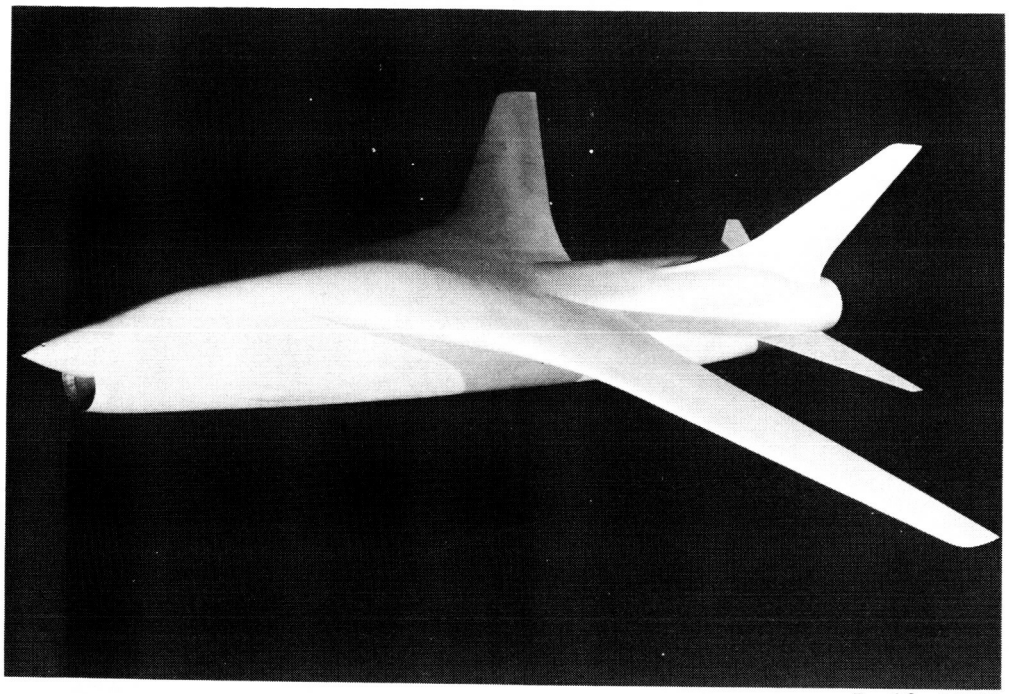

L-69-6079

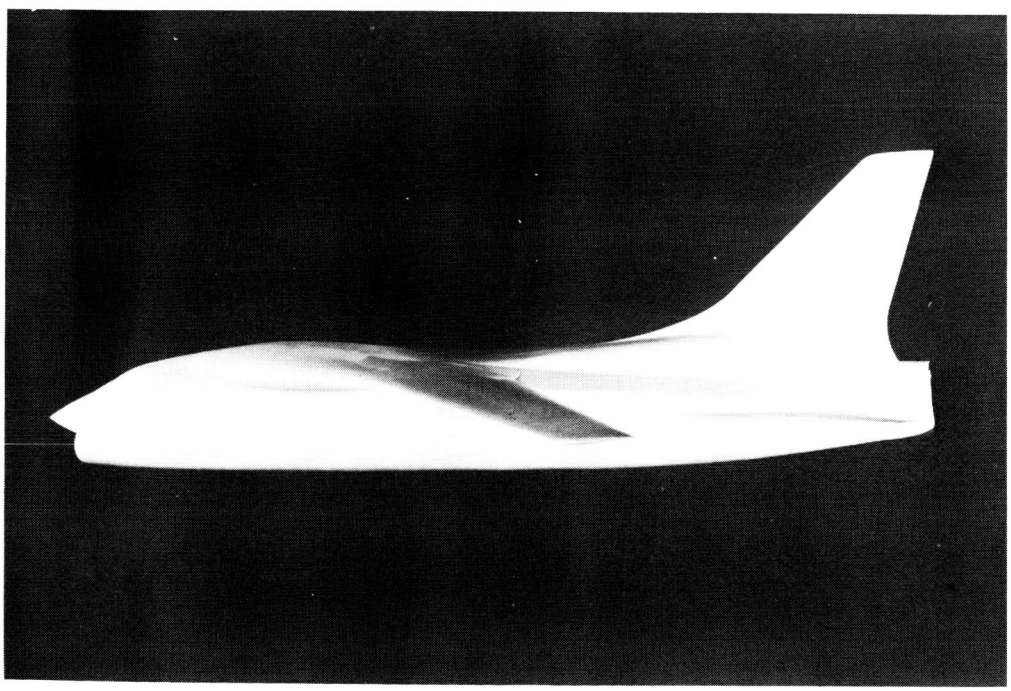

L-69-6083

Figure 2.- Concluded.

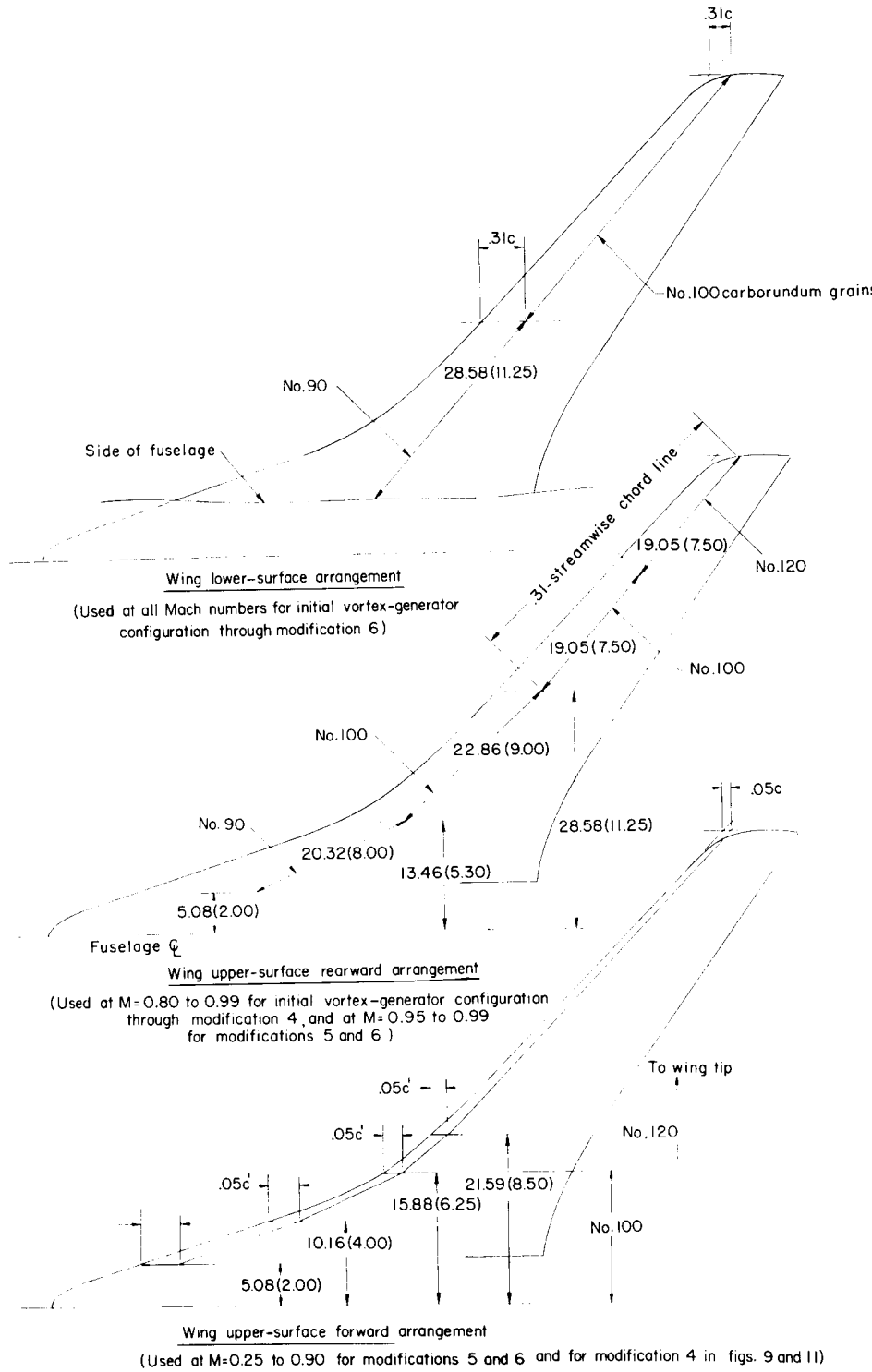


Figure 3.- Boundary-layer-trip arrangements. Dimensions are given in centimeters (inches).

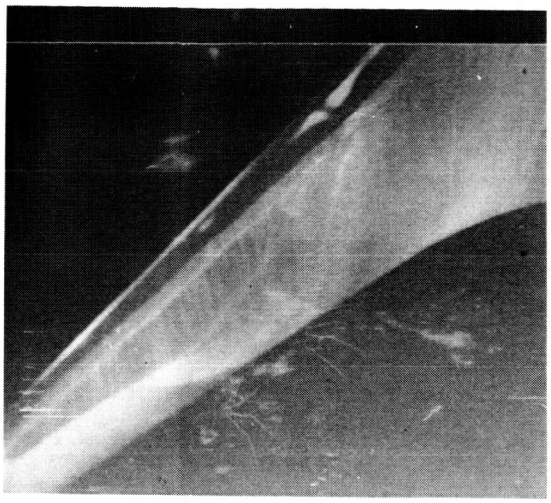

$\alpha = 5.2^{O}$; $C_L = 0.65$

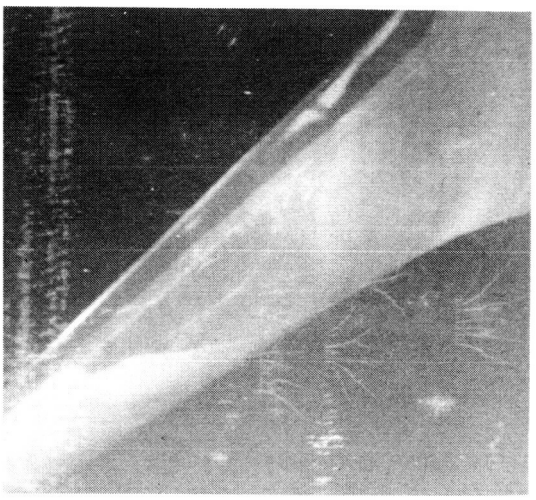

$\alpha = 6.7^{O}$; $C_L = 0.78$

$\alpha = 8.1^{O}$; $C_L = 0.86$

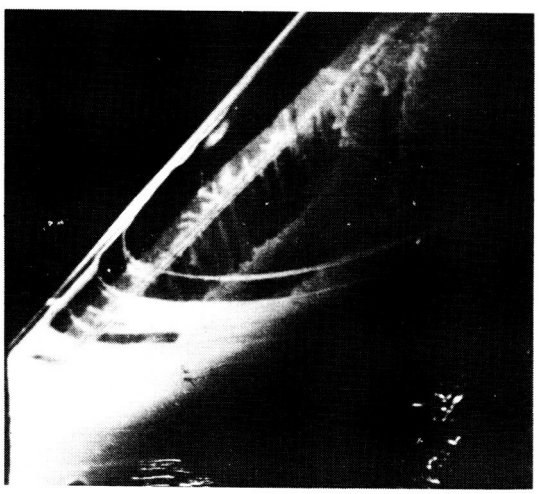

$\alpha = 9.4^{O}$; $C_L = 0.92$

(a) Clean wing.

L-73-3093

Figure 4.- Oil-flow photographs of wing upper surface at a Mach number of 0.95. $\beta = 0^{O}$.

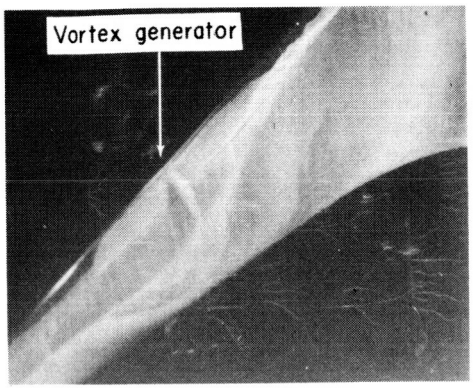


$\alpha = 5.2^{o}$; $C_L = 0.65$

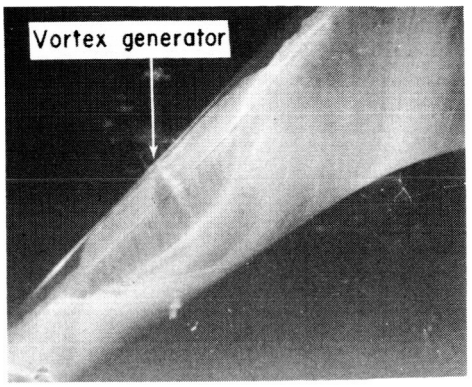


$\alpha = 6.7^{o}$; $C_L = 0.79$

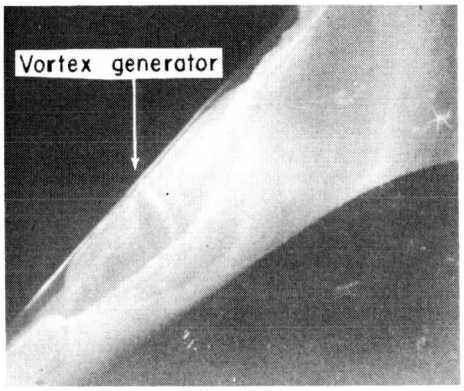


$\alpha = 7.5^{o}$; $C_L = 0.84$

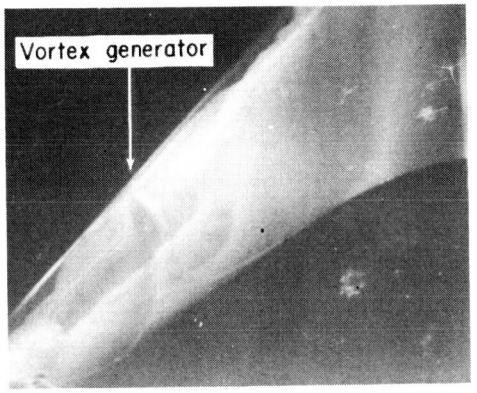


$\alpha = 8.1^{o}$; $C_L = 0.90$

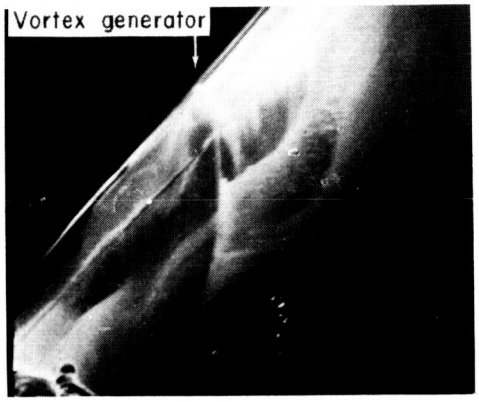


$\alpha = 8.8^{o}$; $C_L = 0.93$

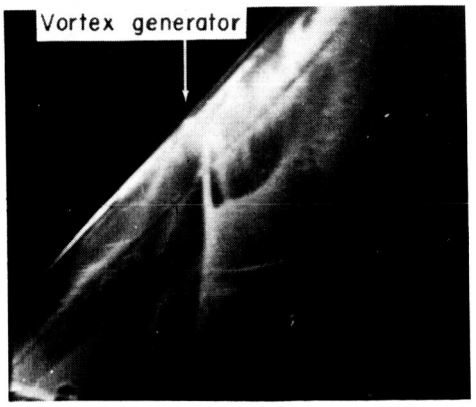


$\alpha = 9.5^{o}$; $C_L = 0.98$

(b) Underwing leading-edge vortex generator. L-73-3094

Figure 4.- Continued.

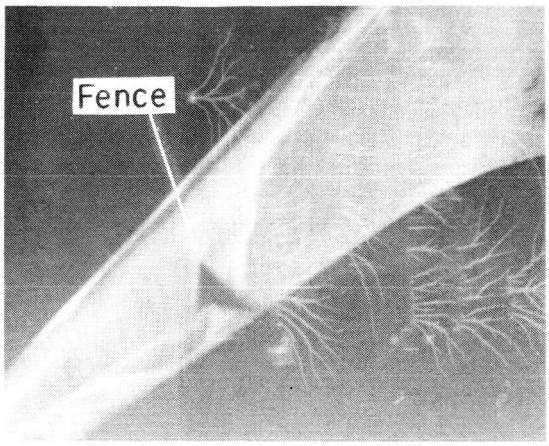


$\alpha = 5.2^{O}$; $C_L = 0.66$

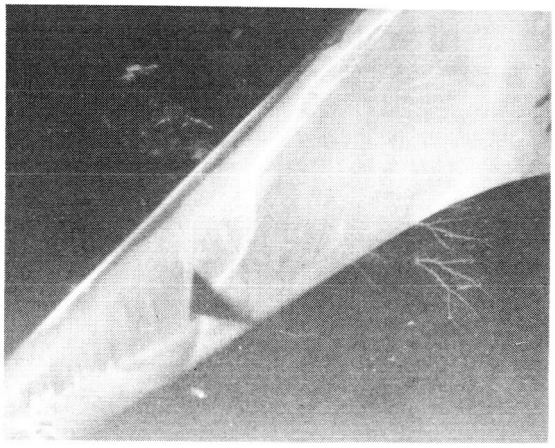

$\alpha = 6.7^{O}$; $C_L = 0.81$

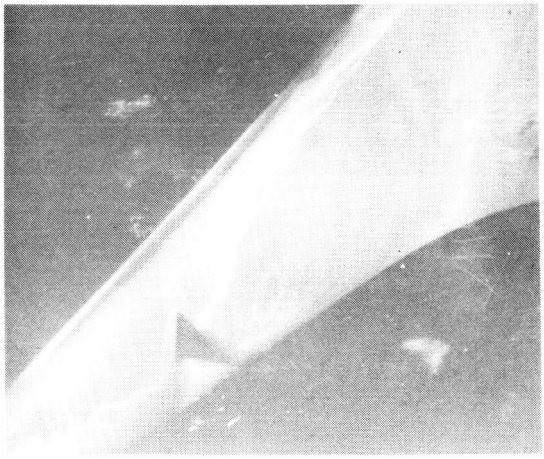

$\alpha = 7.5^{O}$; $C_L = 0.87$

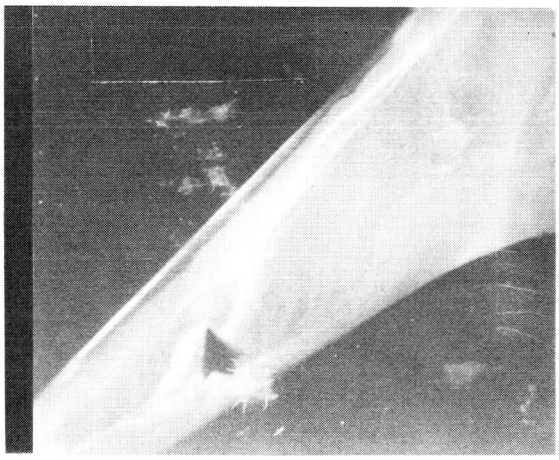

$\alpha = 7.9^{O}$; $C_L = 0.89$

(c) Wing upper-surface fence. L-73-3095

Figure 4.- Concluded.

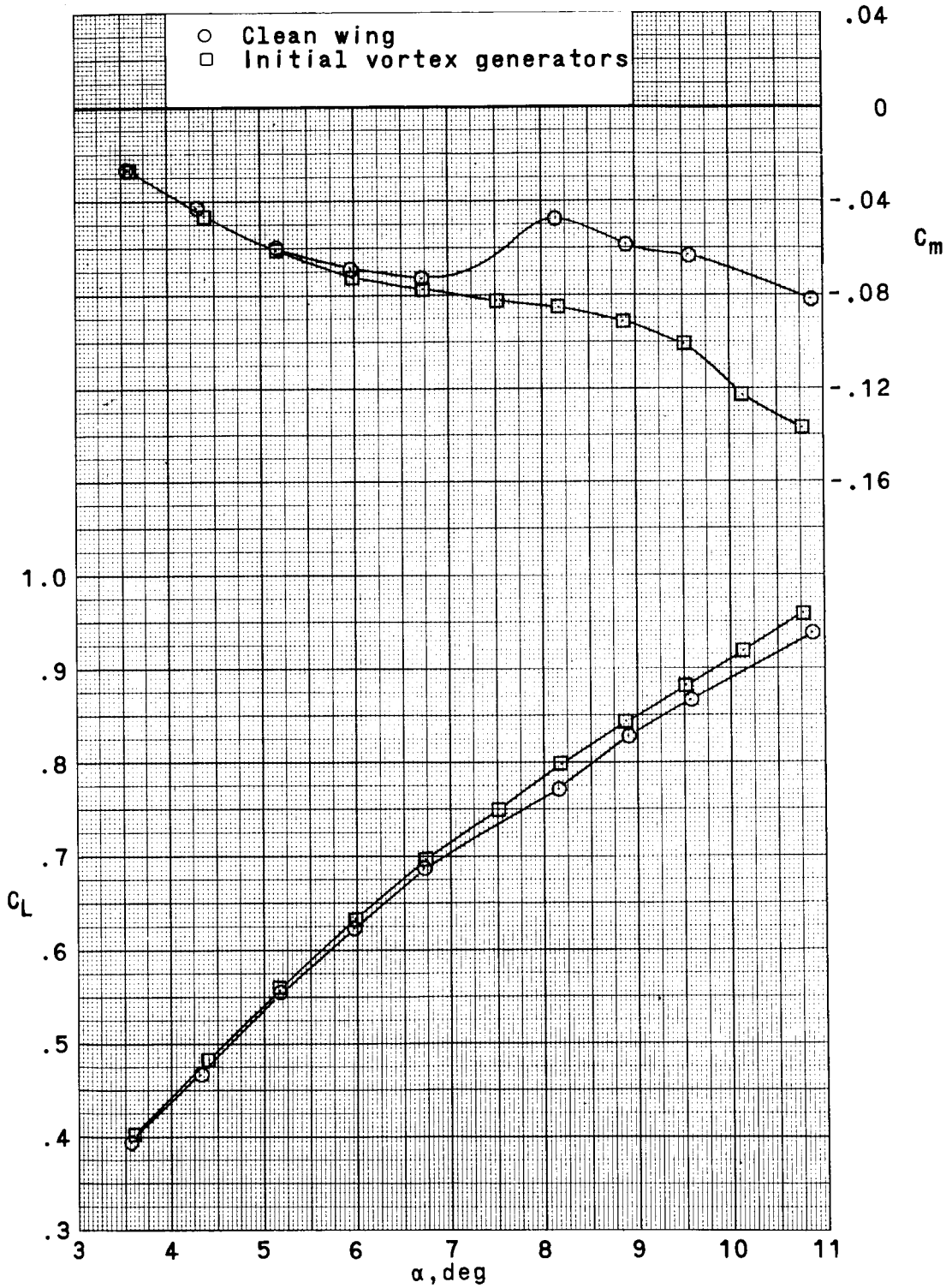


(a) M = 0.80.

Figure 5.- Effect of wing upper-surface fences and initial underwing vortex generators located at 60-percent-semispan station on longitudinal aerodynamic characteristics. Steel wing.

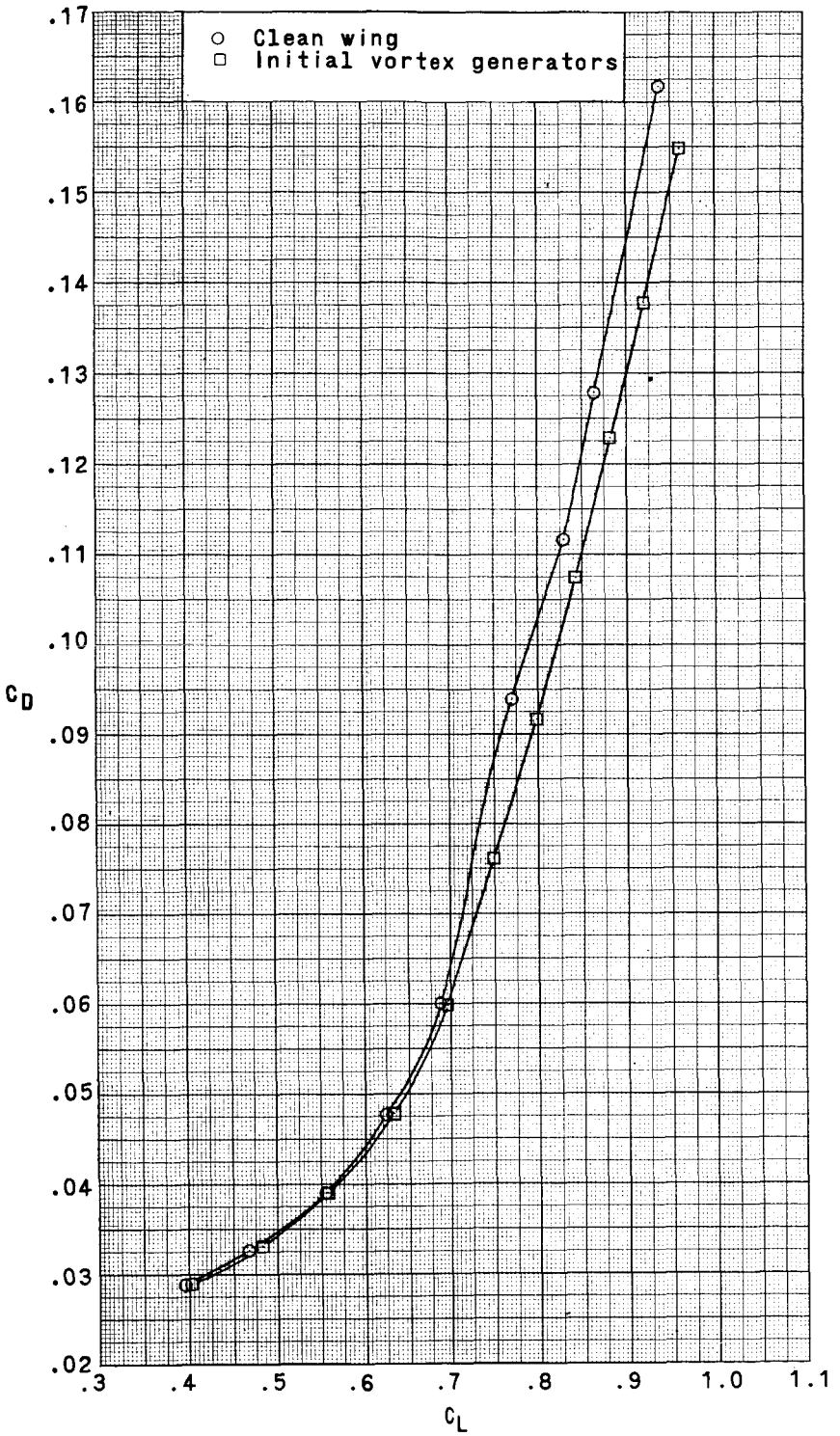


(a) M = 0.80. Concluded.

Figure 5.- Continued.

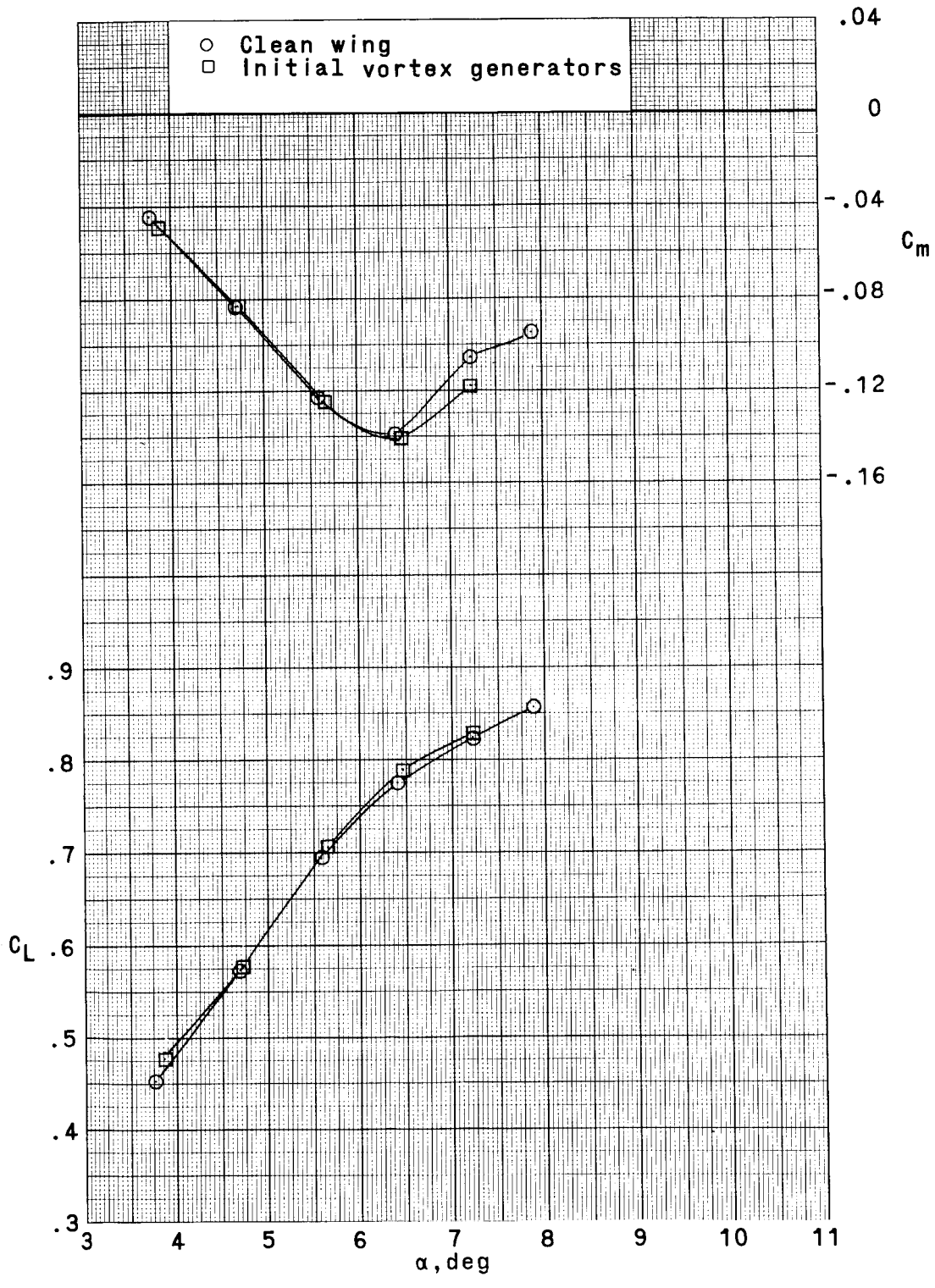


(b) M = 0.90.

Figure 5.- Continued.

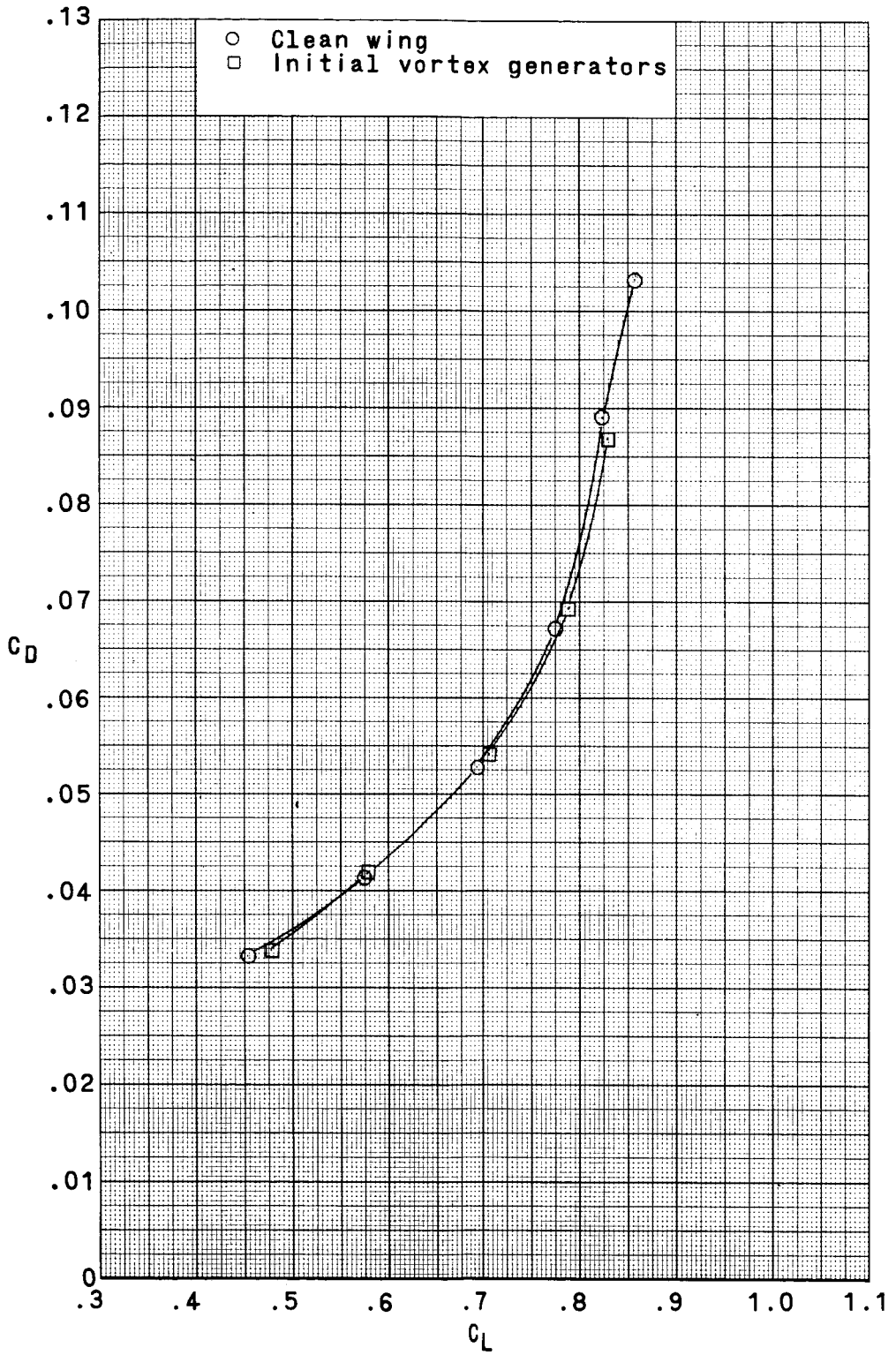


(b) M = 0.90. Concluded.

Figure 5. - Continued.

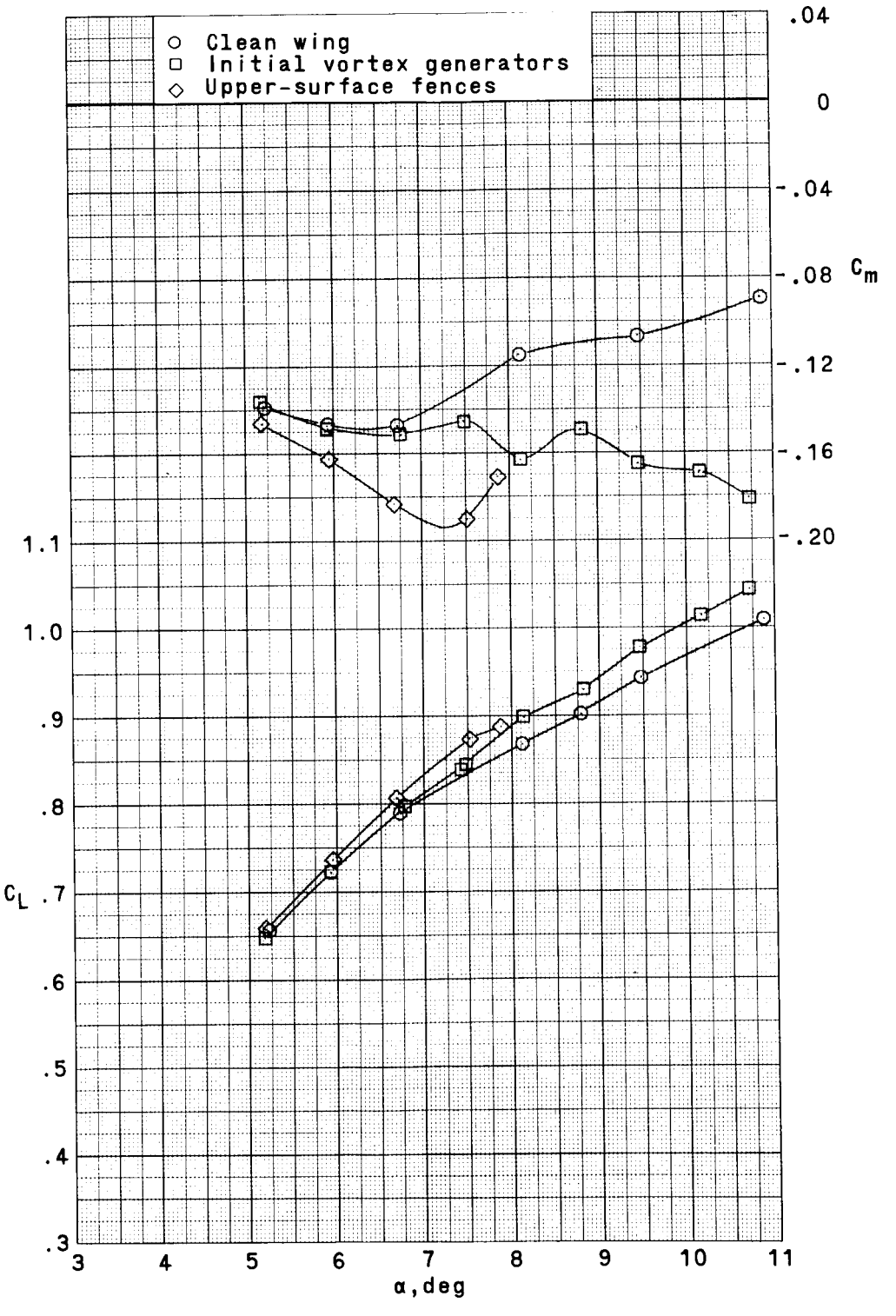


(c) M = 0.95.

Figure 5.- Continued.

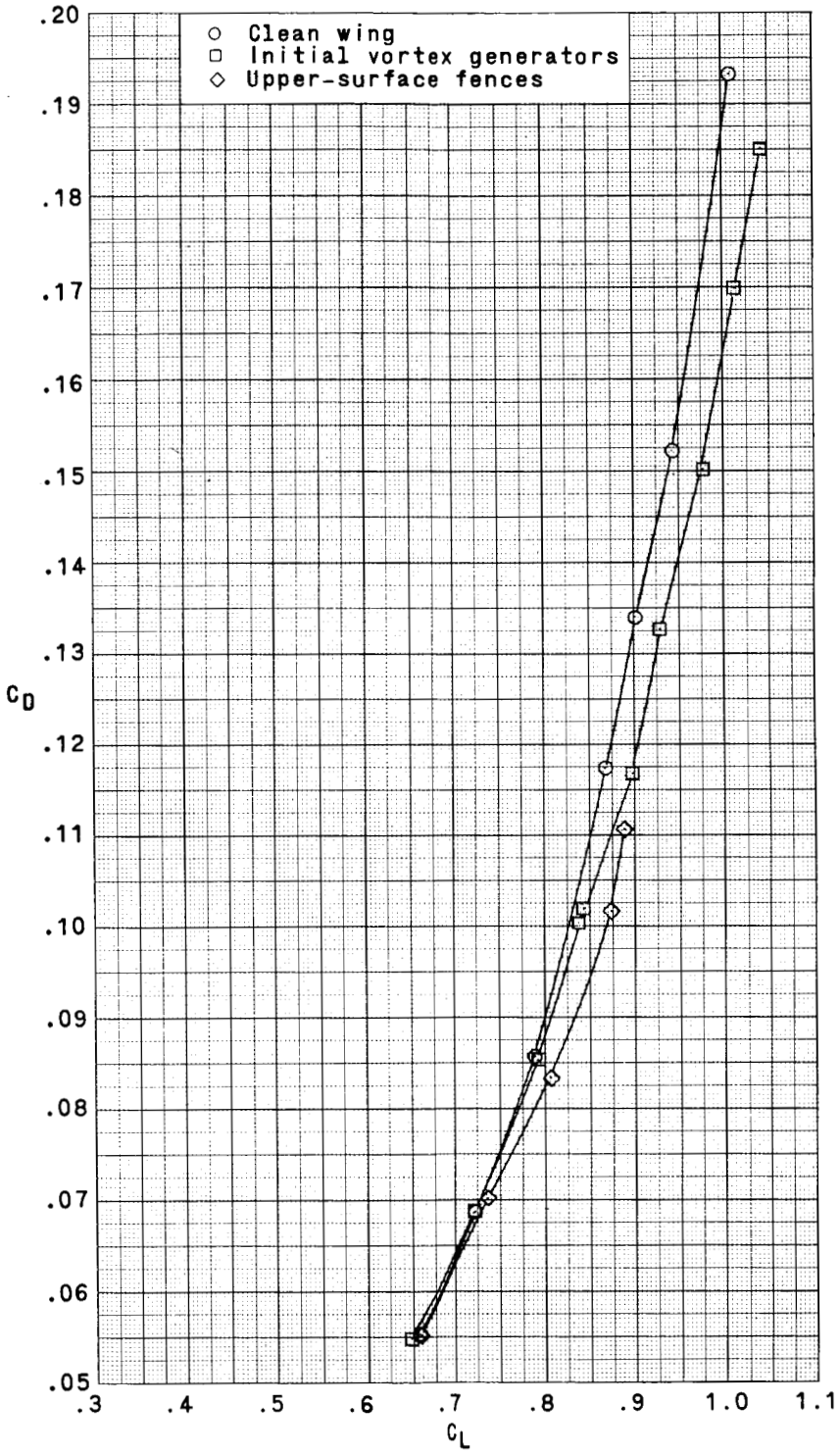


(c) M = 0.95. Concluded.

Figure 5. - Continued.

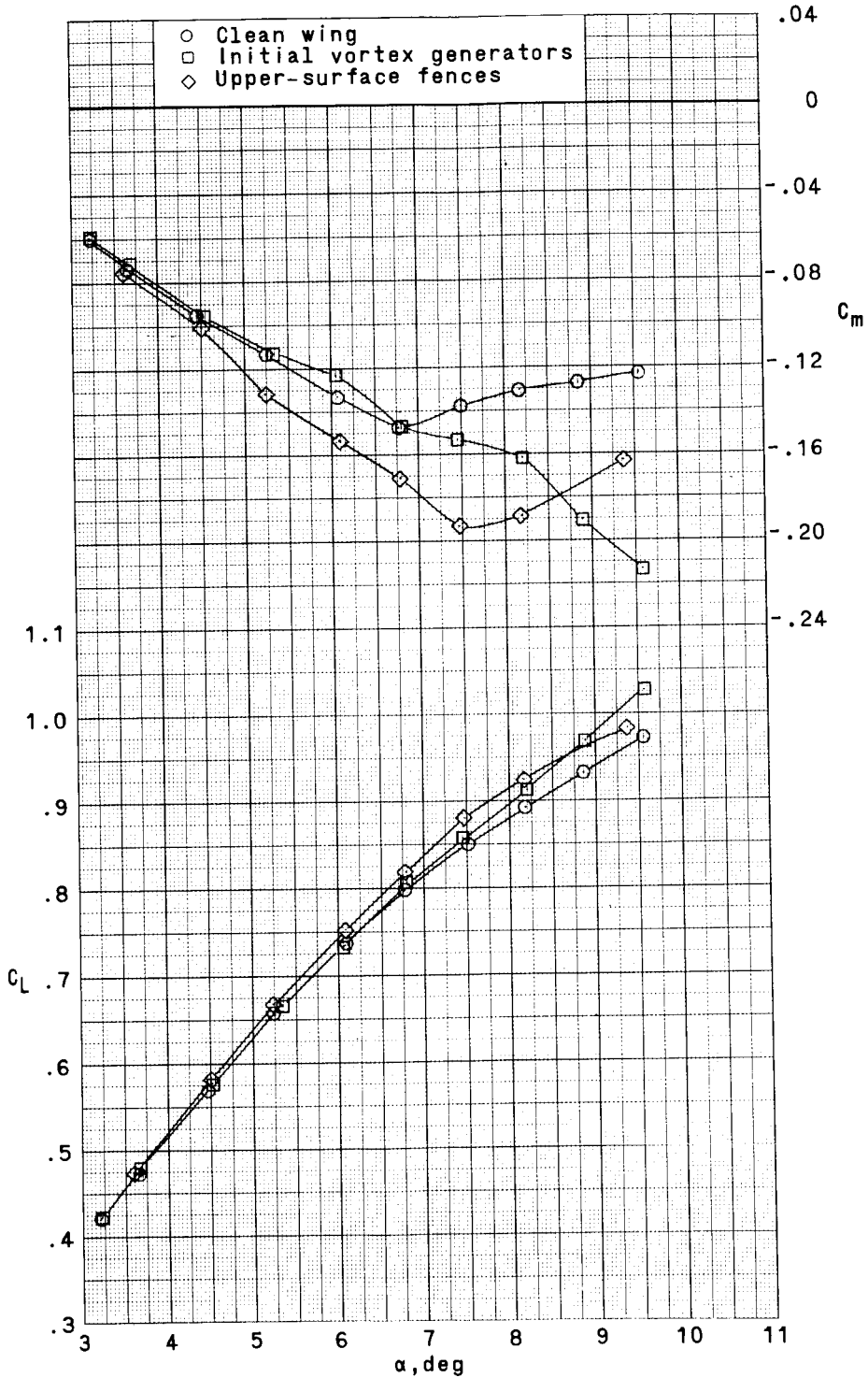


(d) M = 0.99.

Figure 5.- Continued.

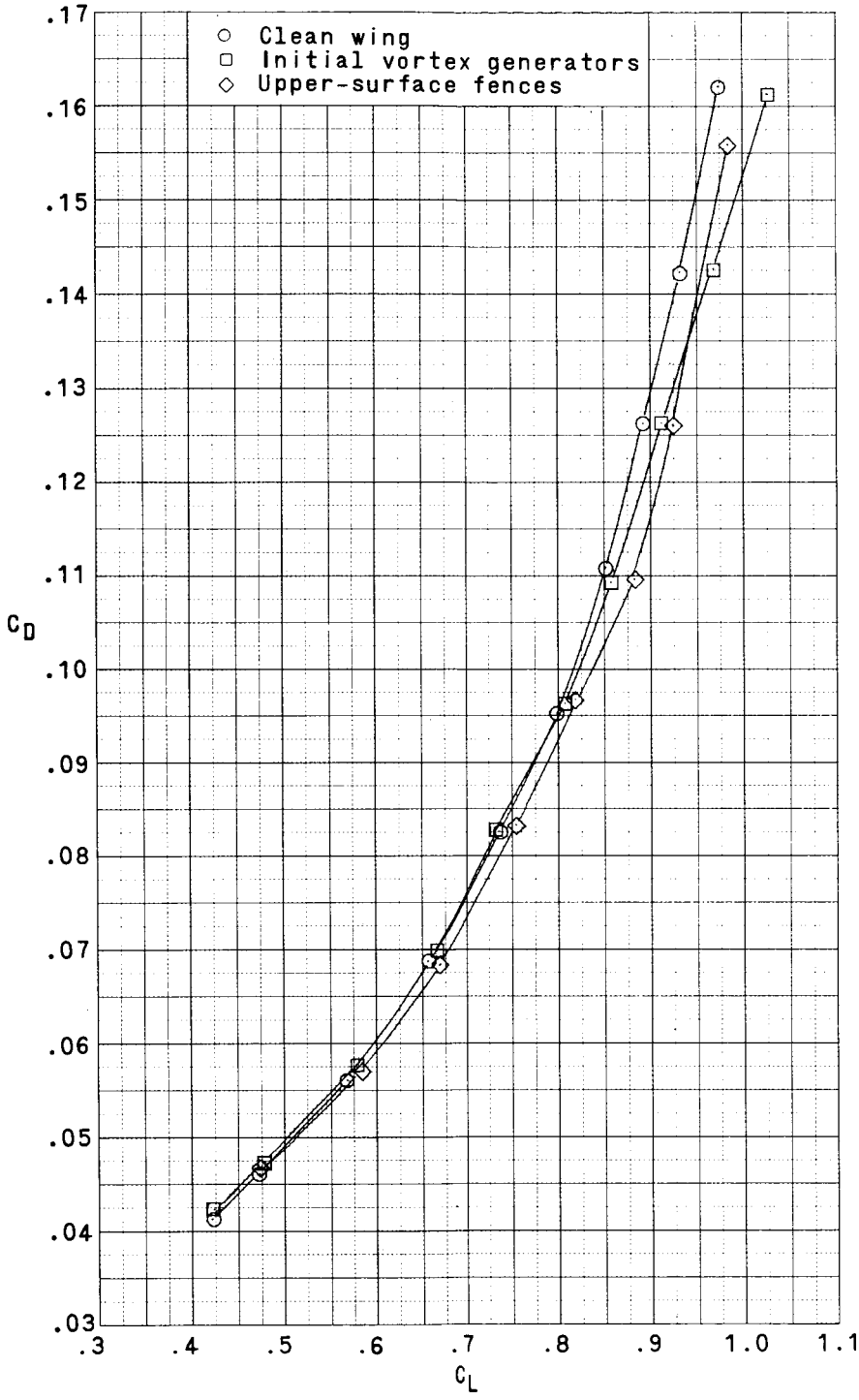


(d) M = 0.99. Concluded.

Figure 5.- Concluded.

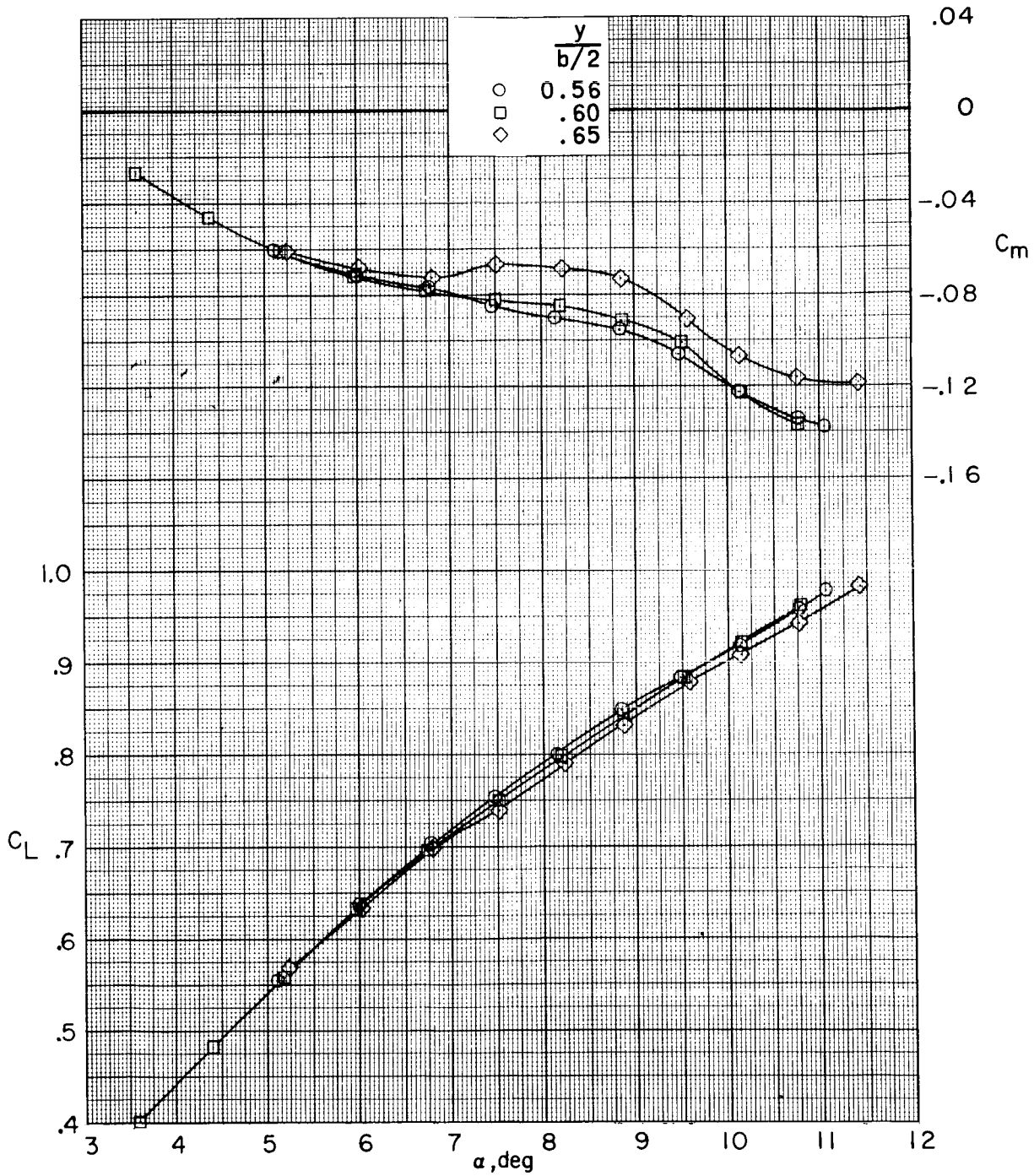


(a) M = 0.80.

Figure 6.- Effect of wing semispan location of initial underwing vortex generators on longitudinal aerodynamic characteristics. Steel wing.

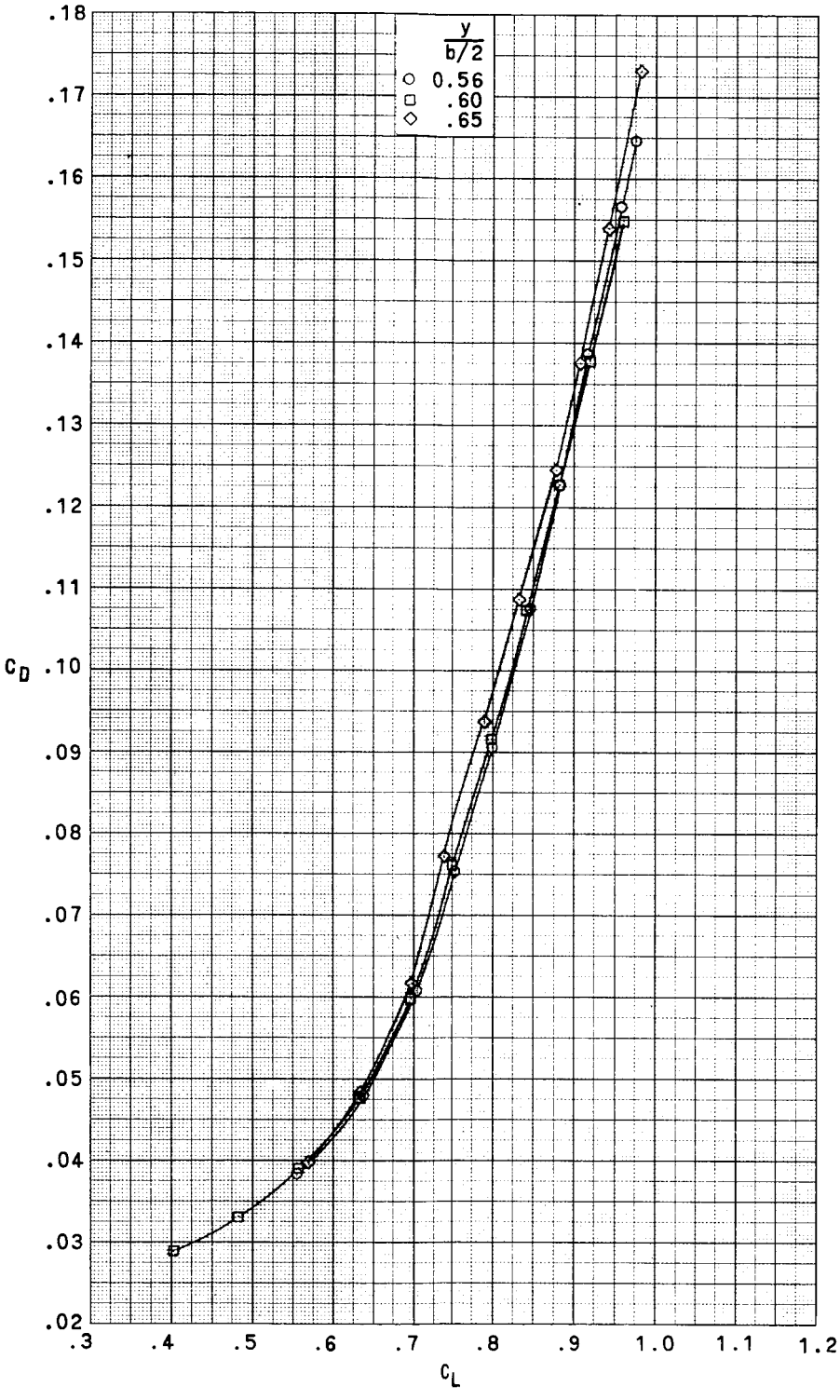


(a) M = 0.80. Concluded.

Figure 6.- Continued.

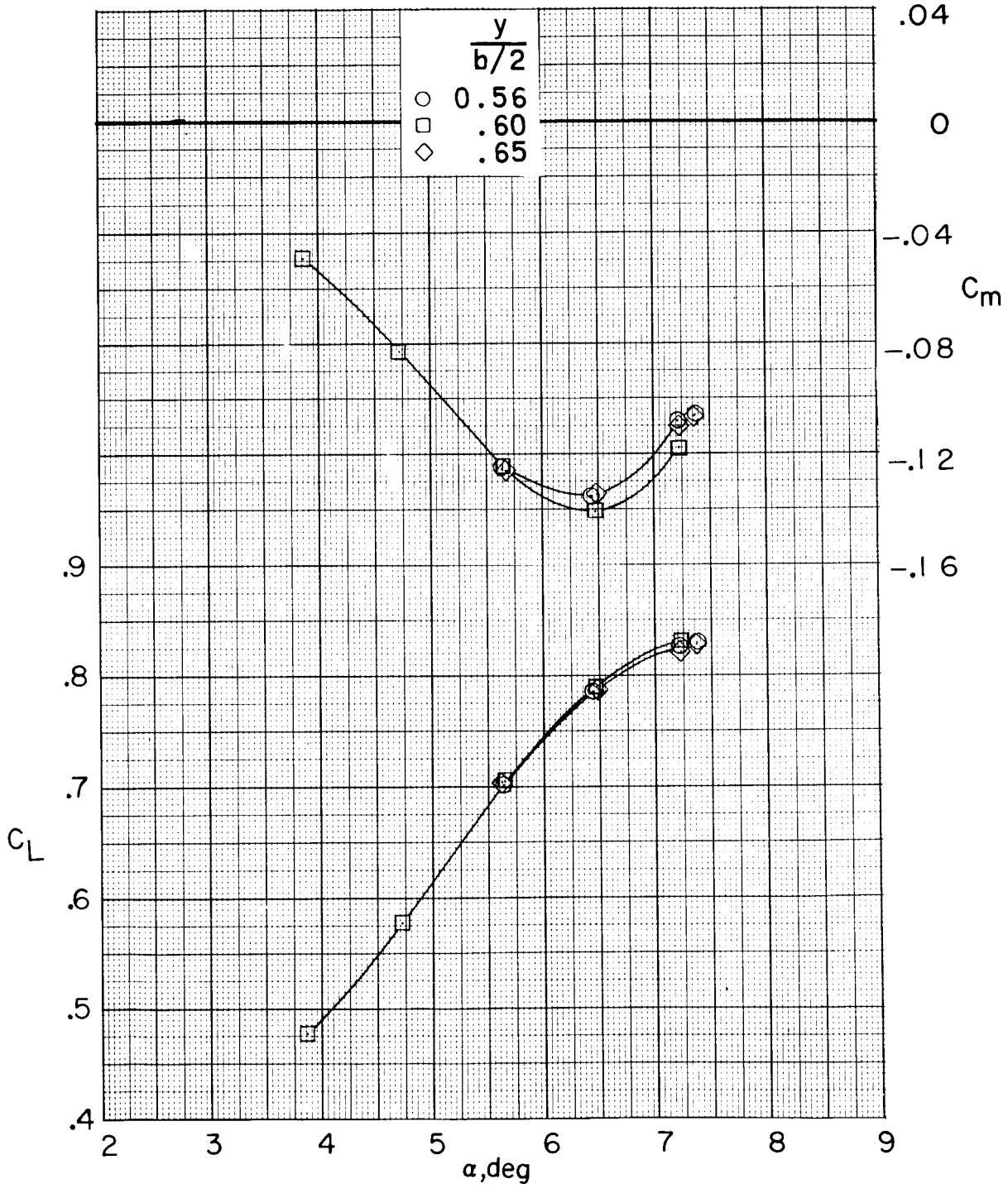


(b) M = 0.90.

Figure 6.- Continued.

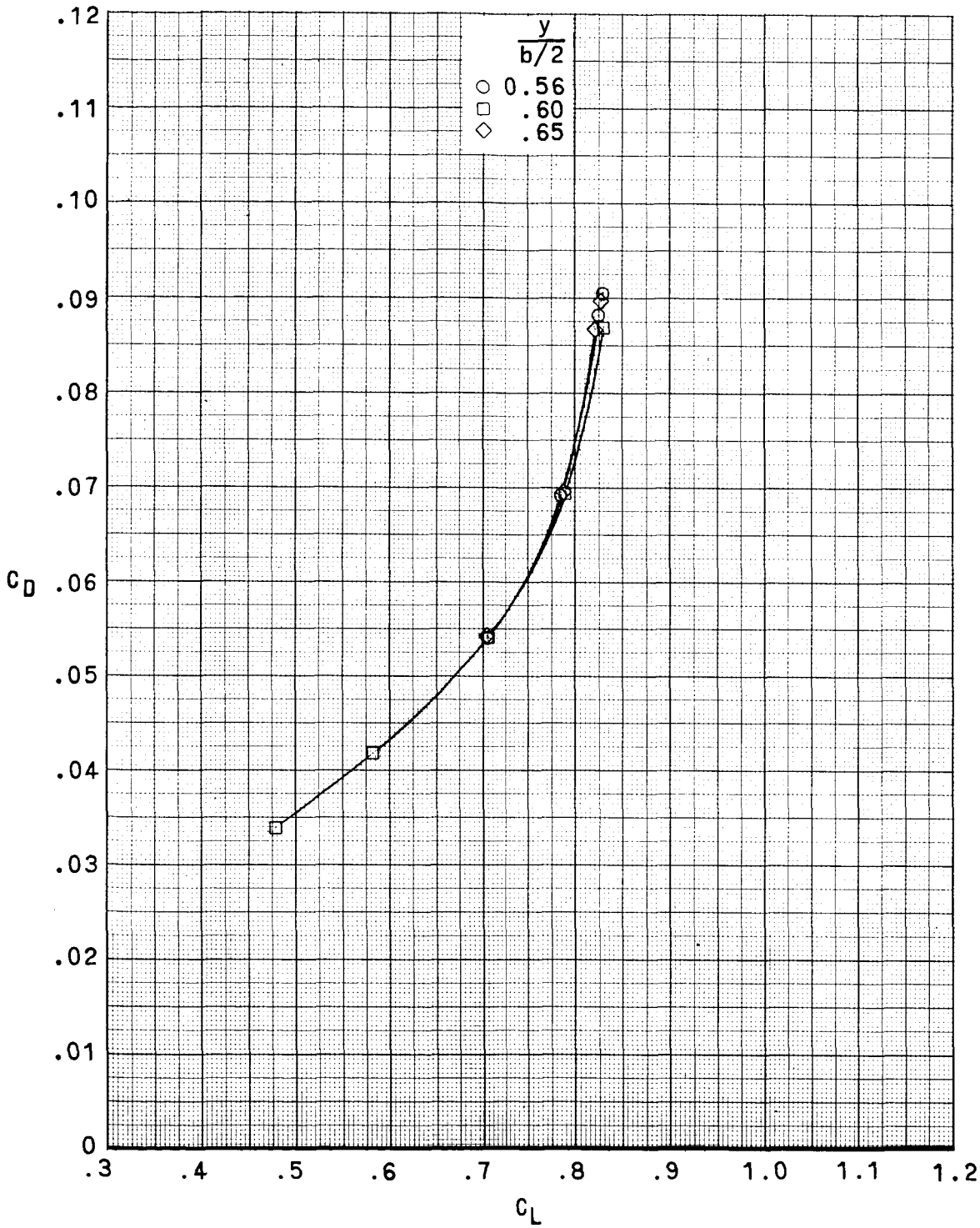


(b) M = 0.90. Concluded.

Figure 6.- Continued.

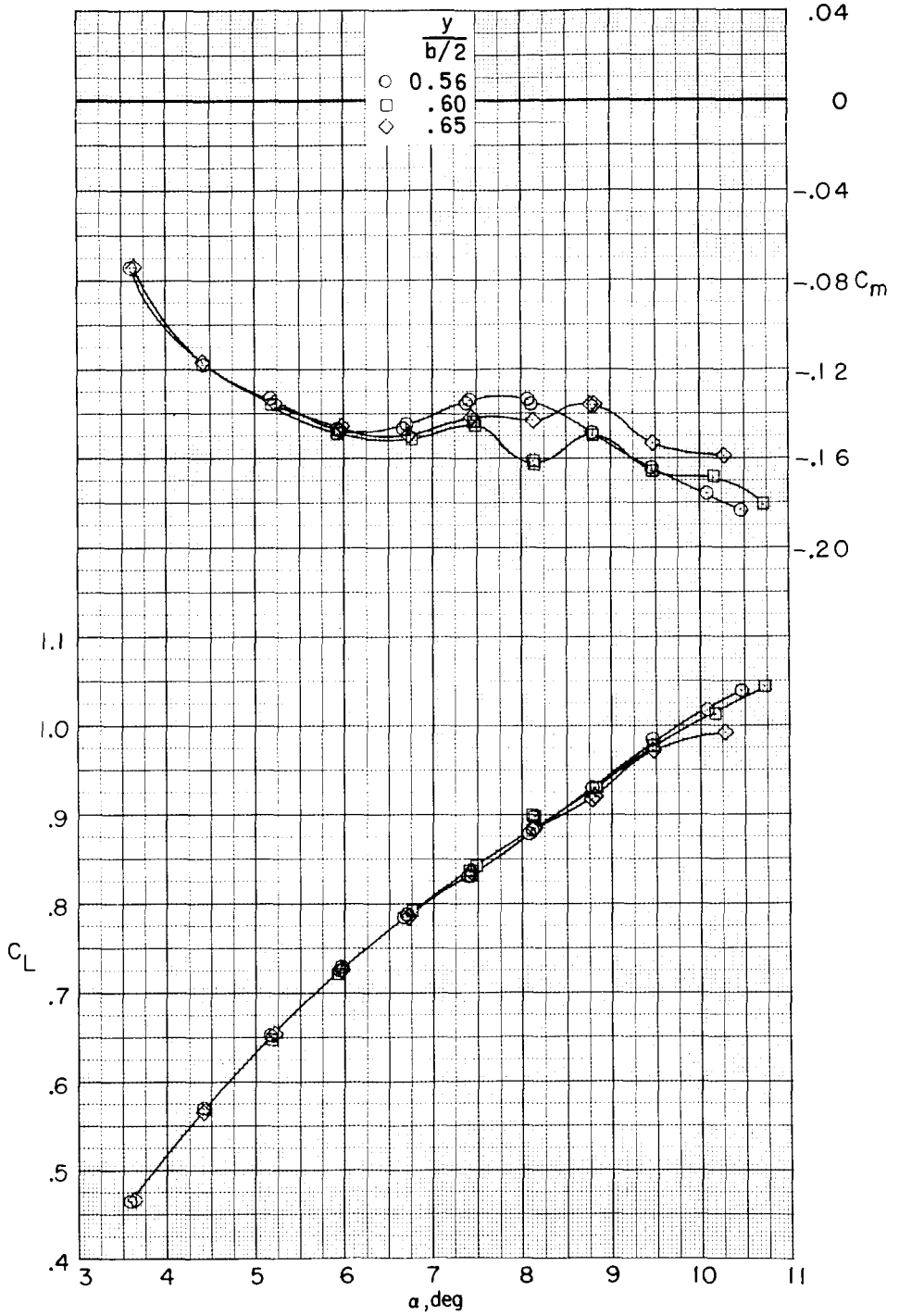


(c) M = 0.95.

Figure 6.- Continued.

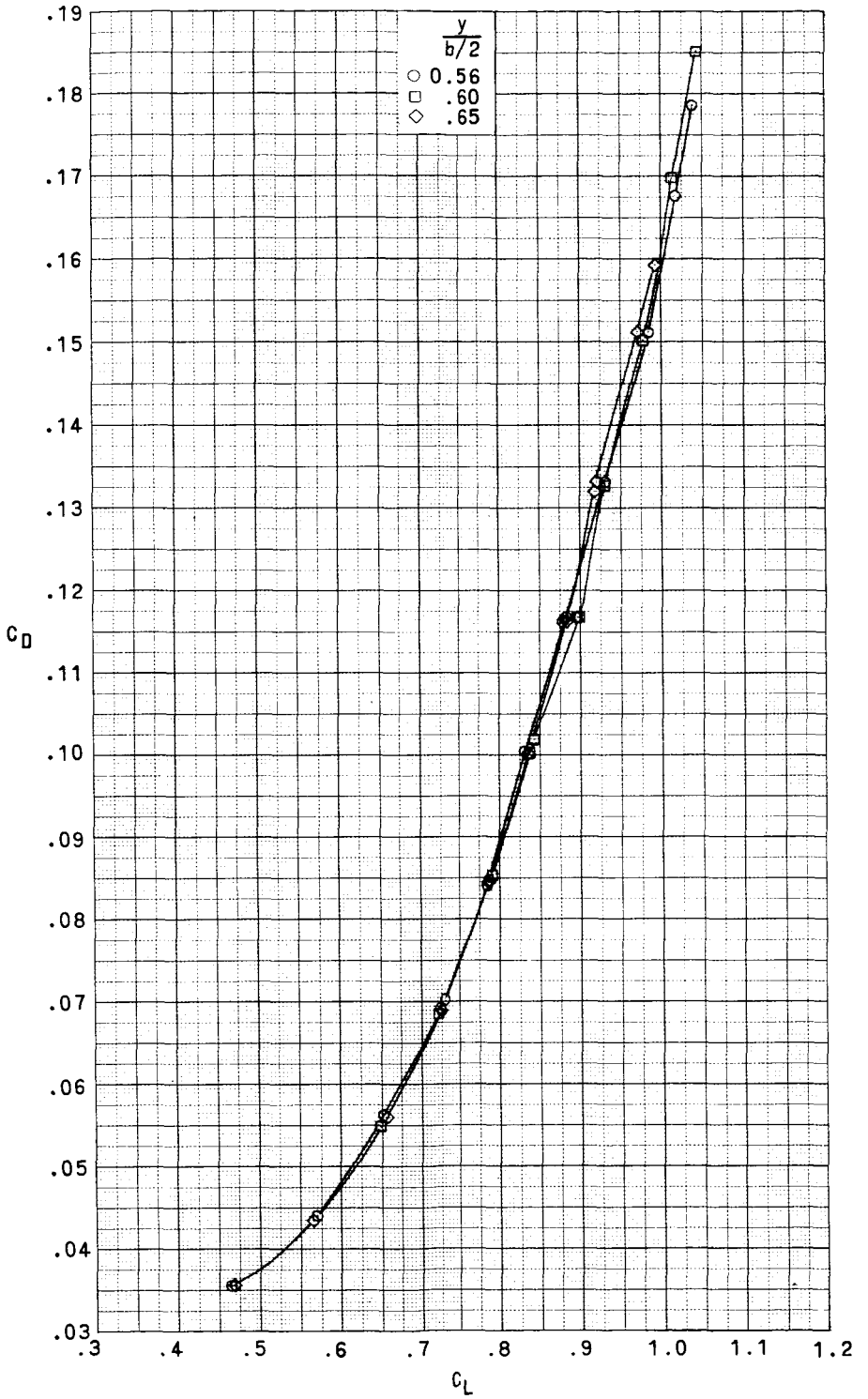


(c) M = 0.95. Concluded.

Figure 6.- Concluded.

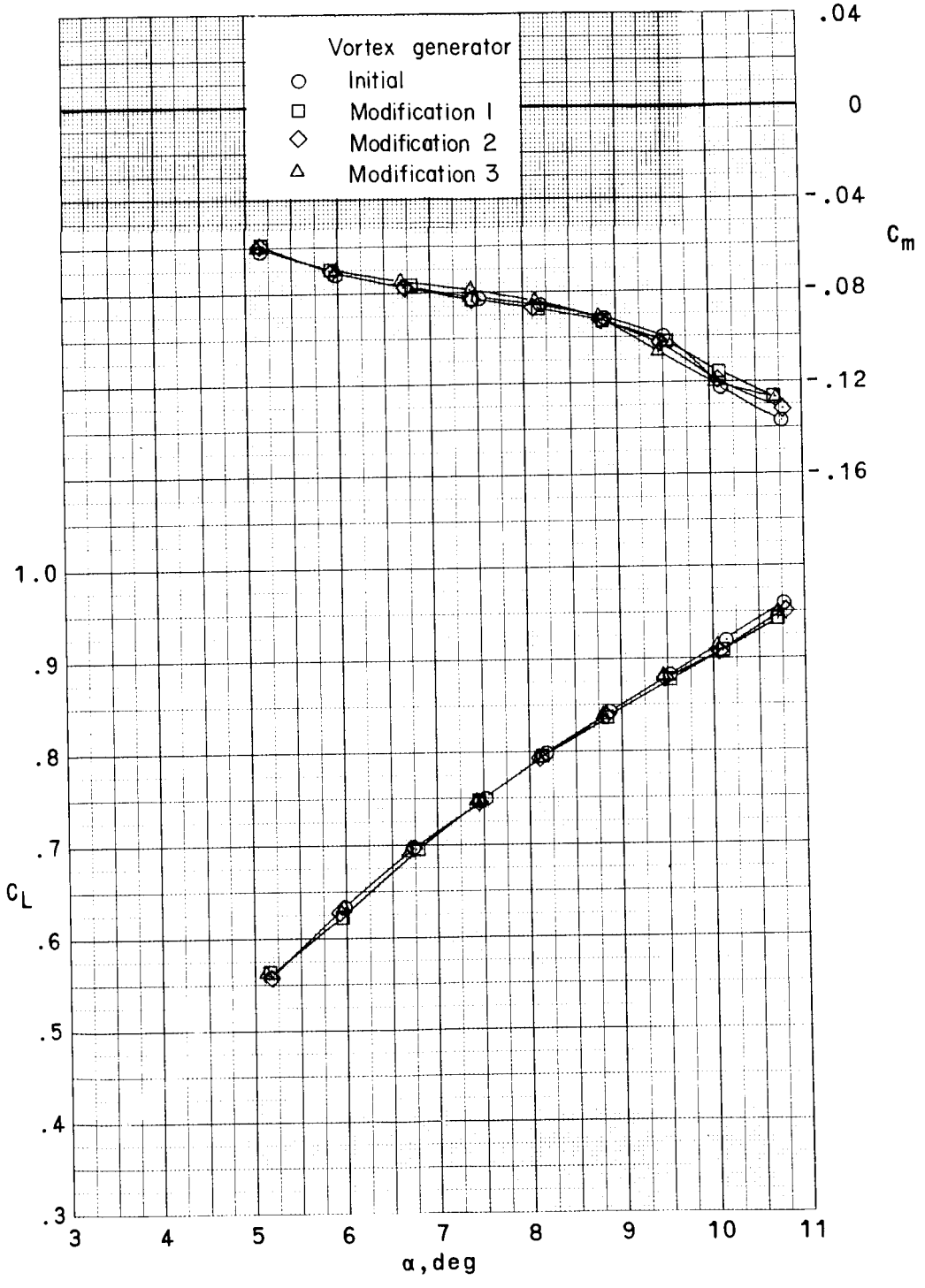


(a) M = 0.80.

Figure 7.- Effect of vortex-generator modifications 1, 2, and 3 on longitudinal aerodynamic characteristics. Steel wing.

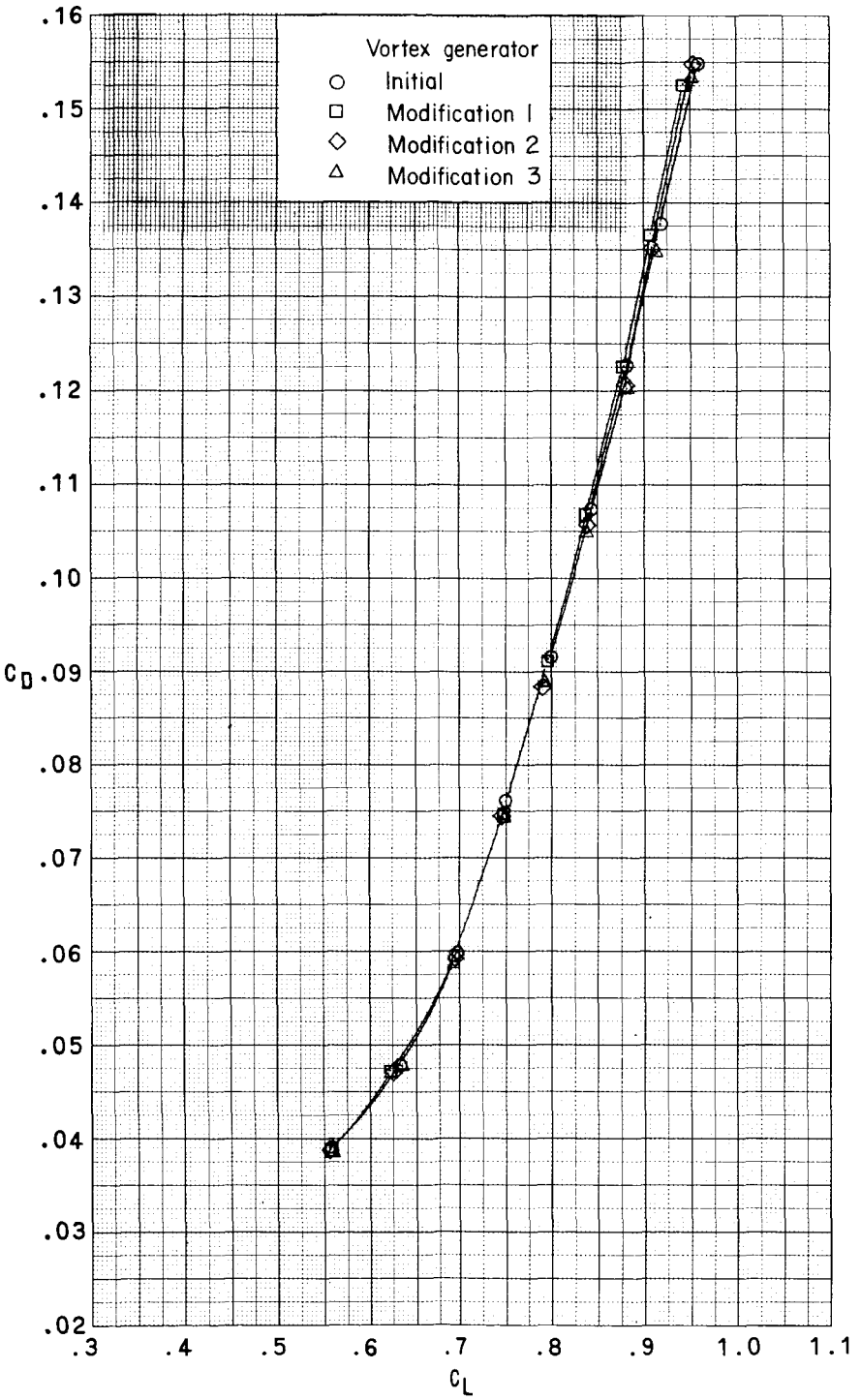


(a) M = 0.80. Concluded.

Figure 7.- Continued.

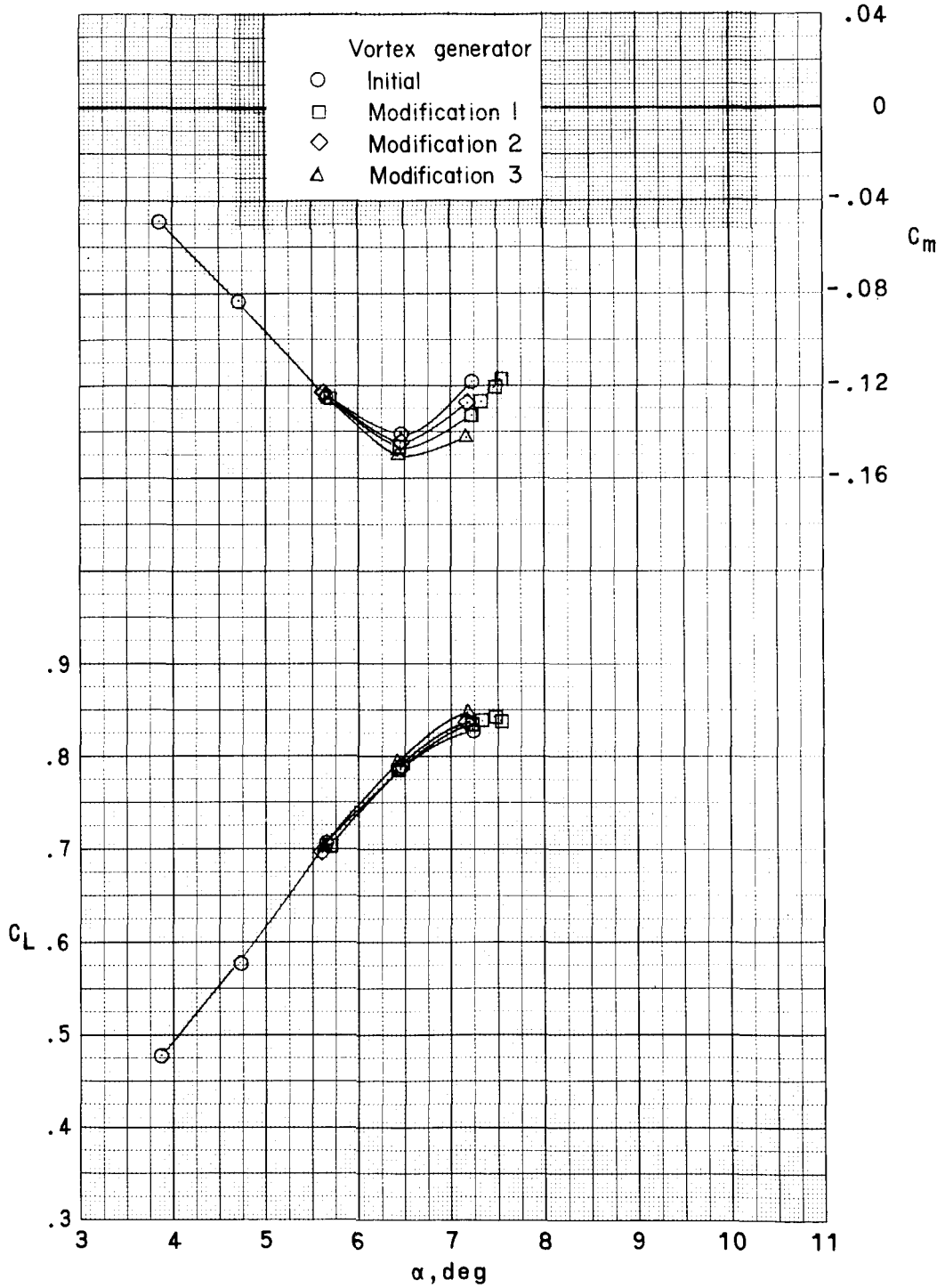


(b) M = 0.90.

Figure 7.- Continued.

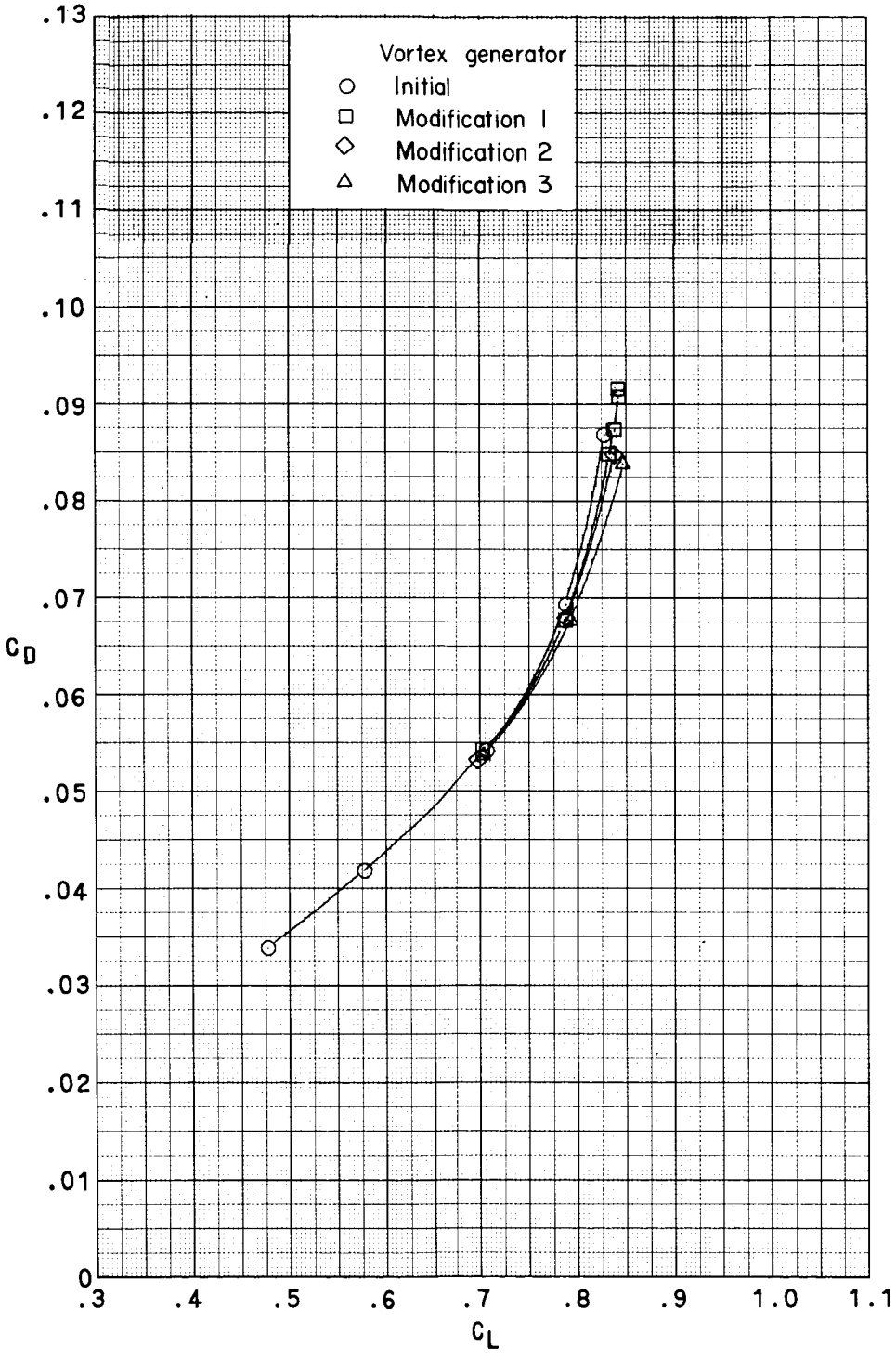


(b) M = 0.90. Concluded.

Figure 7.- Continued.

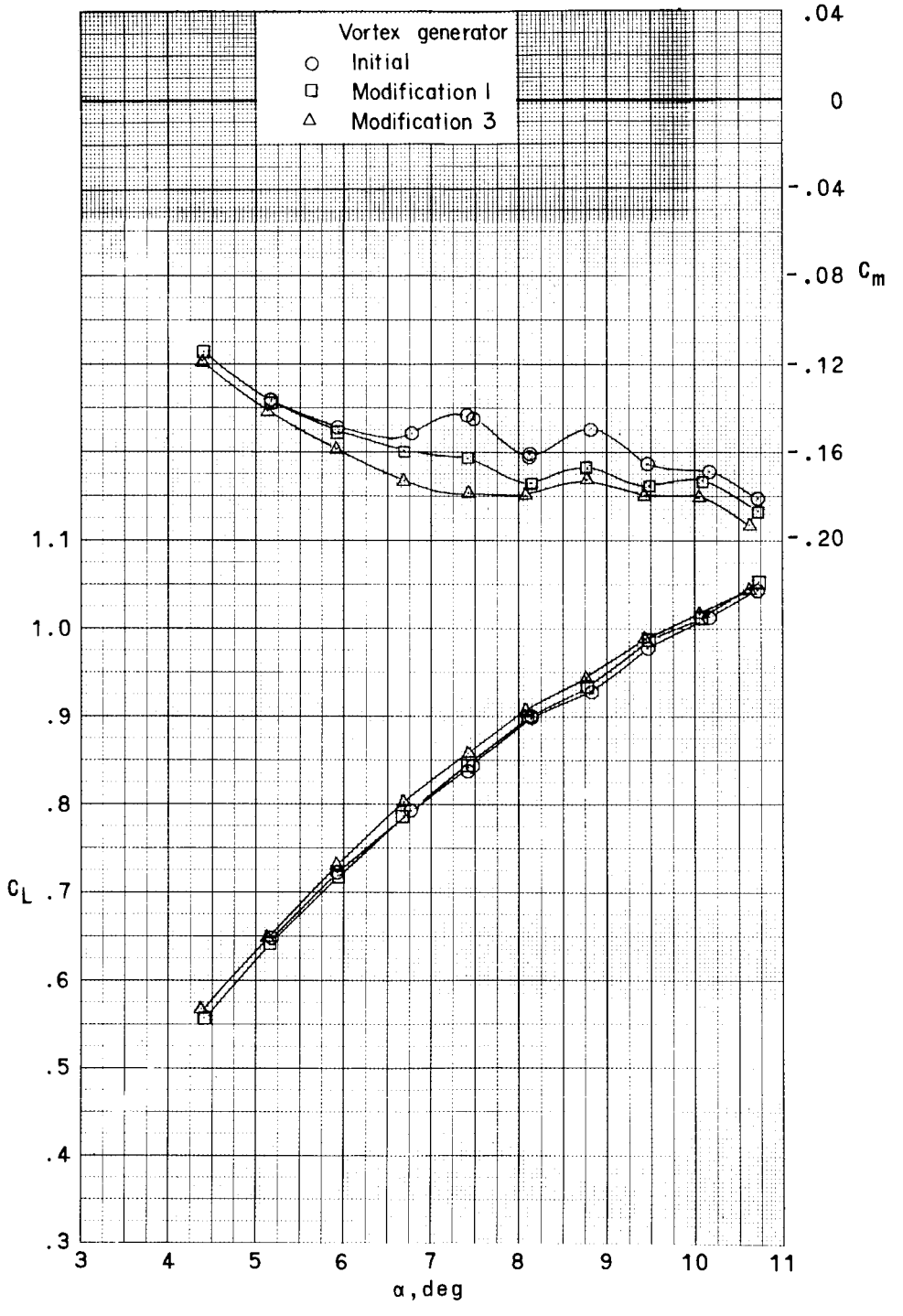


(c) M = 0.95.

Figure 7.- Continued.

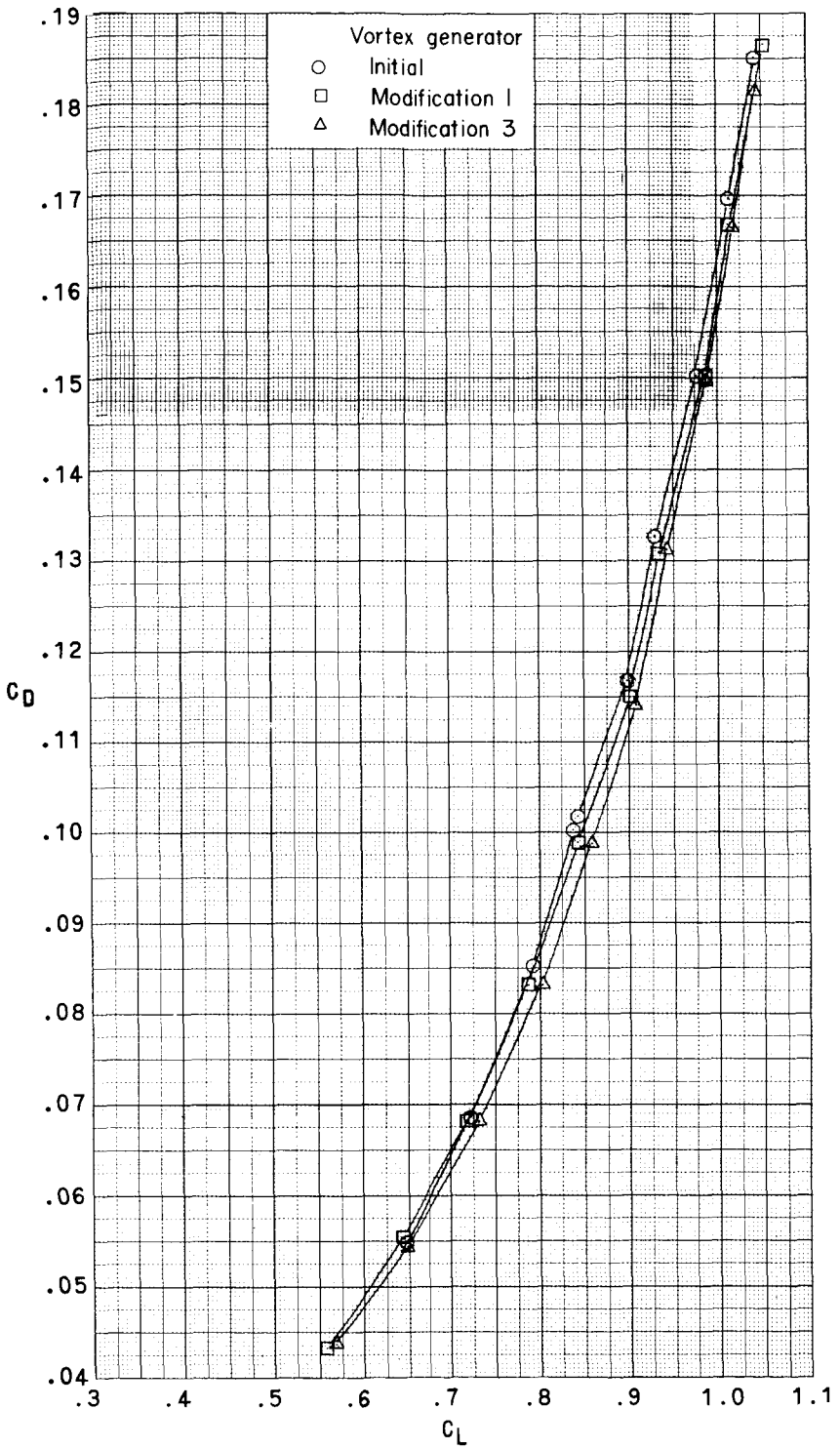


(c) M = 0.95. Concluded.

Figure 7.- Continued.

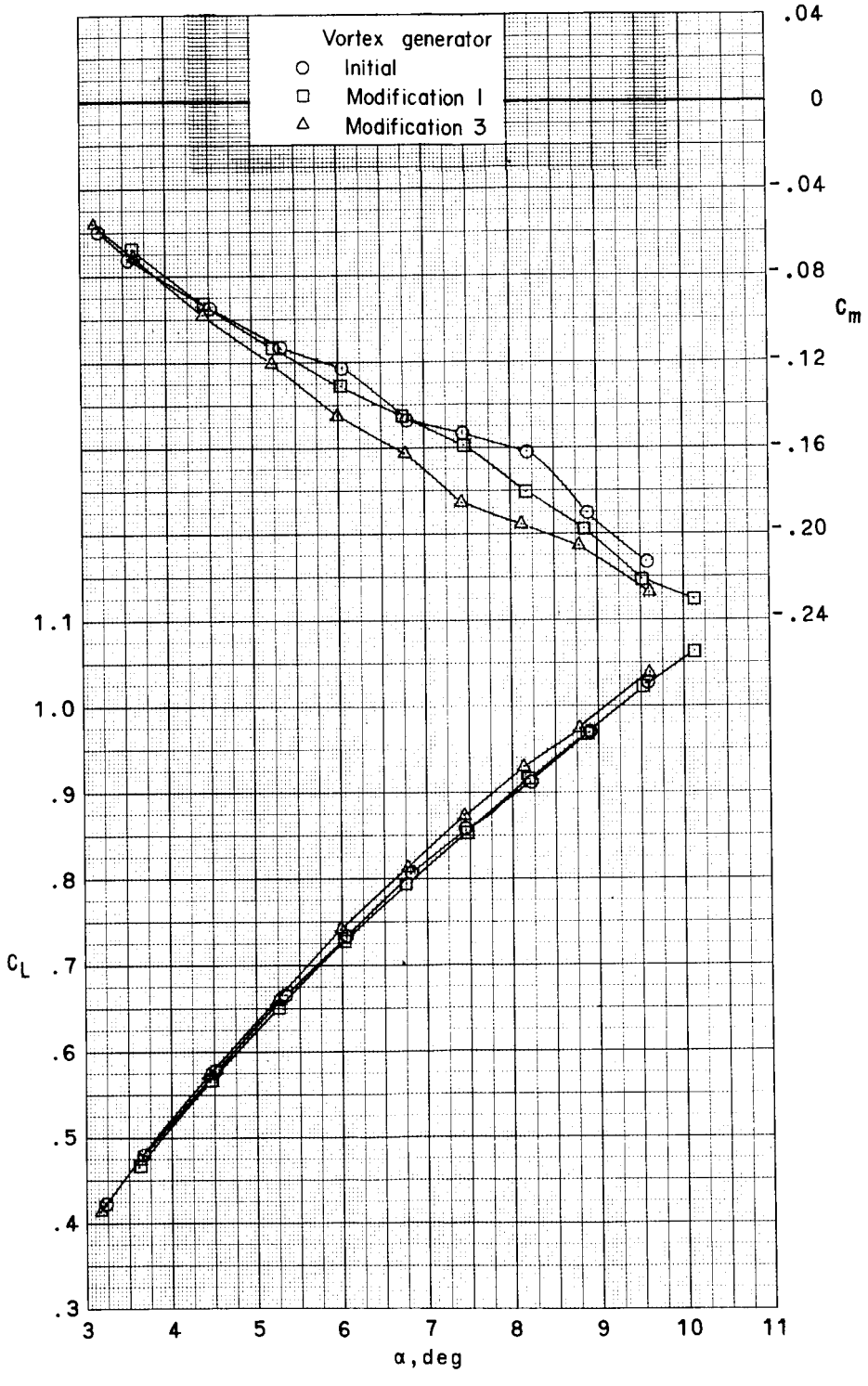


(d) M = 0.99.

Figure 7.- Continued.

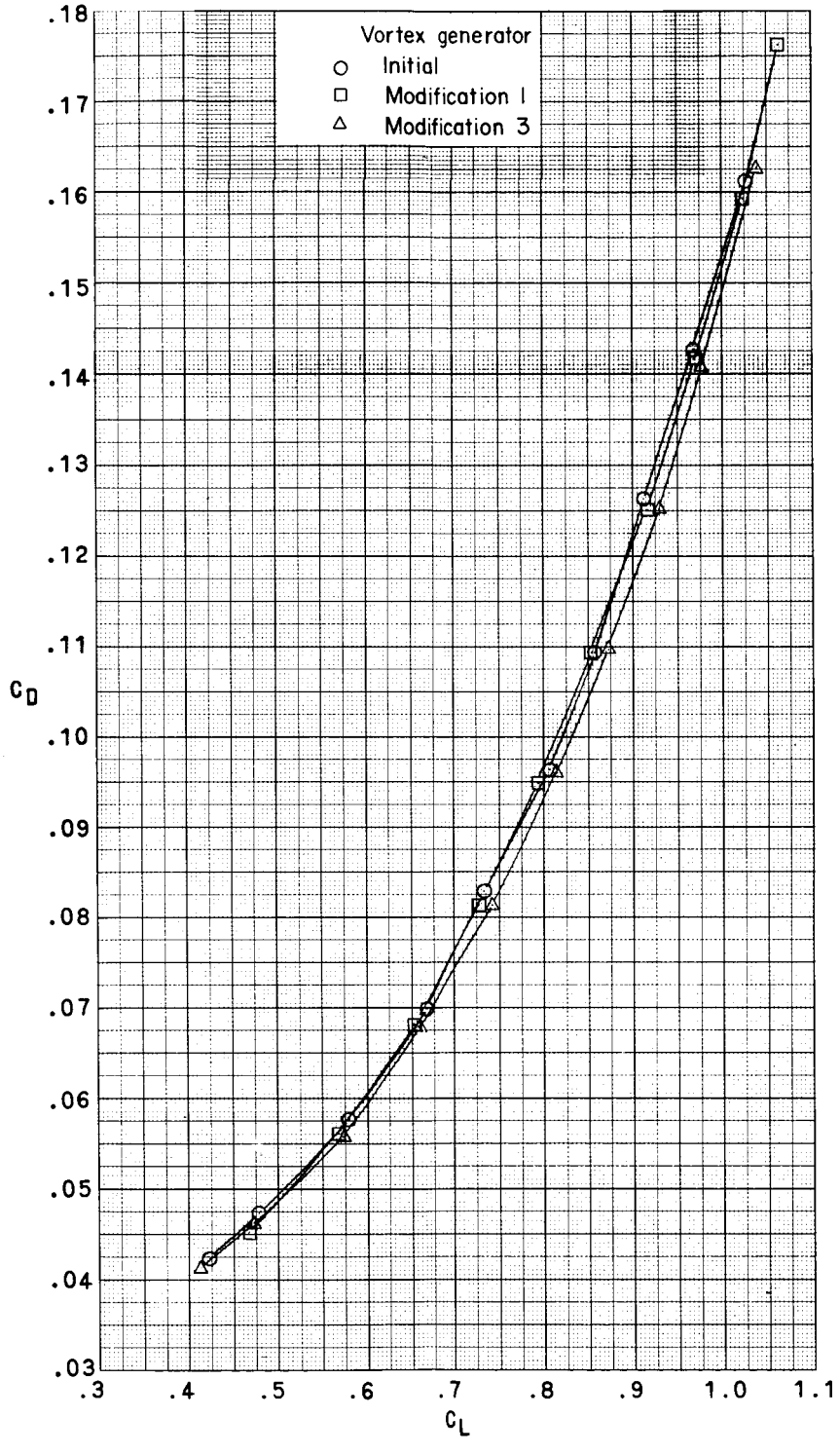


(d) M = 0.99. Concluded.

Figure 7.- Concluded.

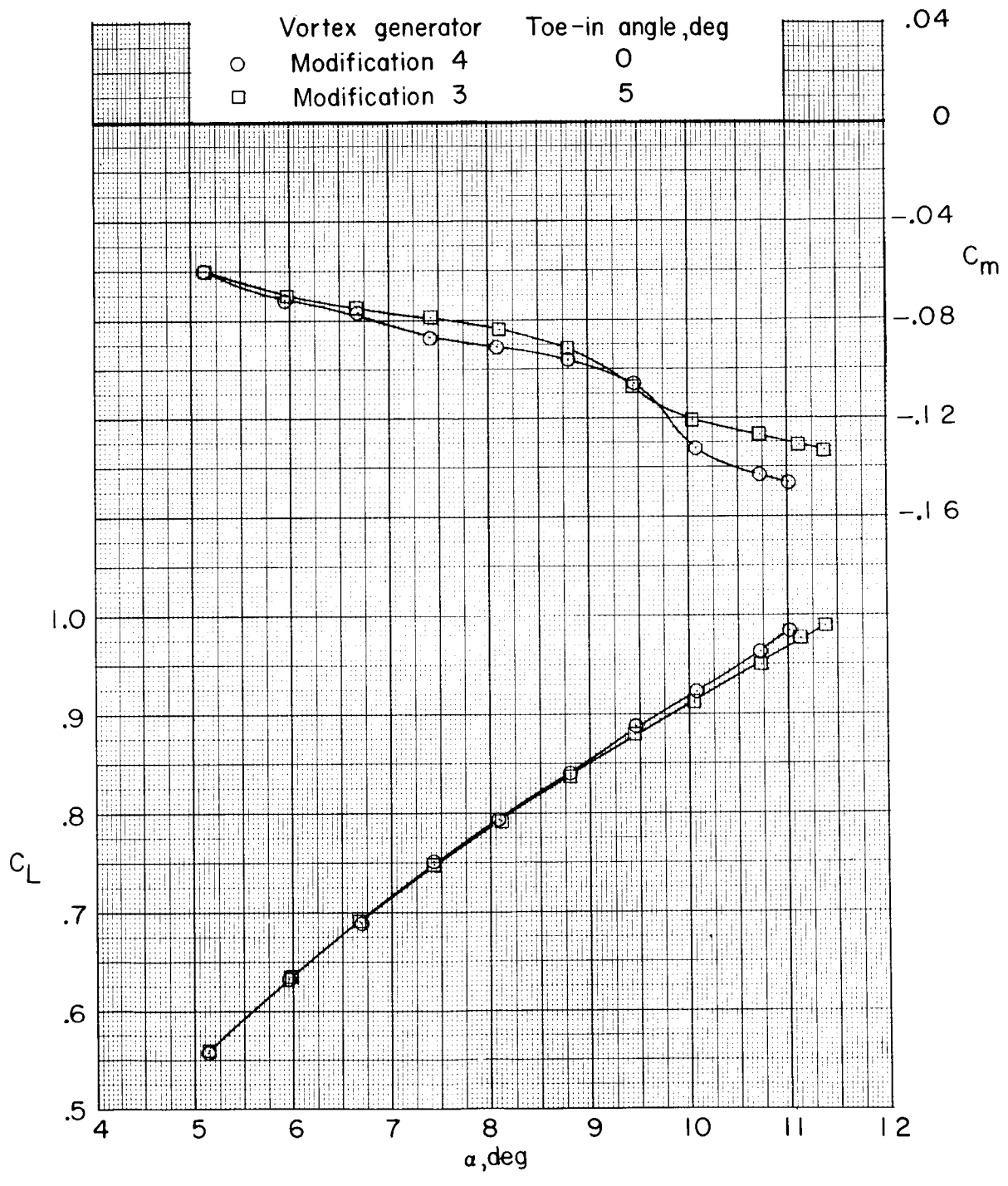


(a) M = 0.80.

Figure 8.- Effect of vortex-generator toe-in angle on longitudinal aerodynamic characteristics. Steel wing.

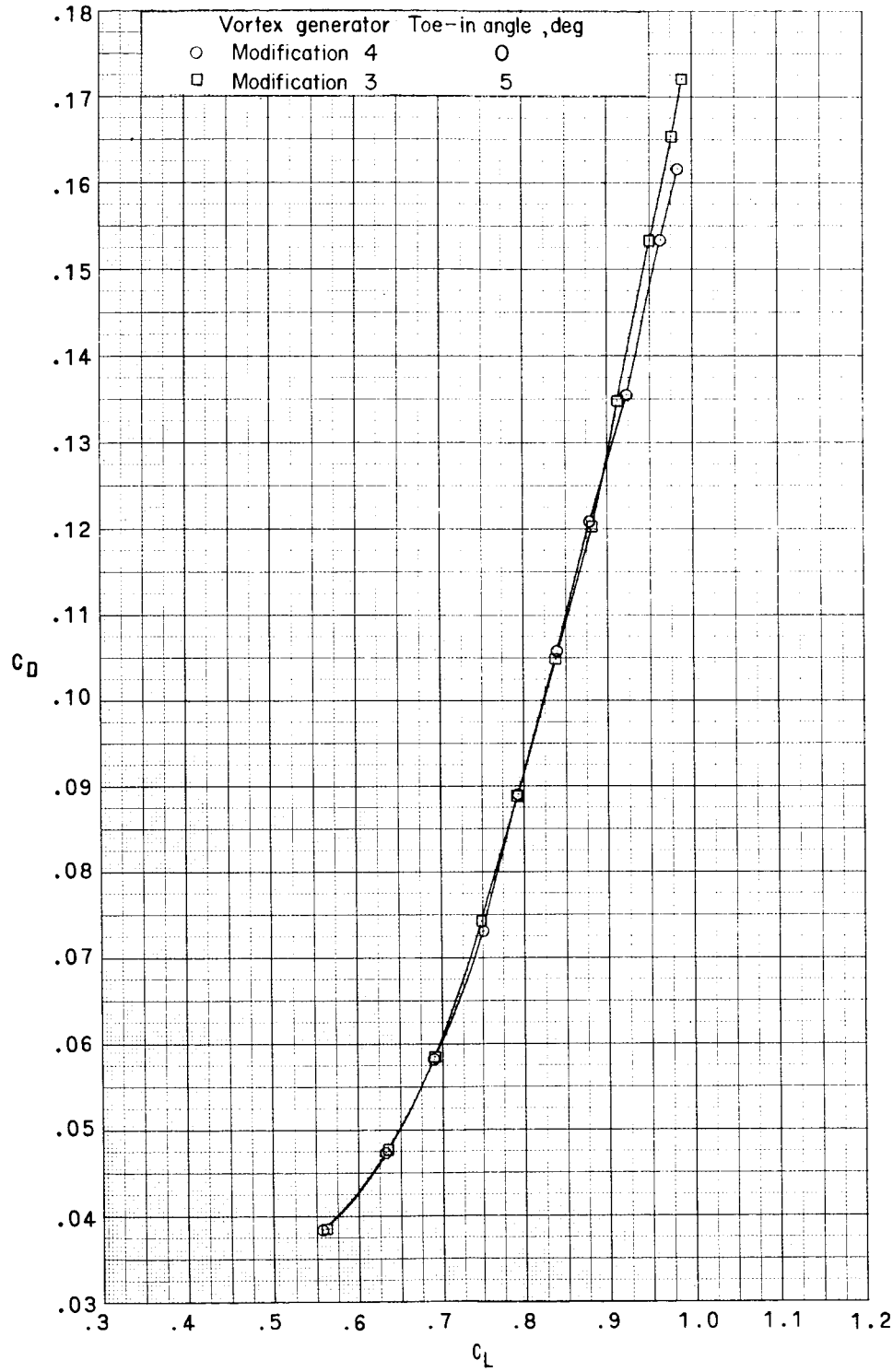


(a) M = 0.80. Concluded.

Figure 8.- Continued.

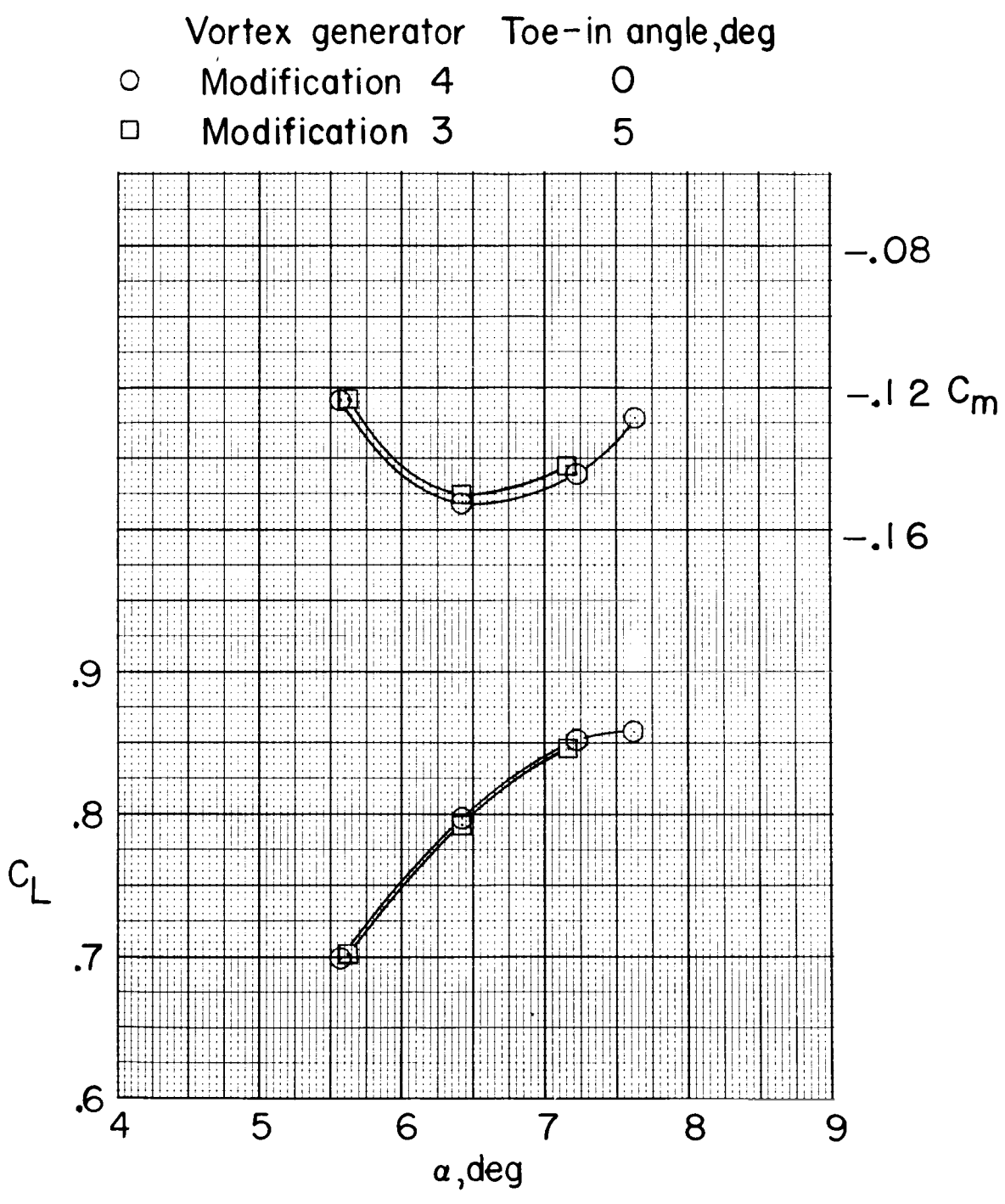


(b) M = 0.90.

Figure 8.- Continued.

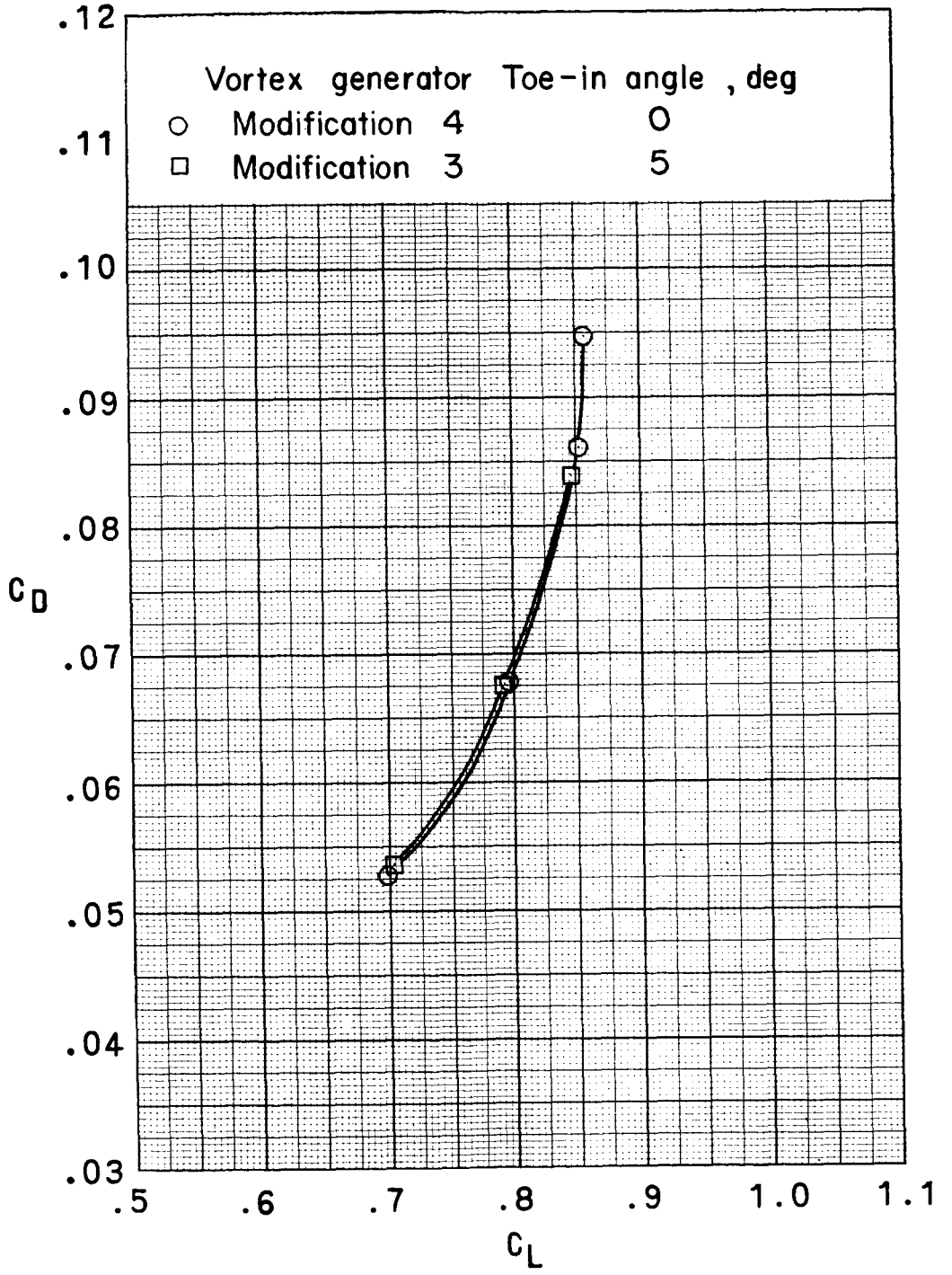


(b) M = 0.90. Concluded.

Figure 8.- Continued.

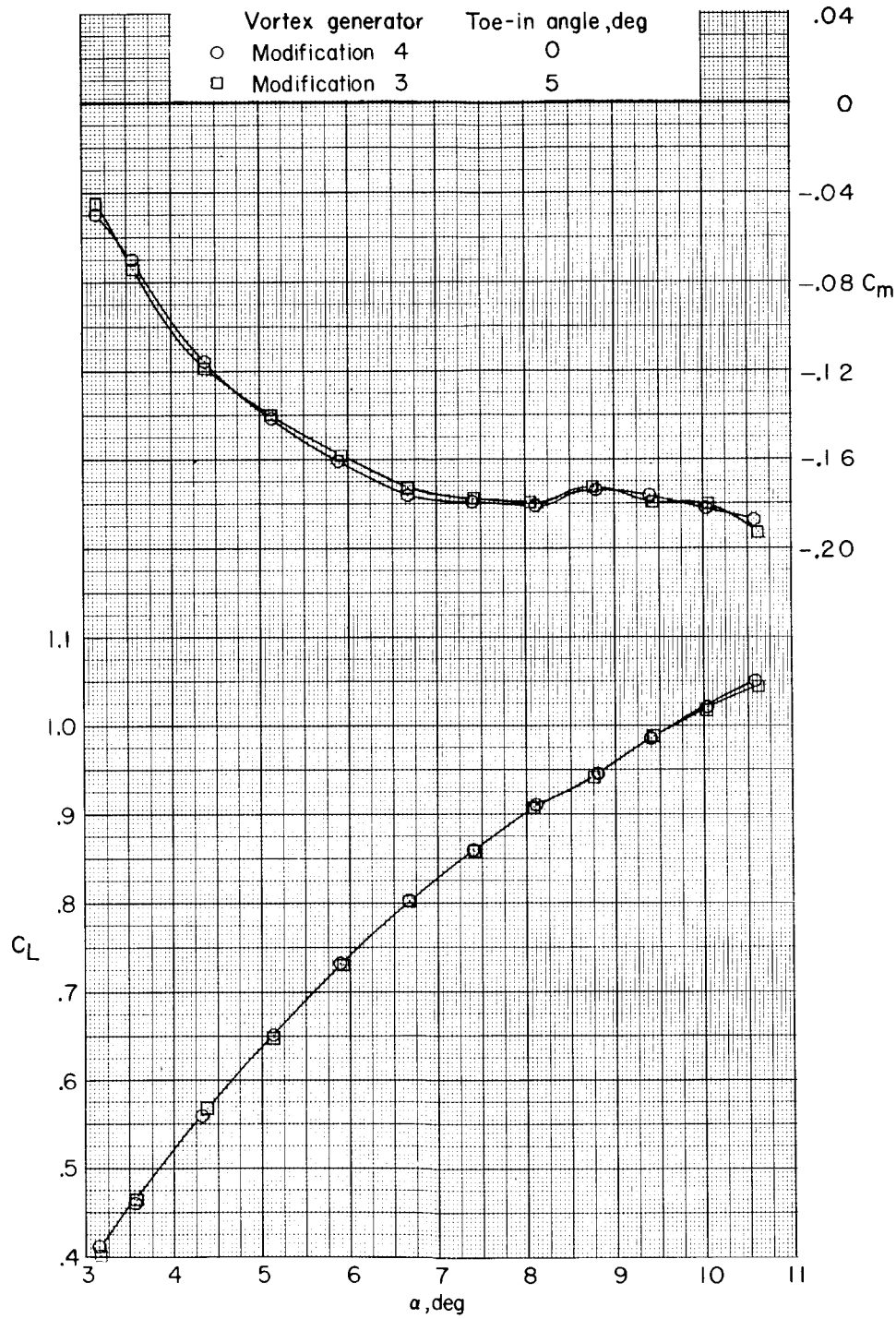


(c) M = 0.95.

Figure 8.- Continued.

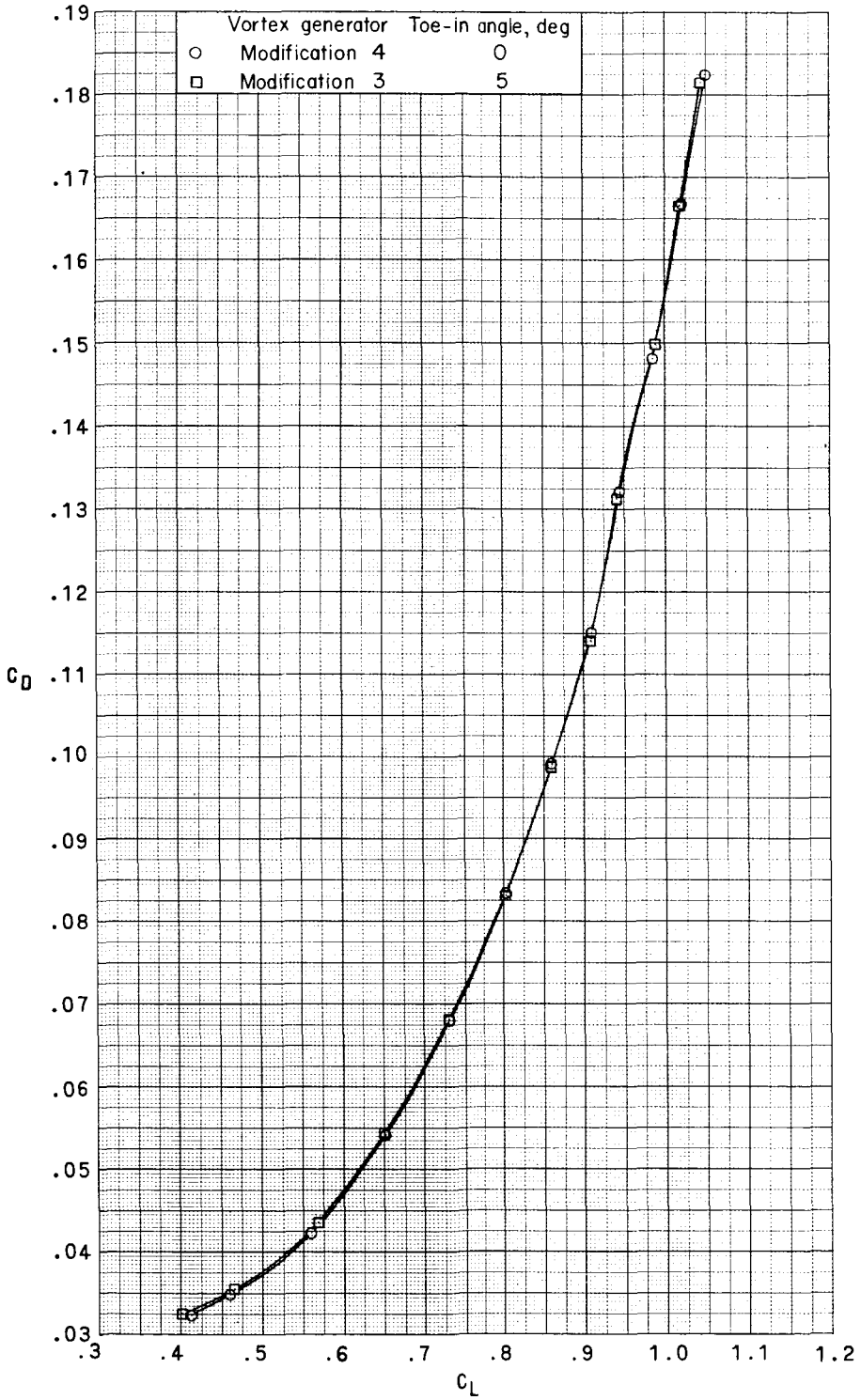


(c) M = 0.95. Concluded.

Figure 8.- Continued.

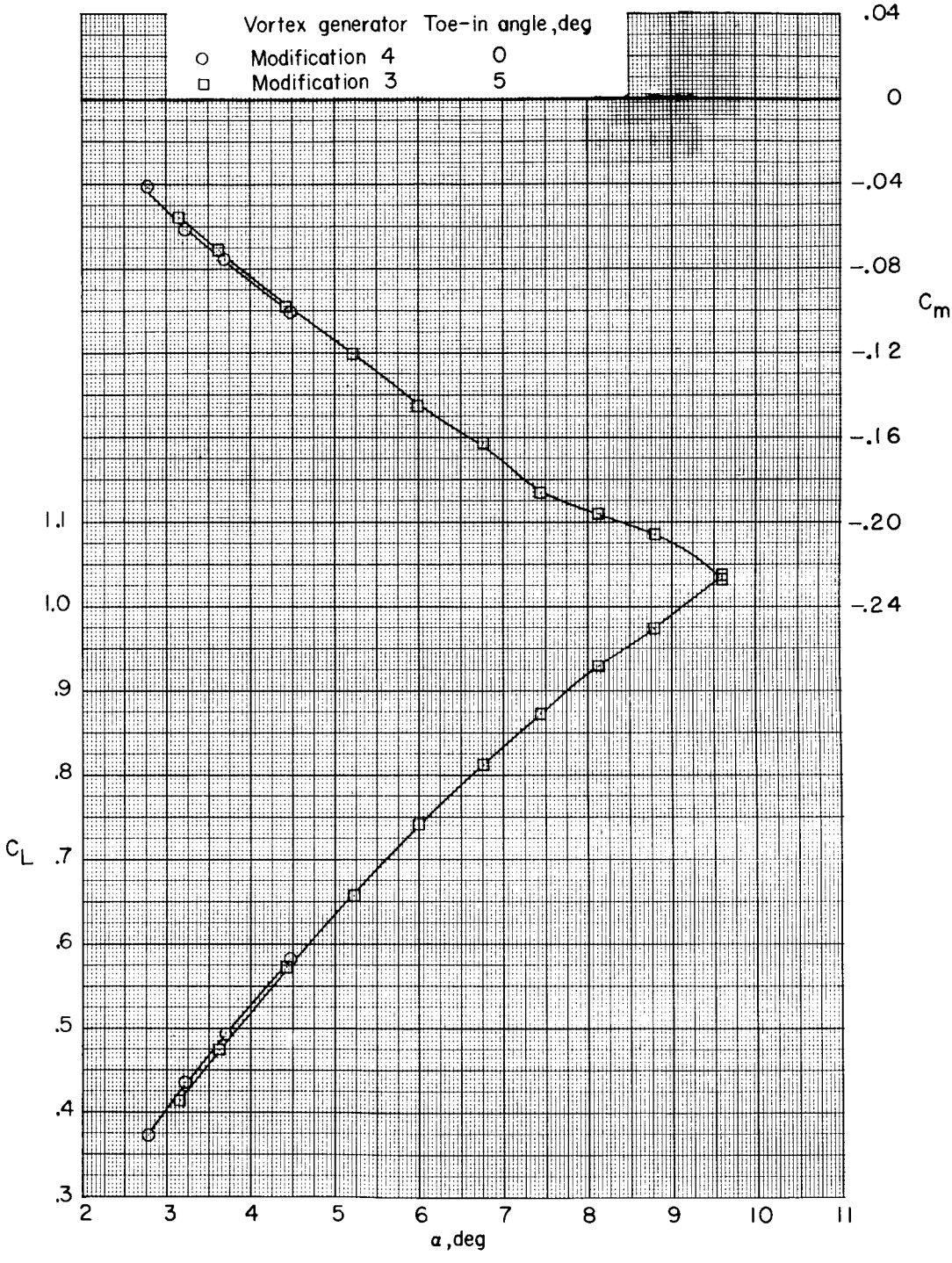


(d) M = 0.99.

Figure 8.- Continued.

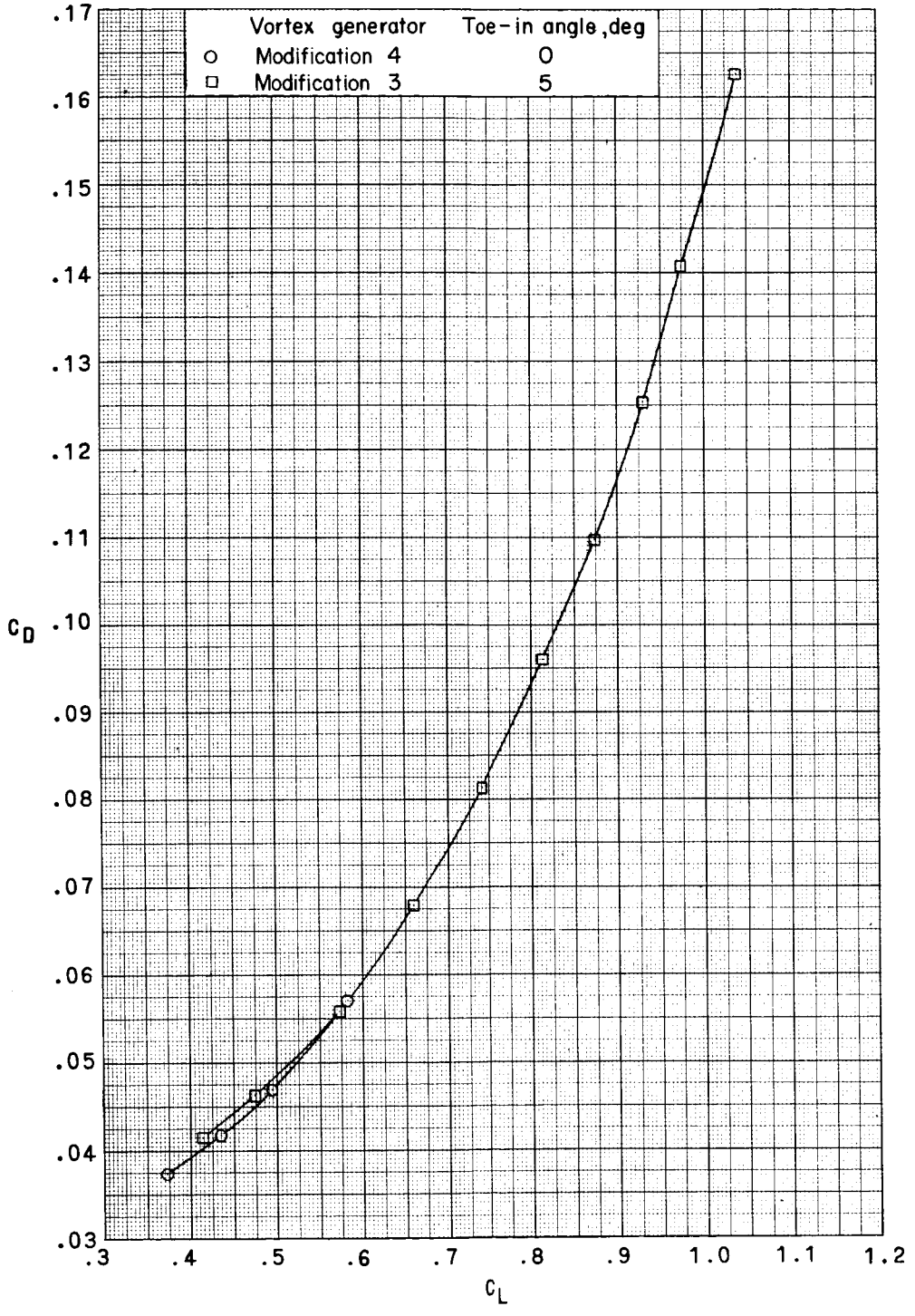


(d) M = 0.99. Concluded.

Figure 8.- Concluded.

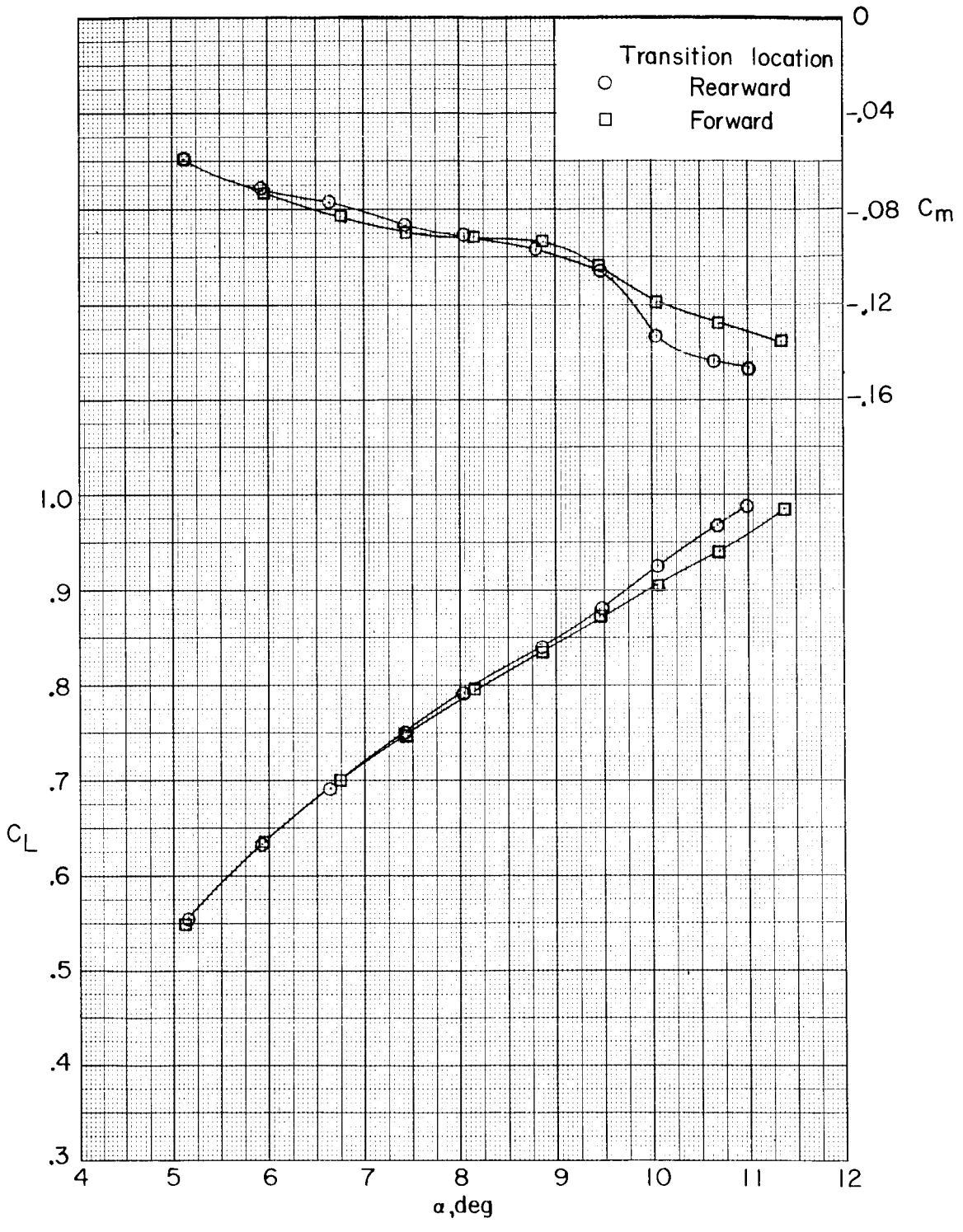


(a) M = 0.80.

Figure 9.- Effect of wing upper-surface boundary-layer-trip location on longitudinal aerodynamic characteristics at Mach numbers of 0.80 and 0.90. Steel wing; vortex-generator modification 4.

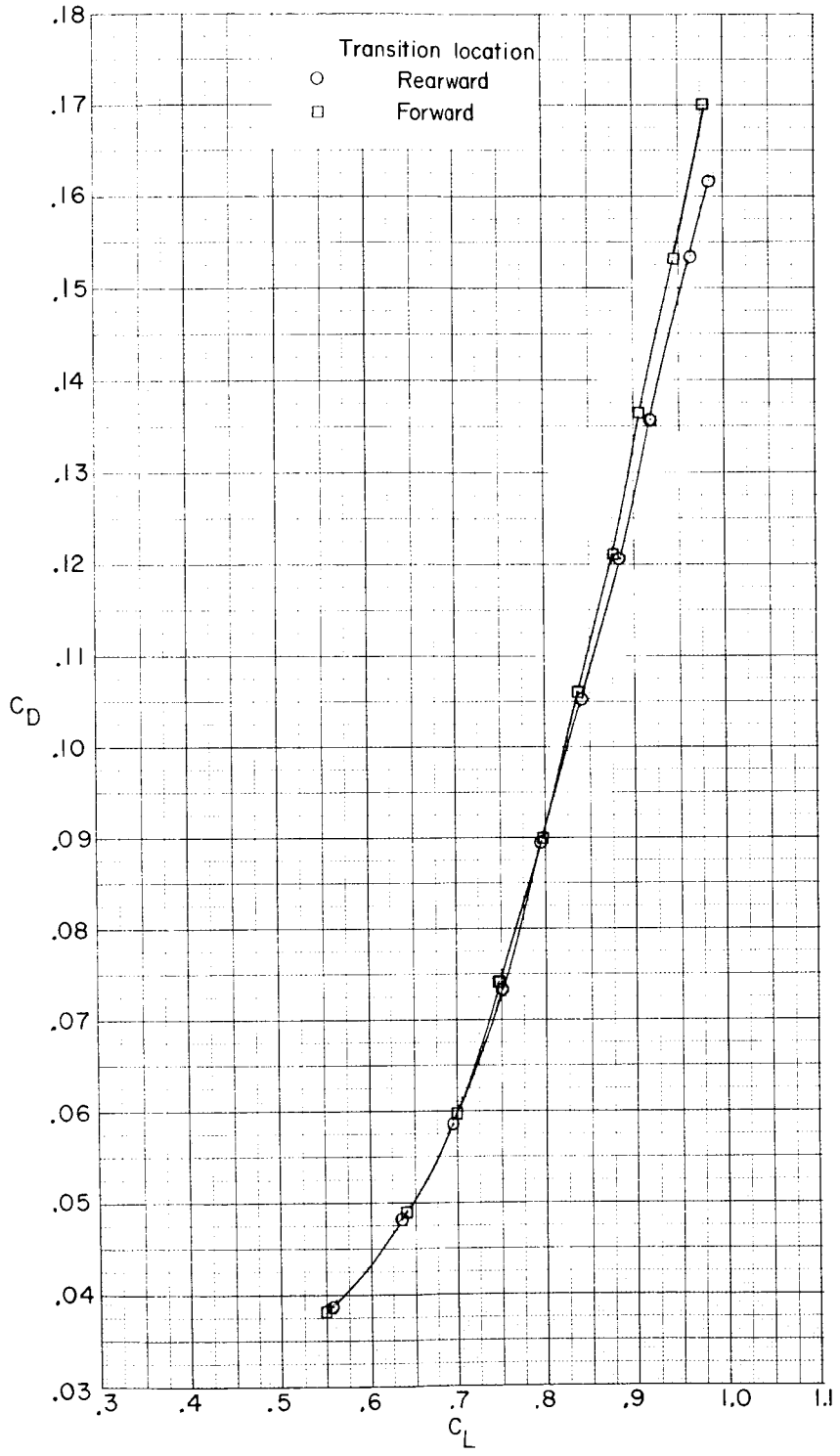


(a) M = 0.80. Concluded.

Figure 9.- Continued.

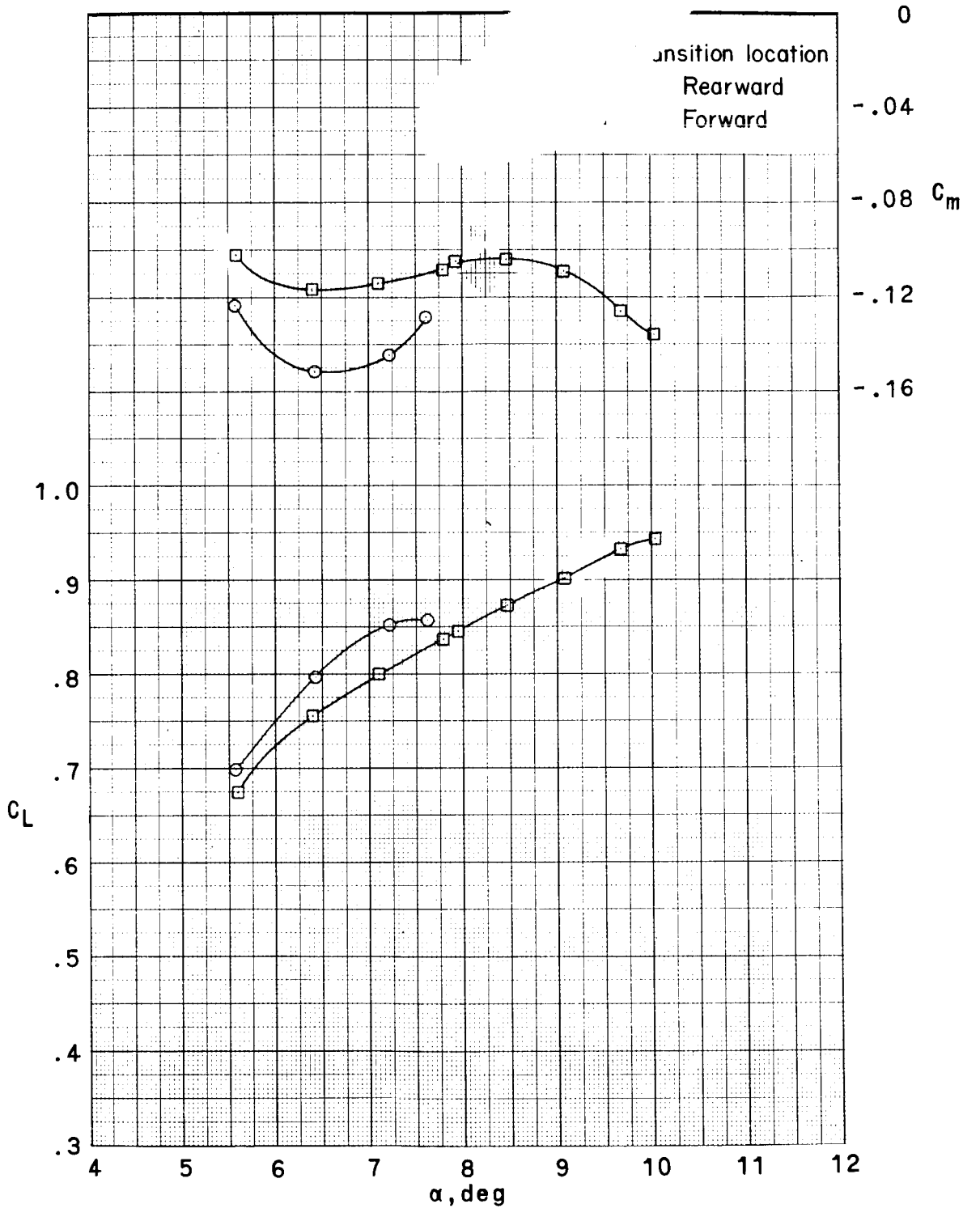


(b) M = 0.90.

Figure 9.- Continued.

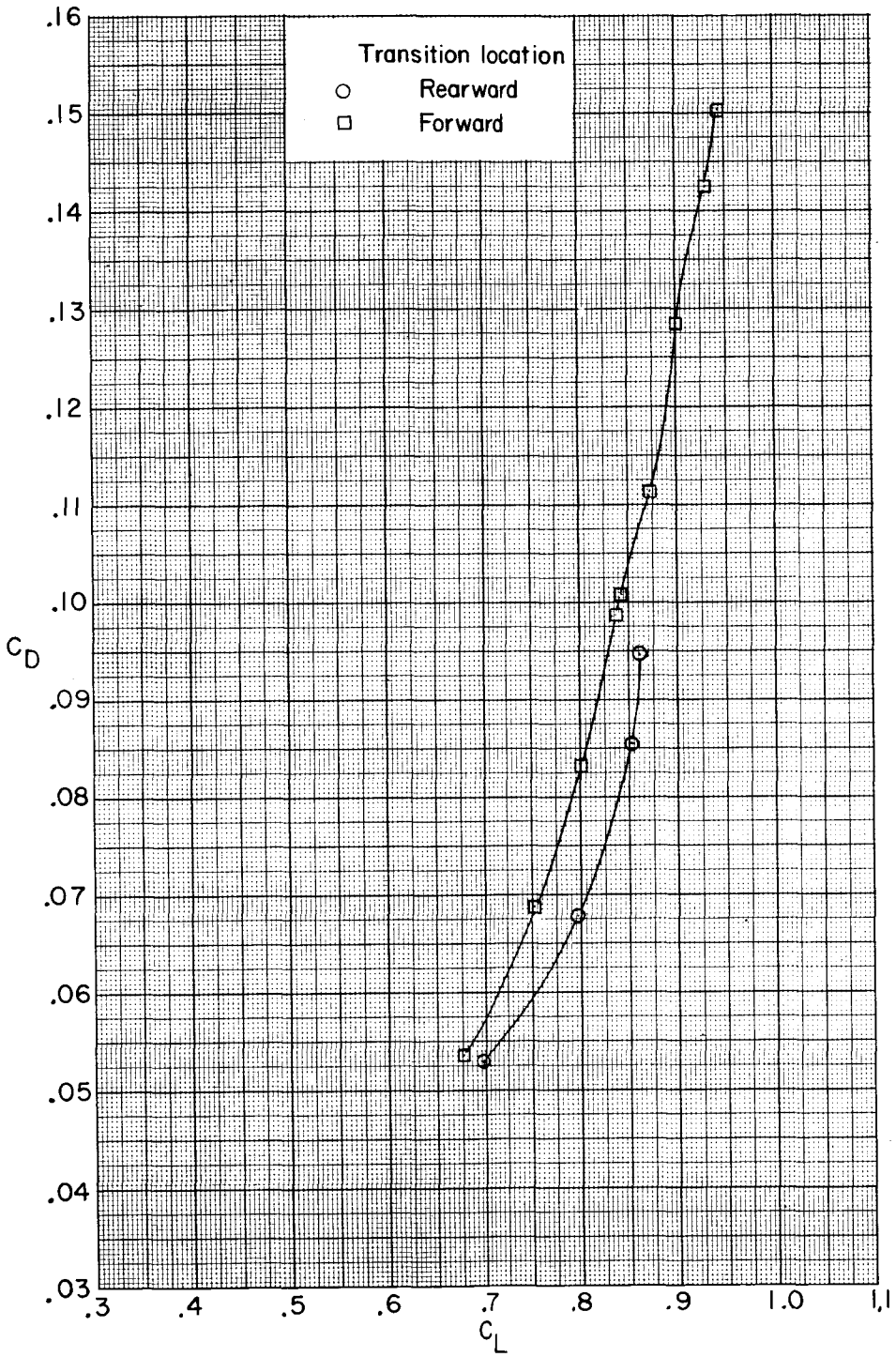


(b) M = 0.90. Concluded.

Figure 9.- Concluded.

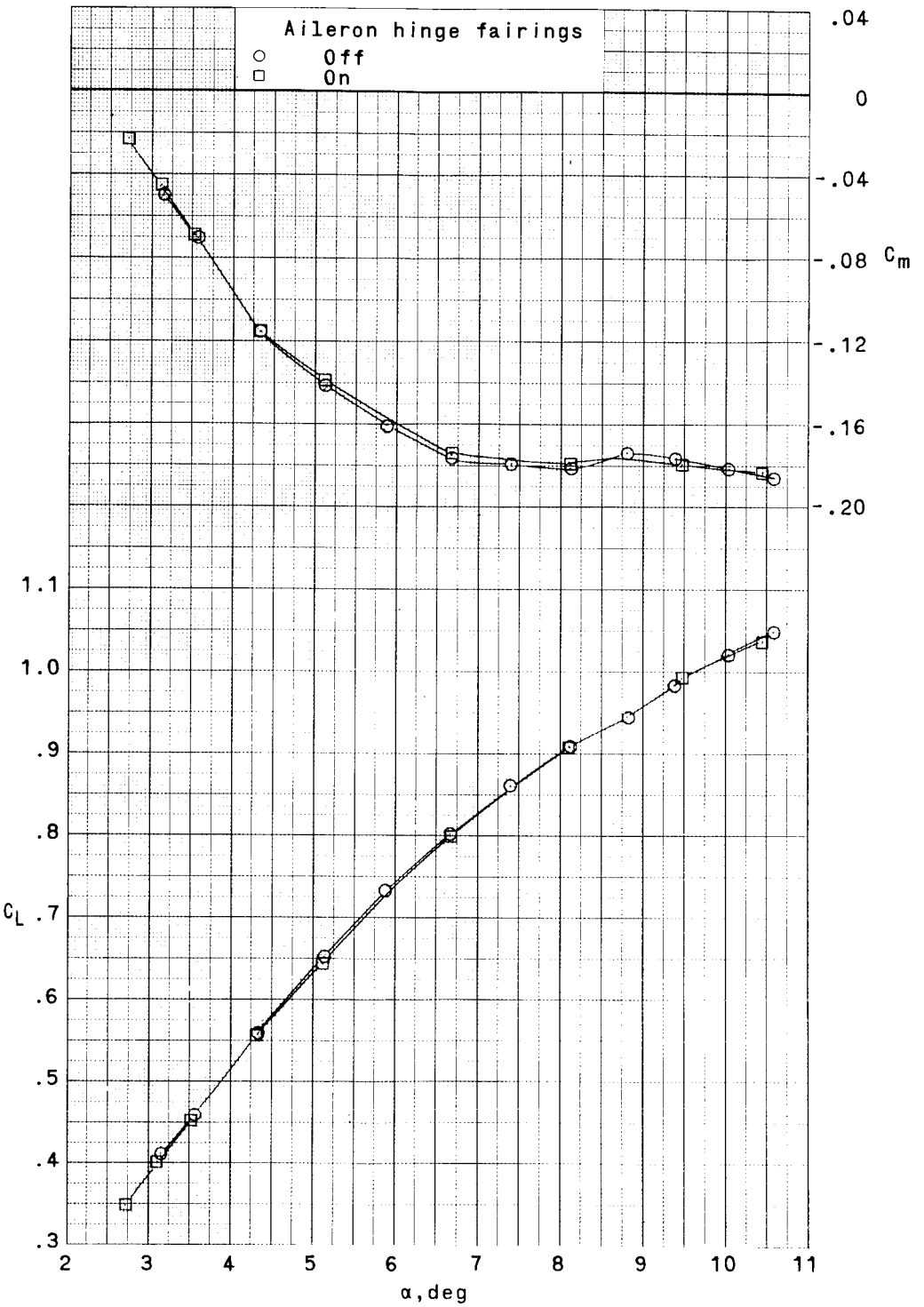


(a) M = 0.95.

Figure 10.- Effect of aileron hinge fairings on longitudinal aerodynamic characteristics at Mach numbers of 0.95 and 0.99. Steel wing; vortex-generator modification 4.

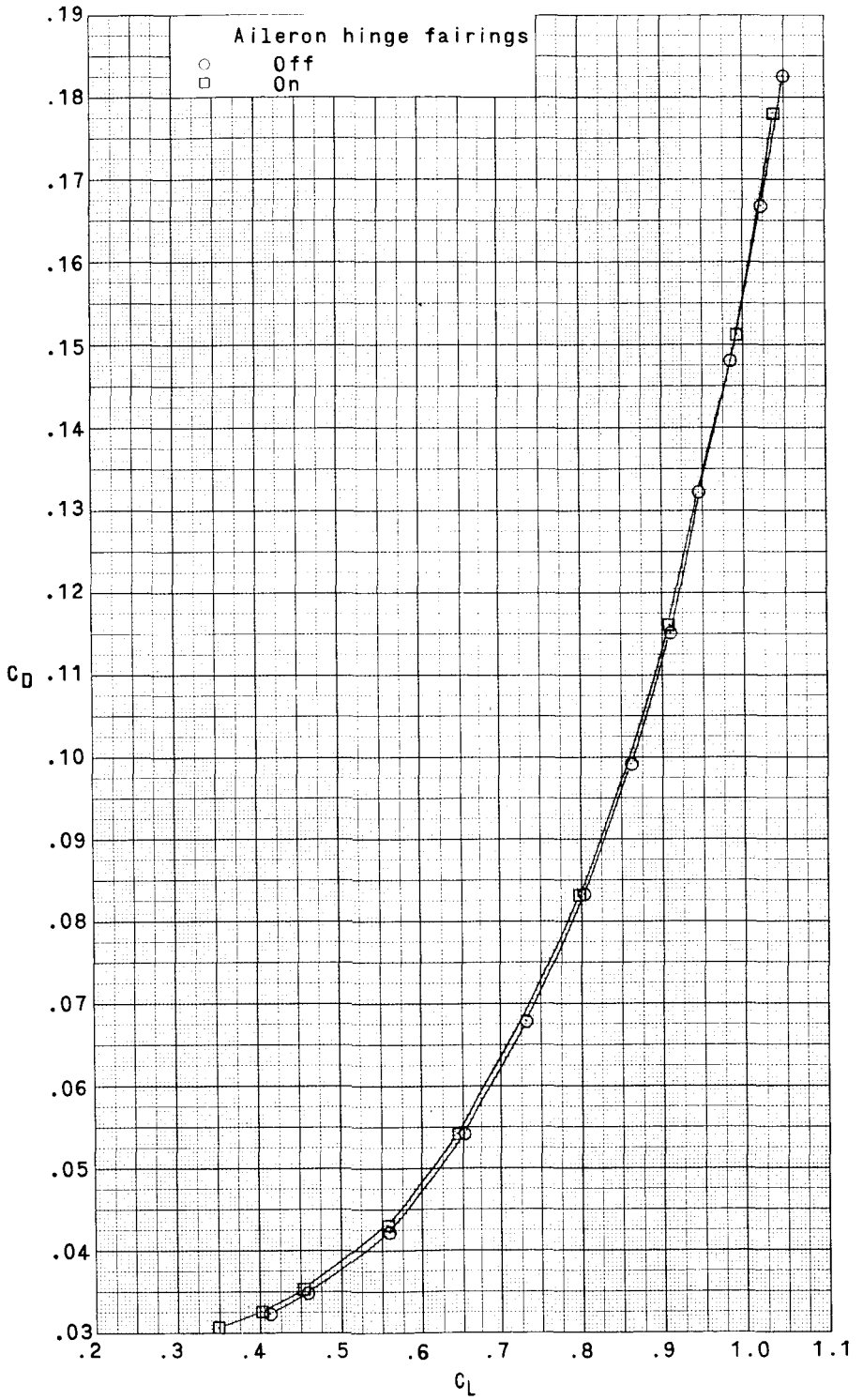


(a) M = 0.95. Concluded.

Figure 10.- Continued.

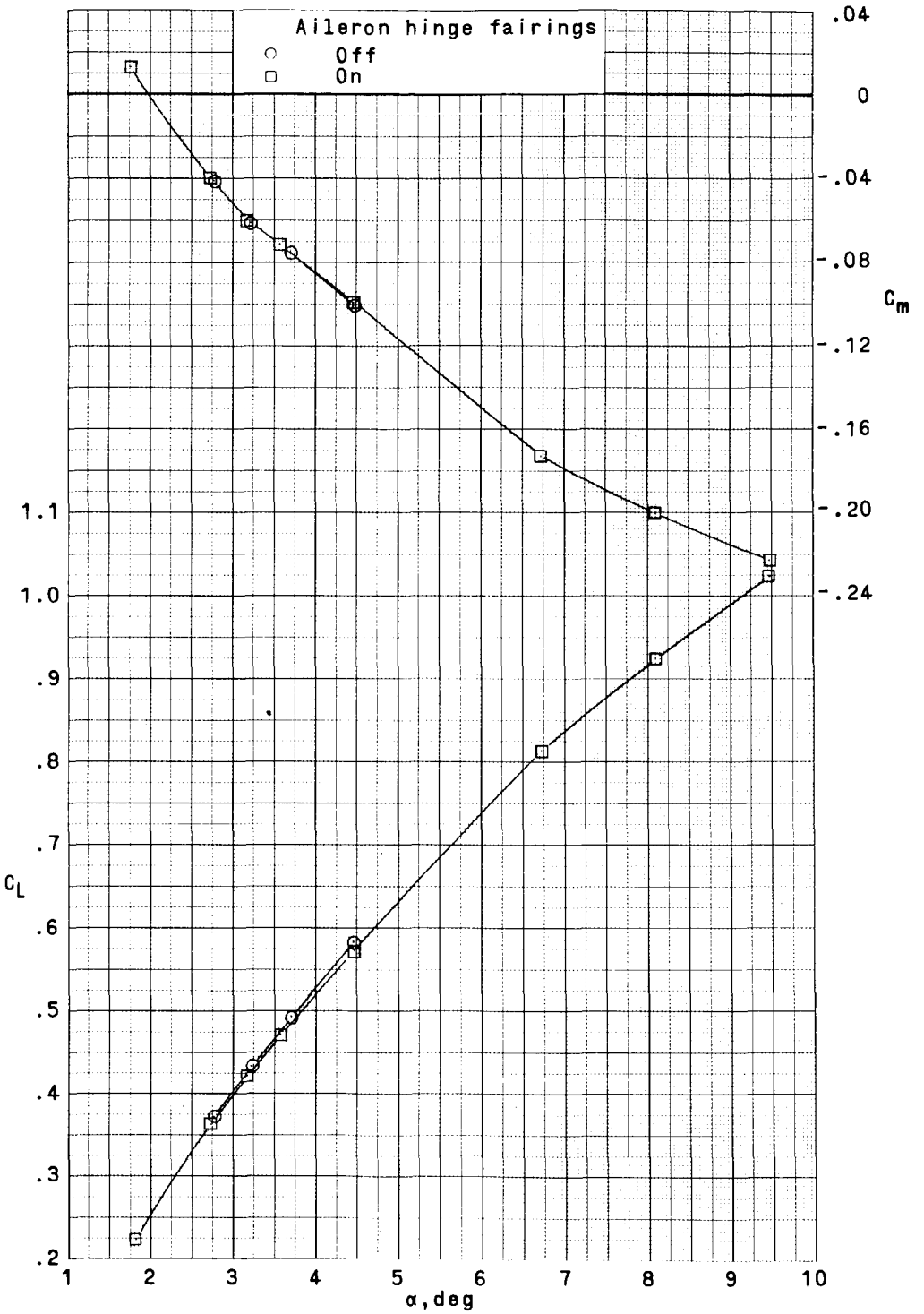


(b) M = 0.99.

Figure 10. - Continued.

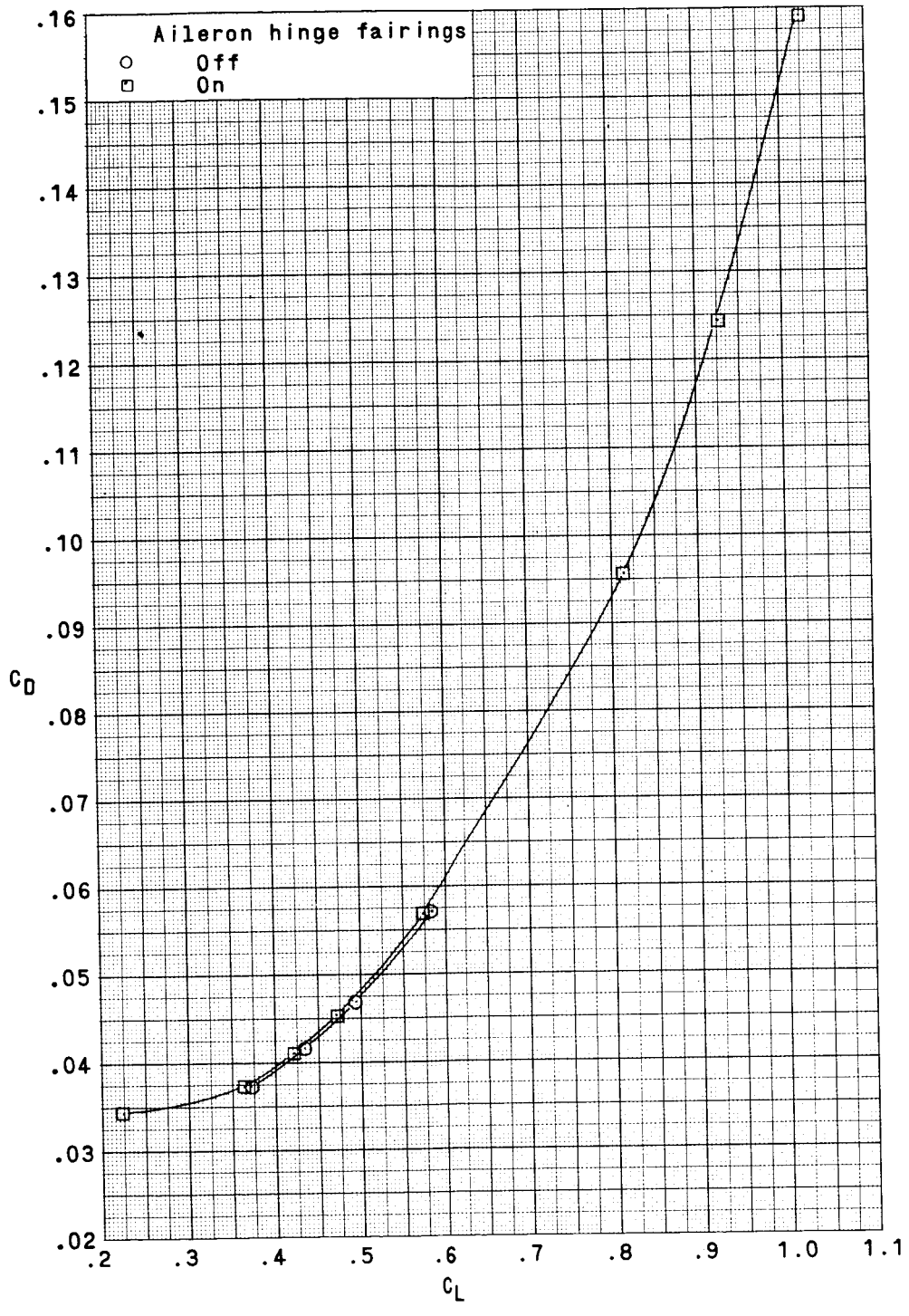


(b) M = 0.99. Concluded.

Figure 10.- Concluded.

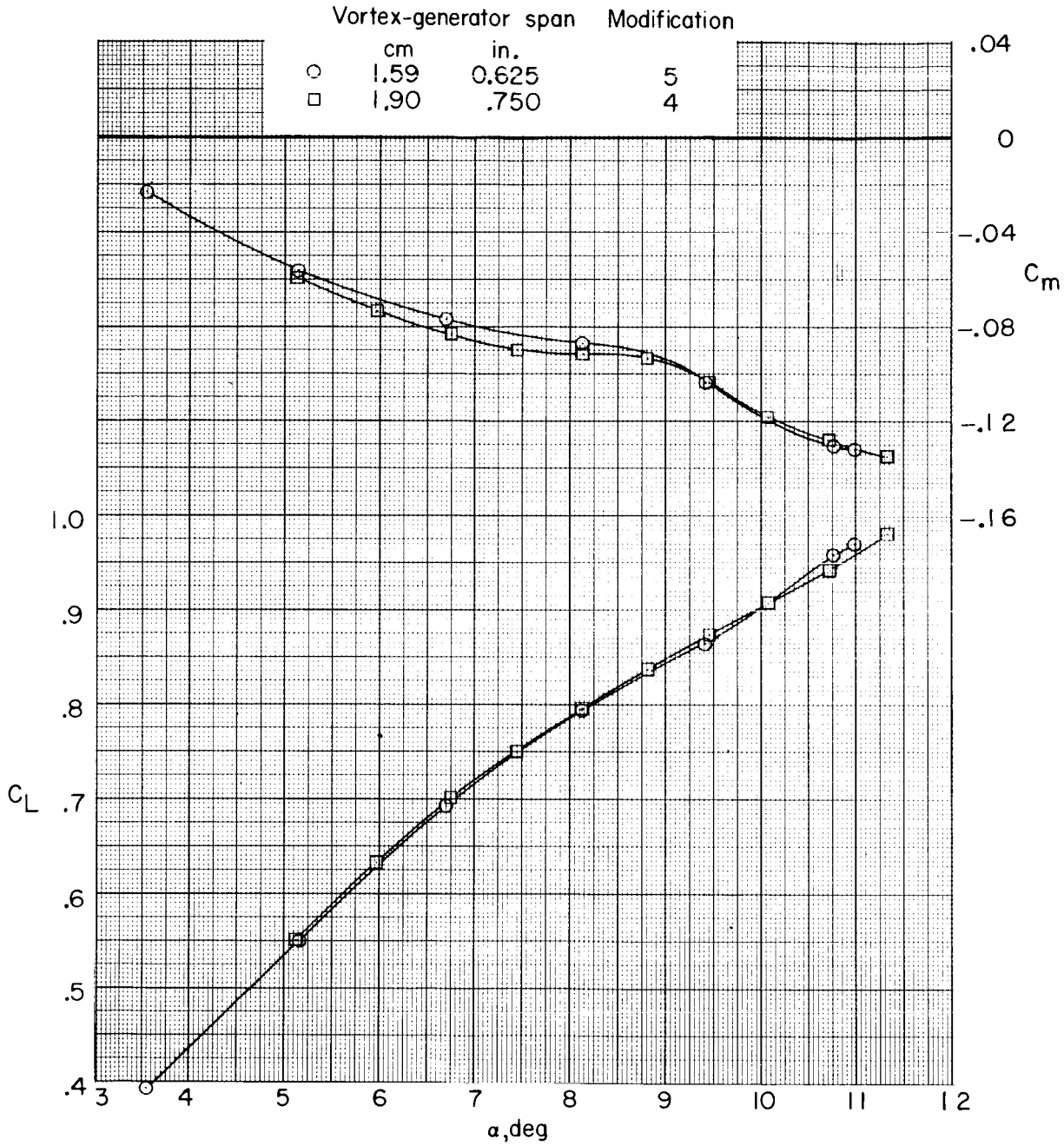


(a) M = 0.80.

Figure 11.- Effect of vortex-generator span on longitudinal aerodynamic characteristics. Steel wing; aileron hinge fairings on.

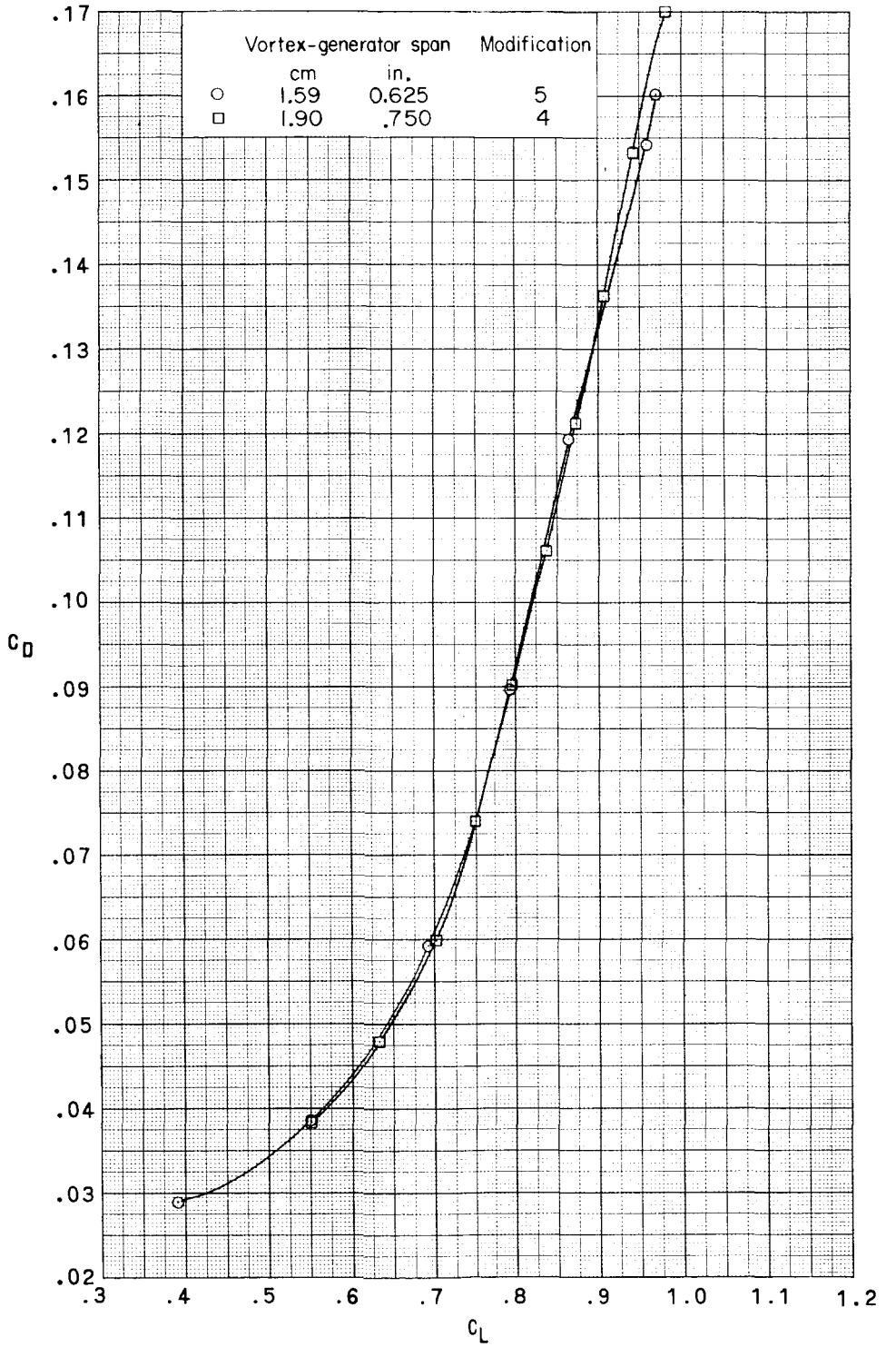


(a) M = 0.80. Concluded.

Figure 11.- Continued.

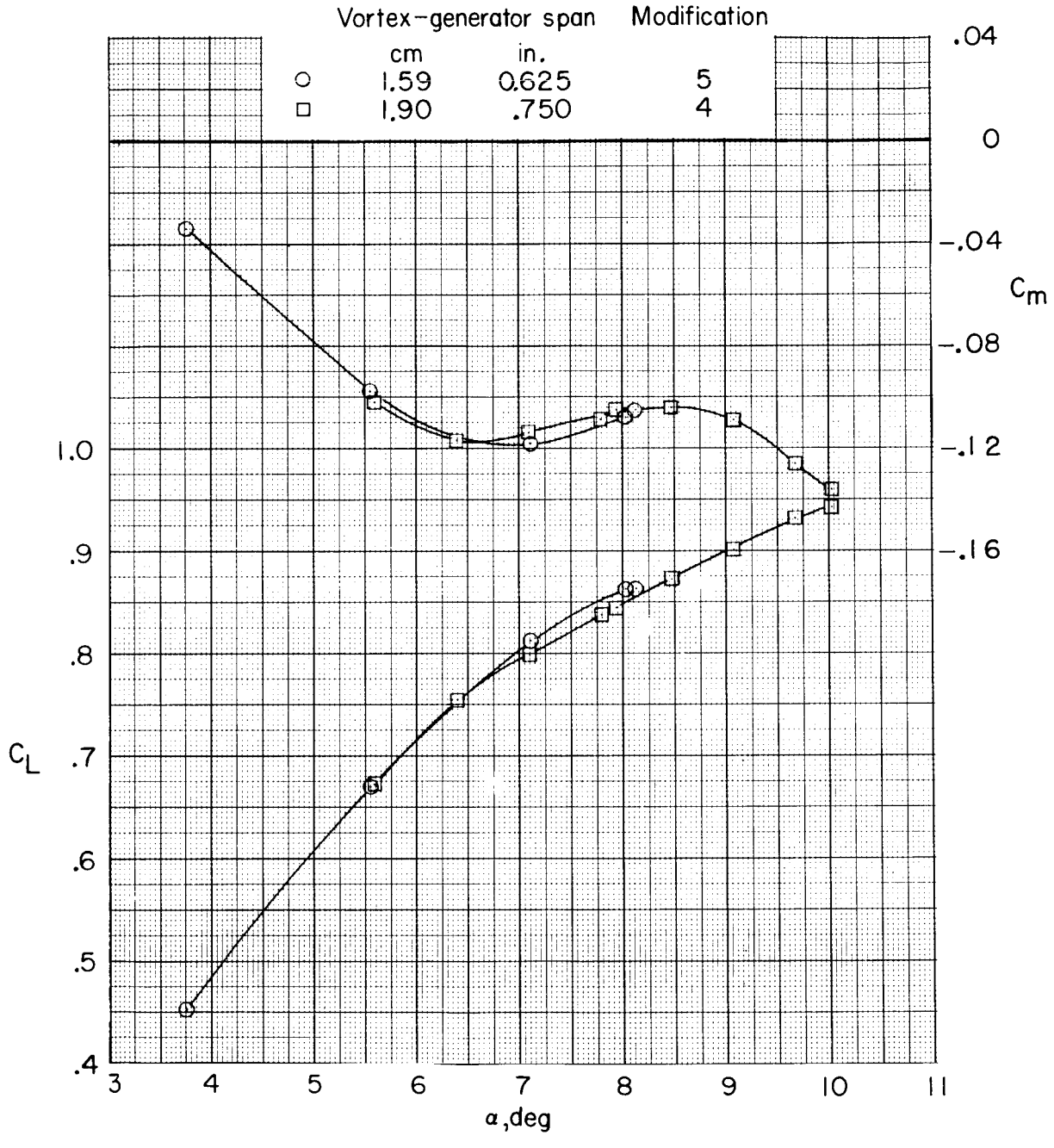


(b) M = 0.90.

Figure 11.- Continued.

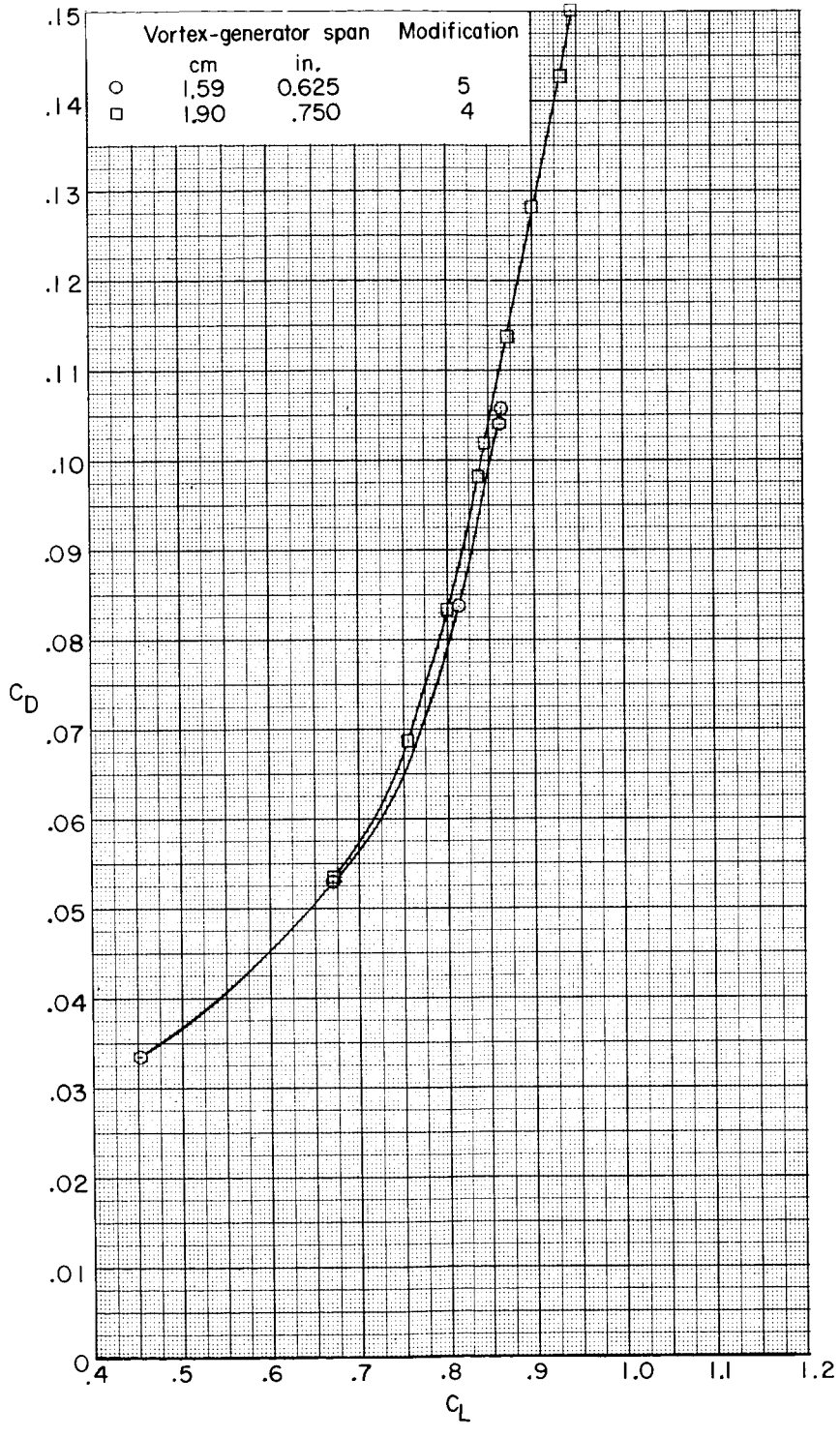


(b) M = 0.90. Concluded.

Figure 11.- Continued.

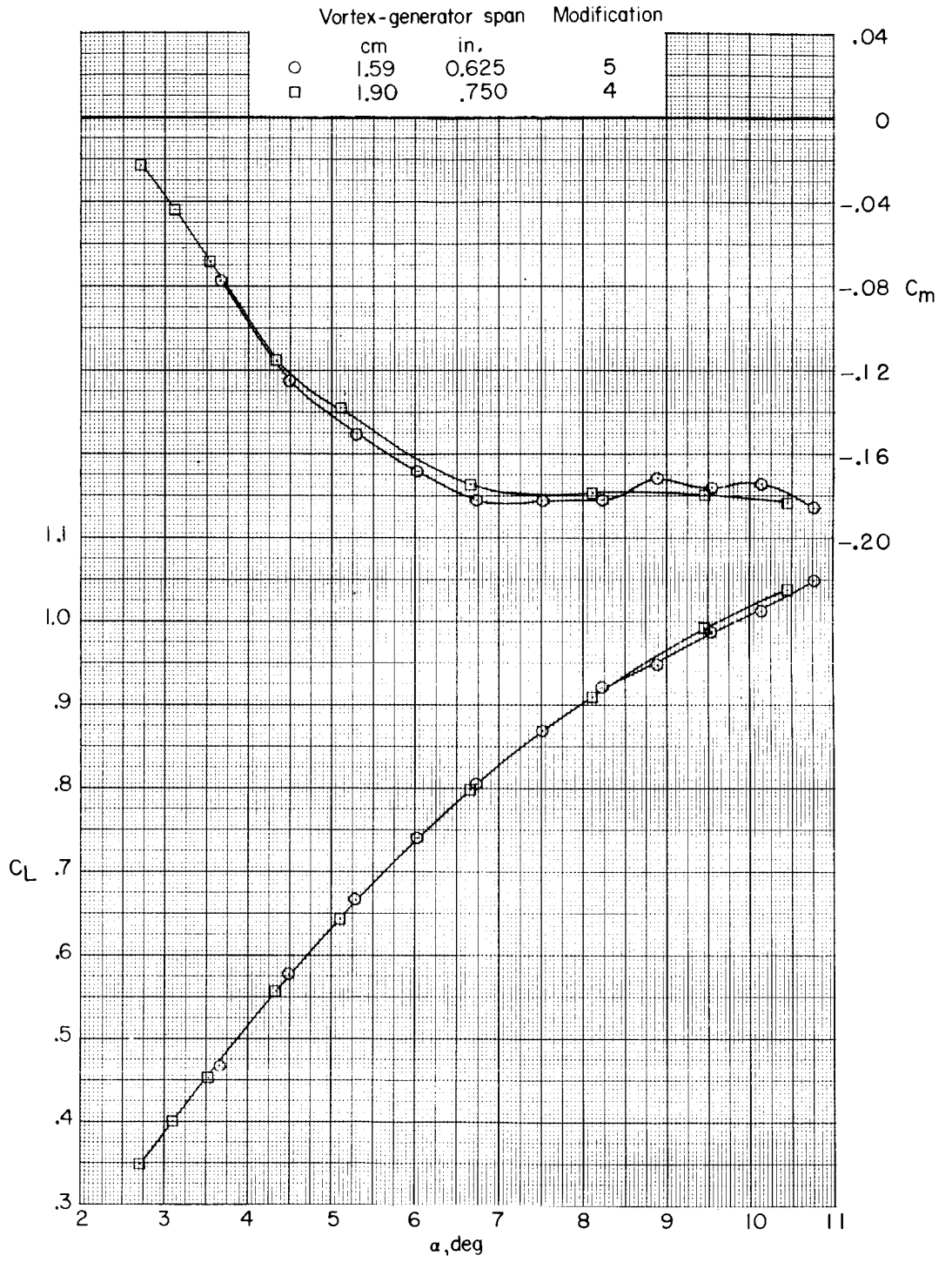


(c) M = 0.95.

Figure 11.- Continued.

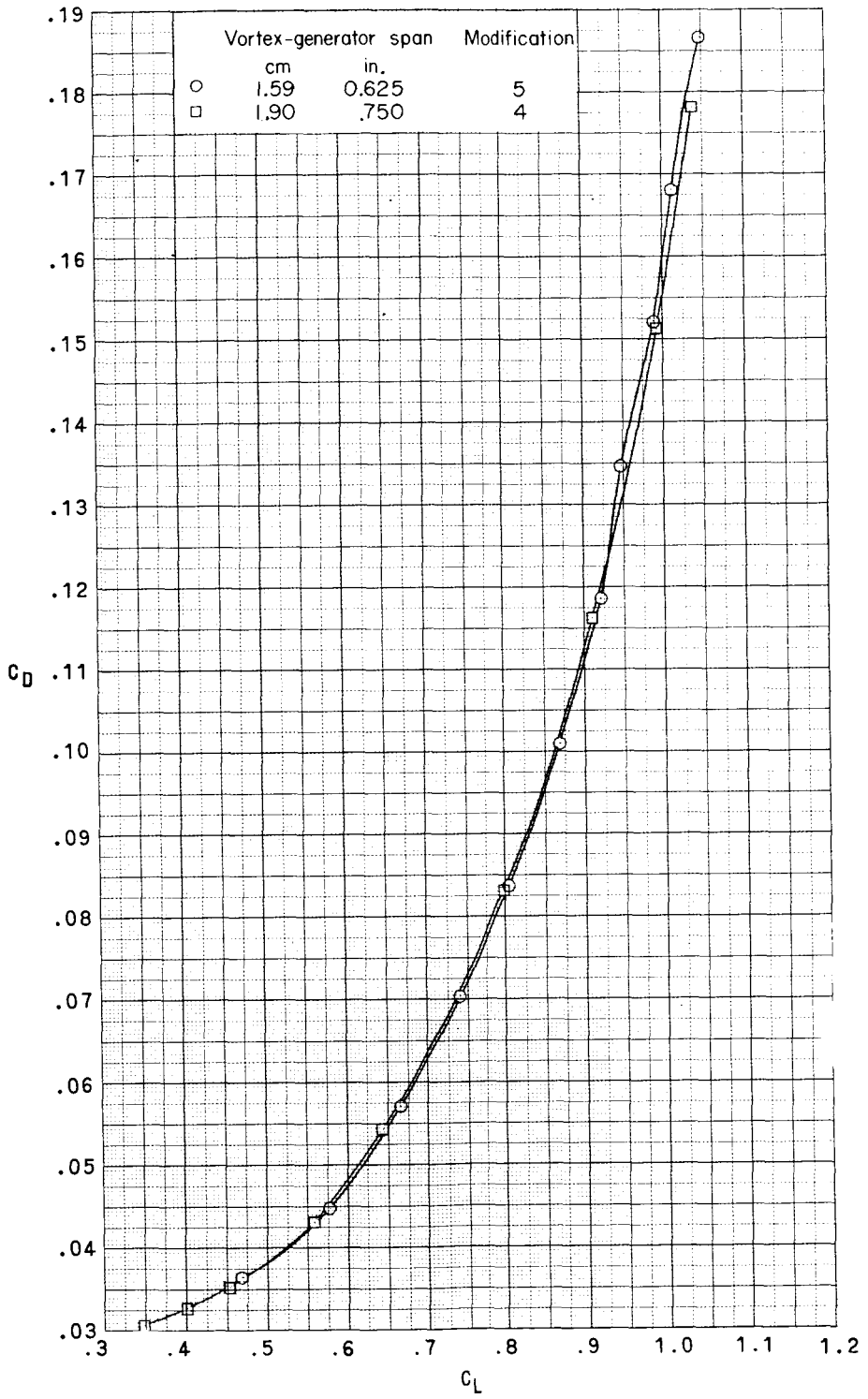


(c) M = 0.95. Concluded.

Figure 11.- Continued.

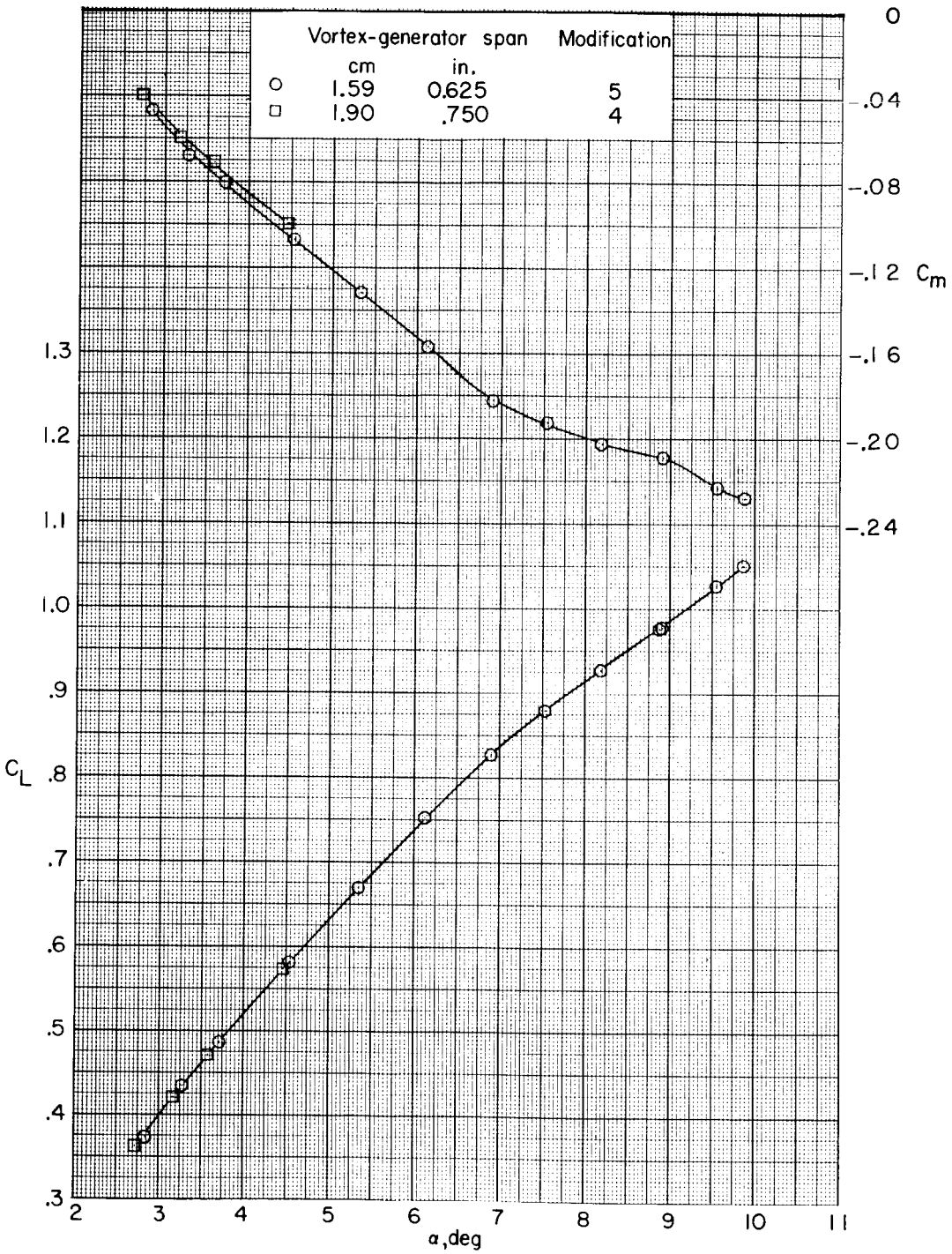


(d) M = 0.99.

Figure 11.- Continued.

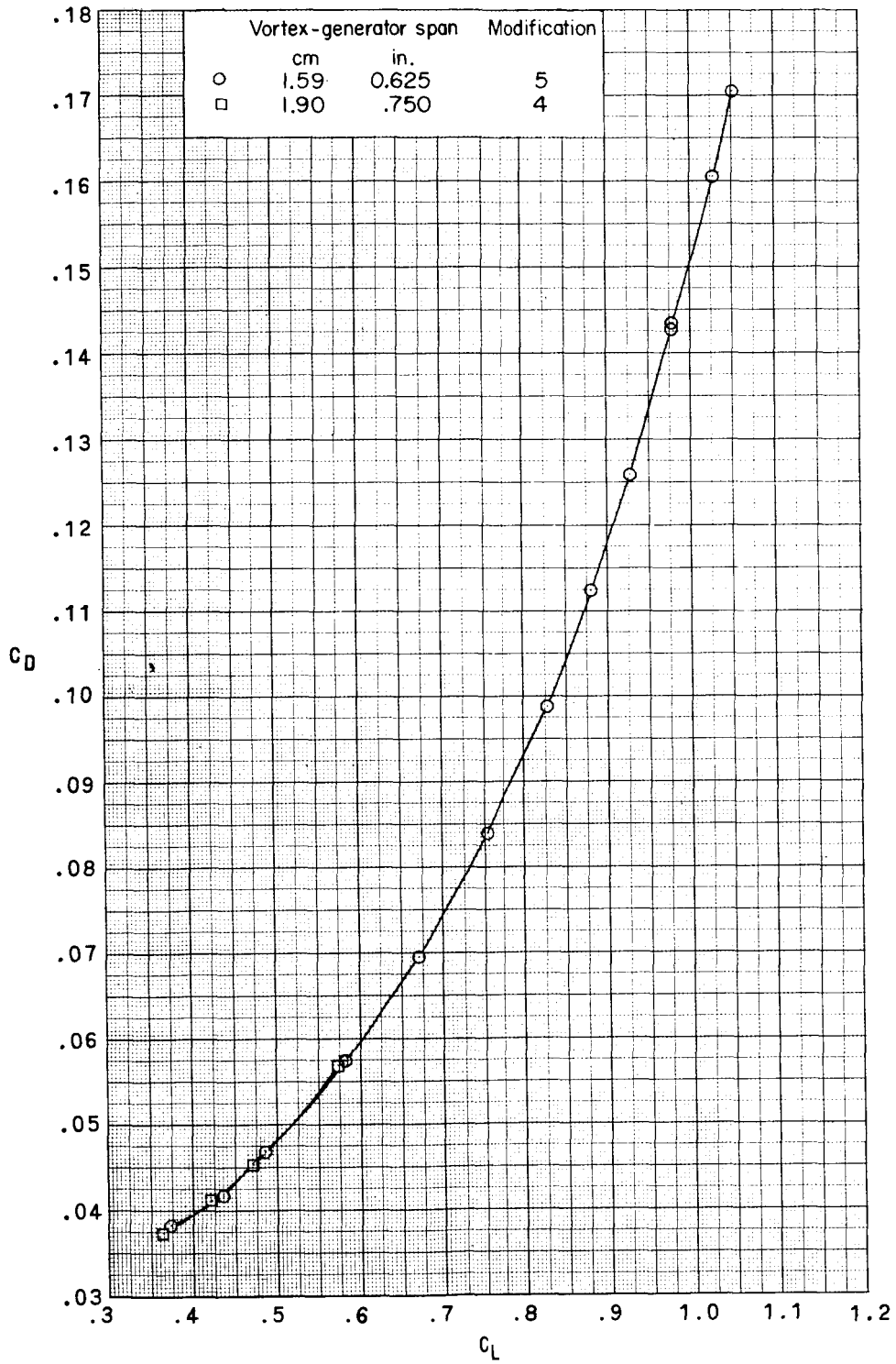


(d) M = 0.99. Concluded.

Figure 11.- Concluded.

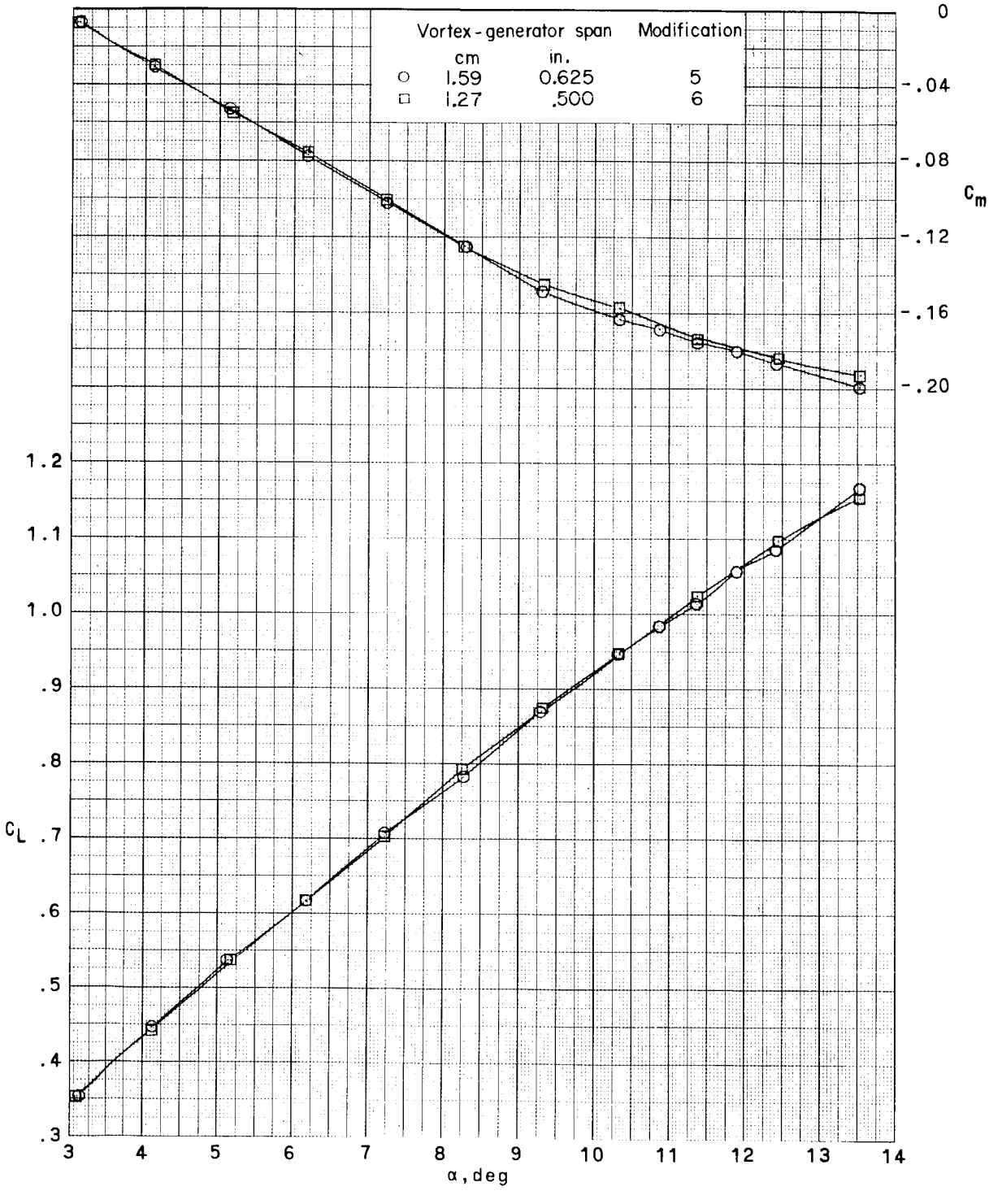


(a) M = 0.25.

Figure 12.- Effect of vortex-generator span on longitudinal aerodynamic characteristics. Aluminum wing.

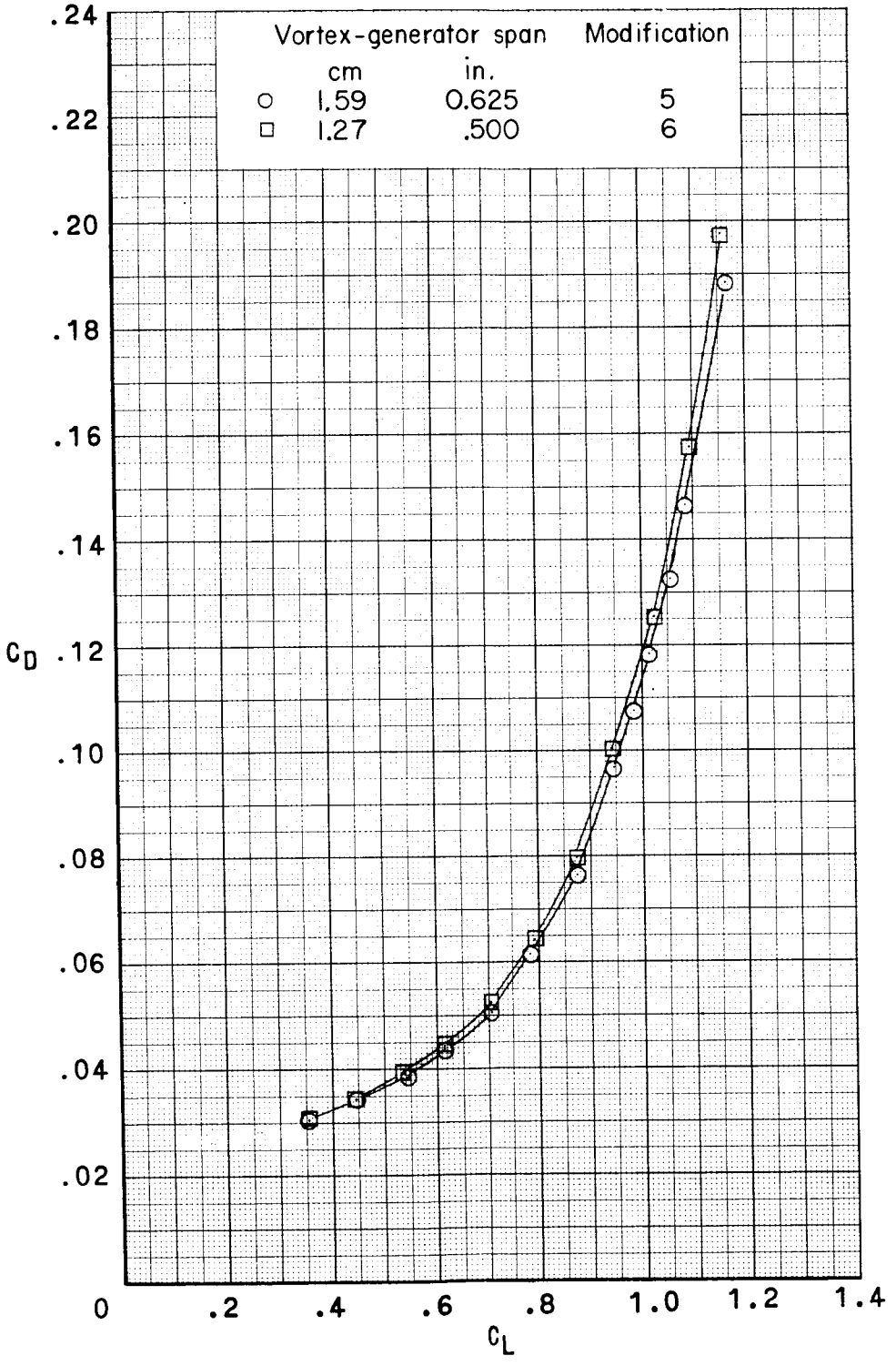


(a) M = 0.25. Concluded.

Figure 12.- Continued.

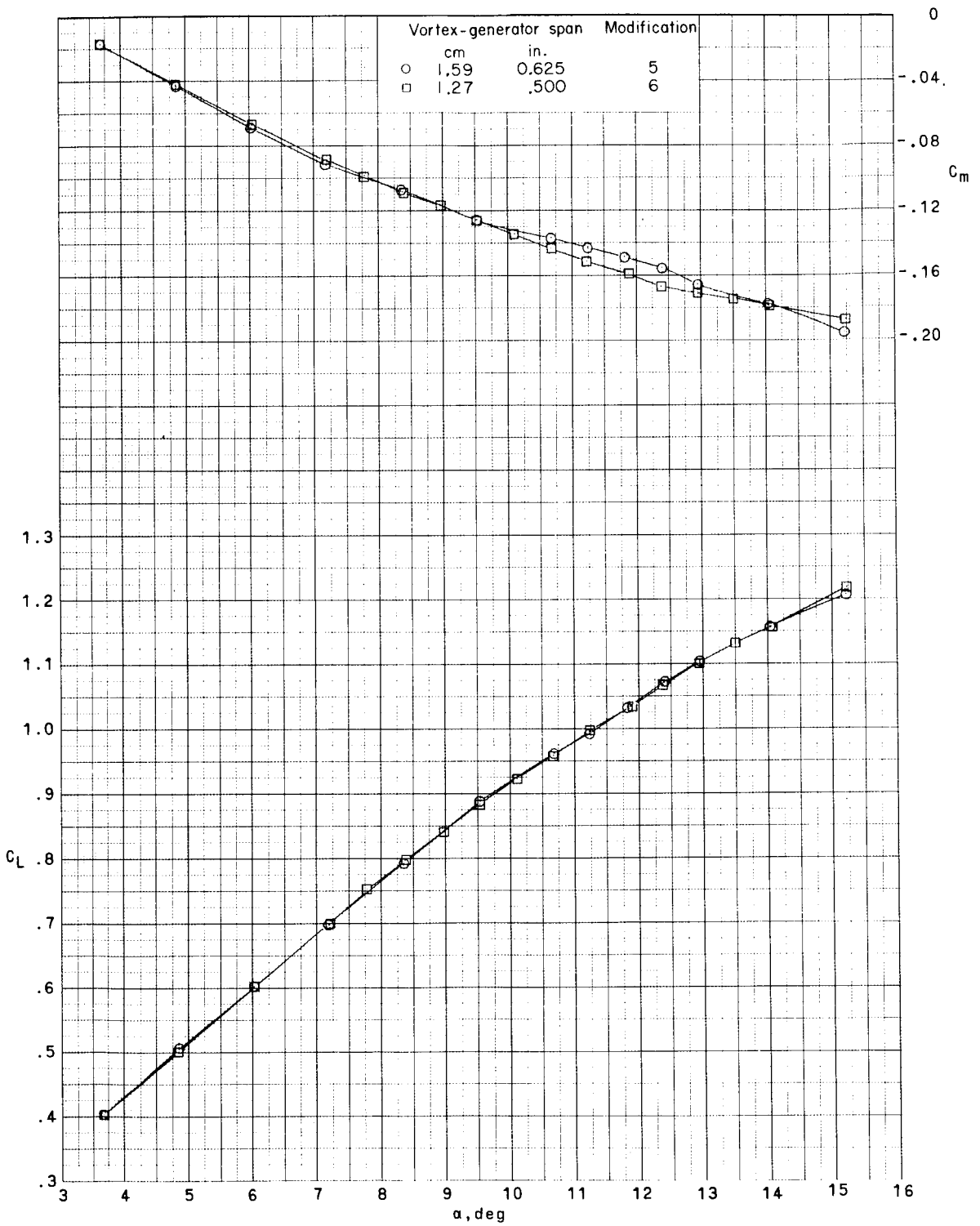


(b) M = 0.50.

Figure 12.- Continued.

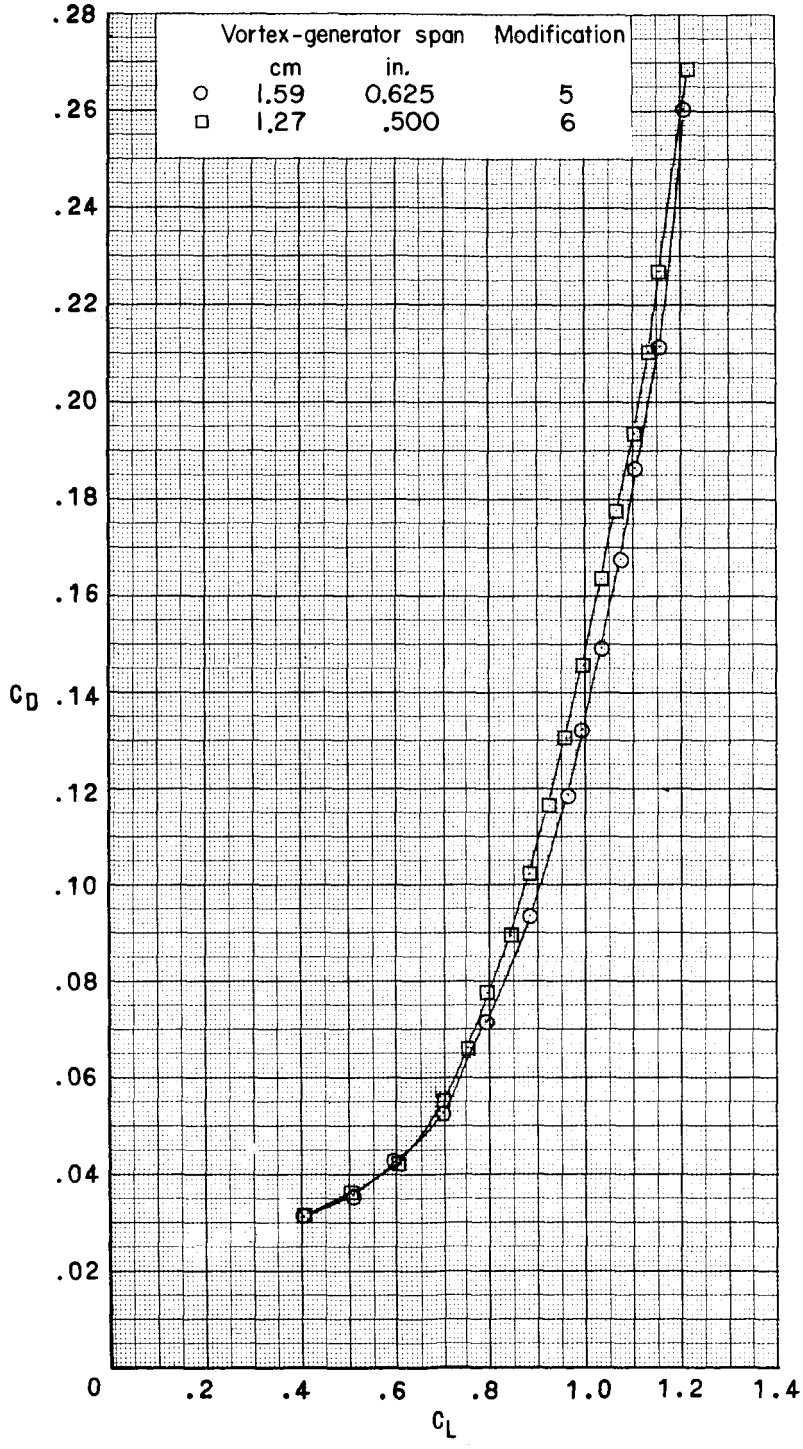


(b) M = 0.50. Concluded.

Figure 12.- Continued.

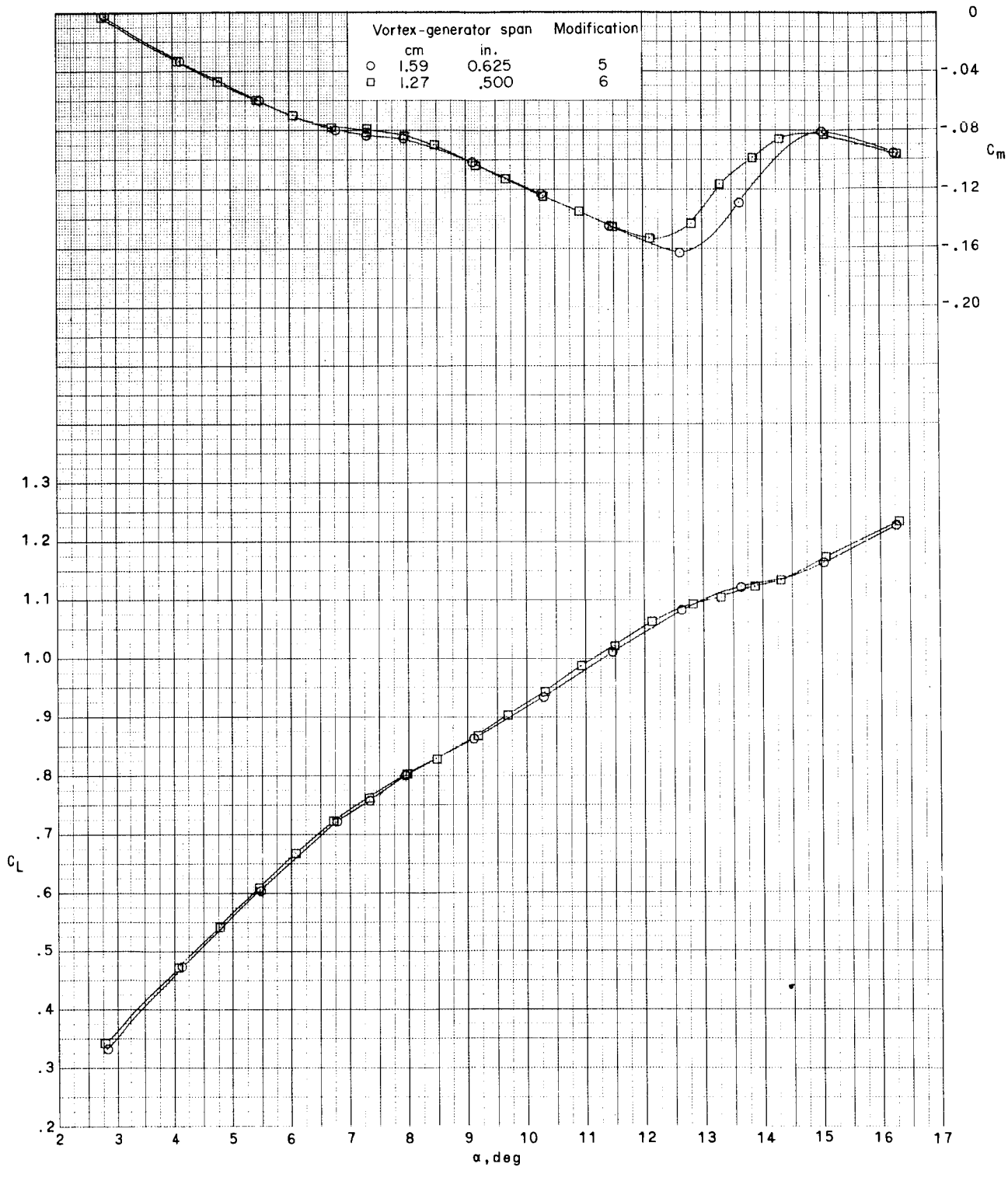


(c) M = 0.80.

Figure 12.- Continued.

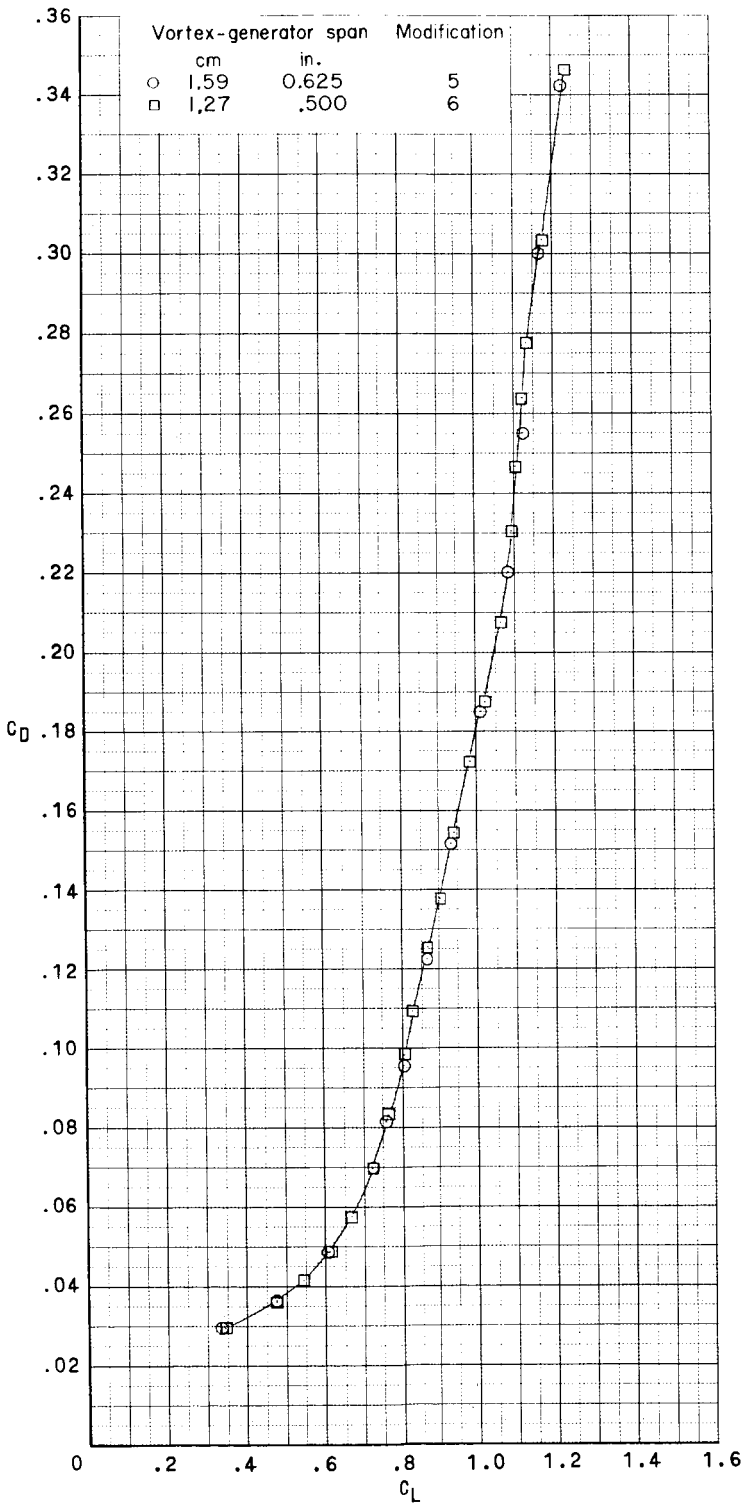


(c) M = 0.80. Concluded.

Figure 12.- Continued.

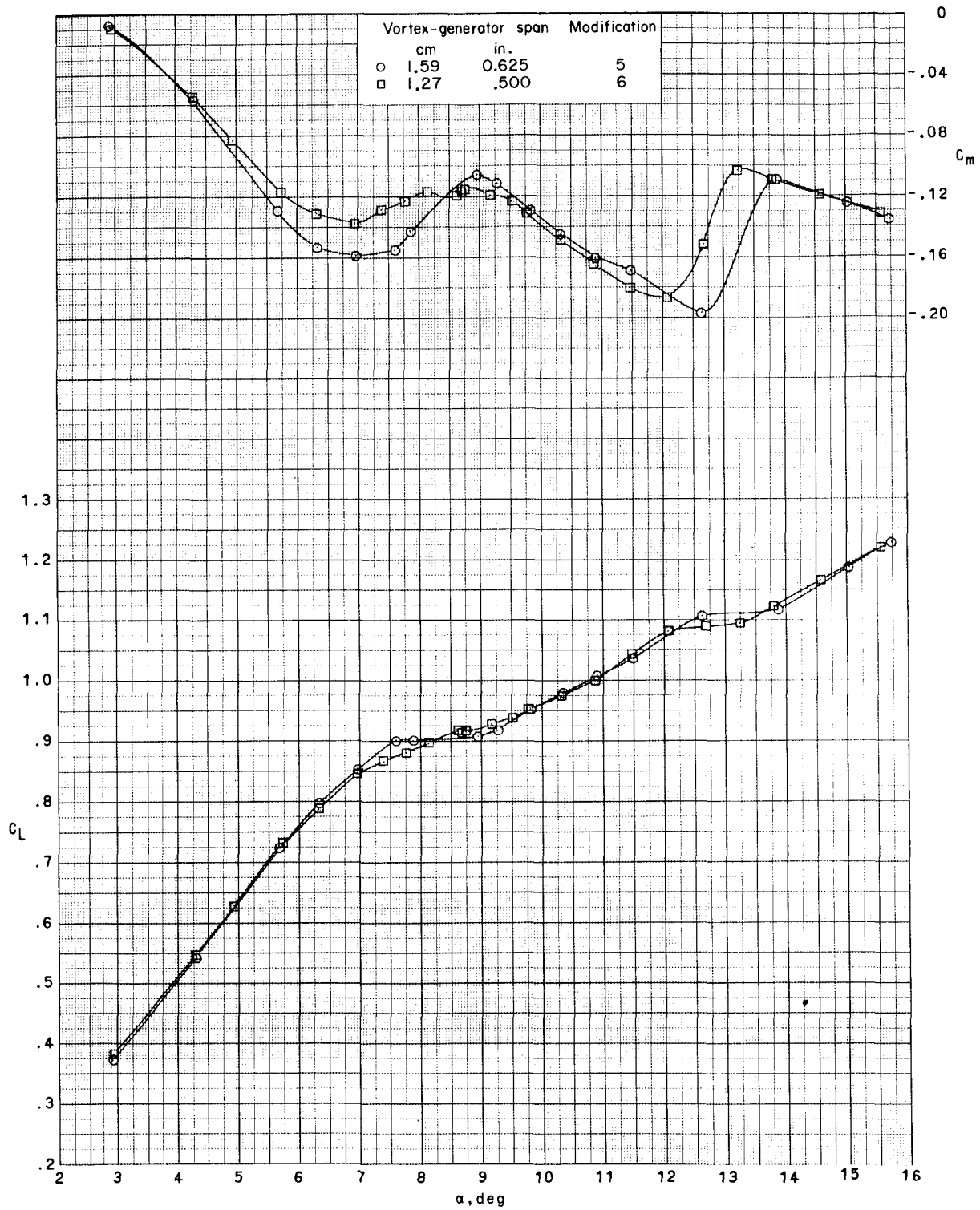


(d) M = 0.90.

Figure 12. - Continued.

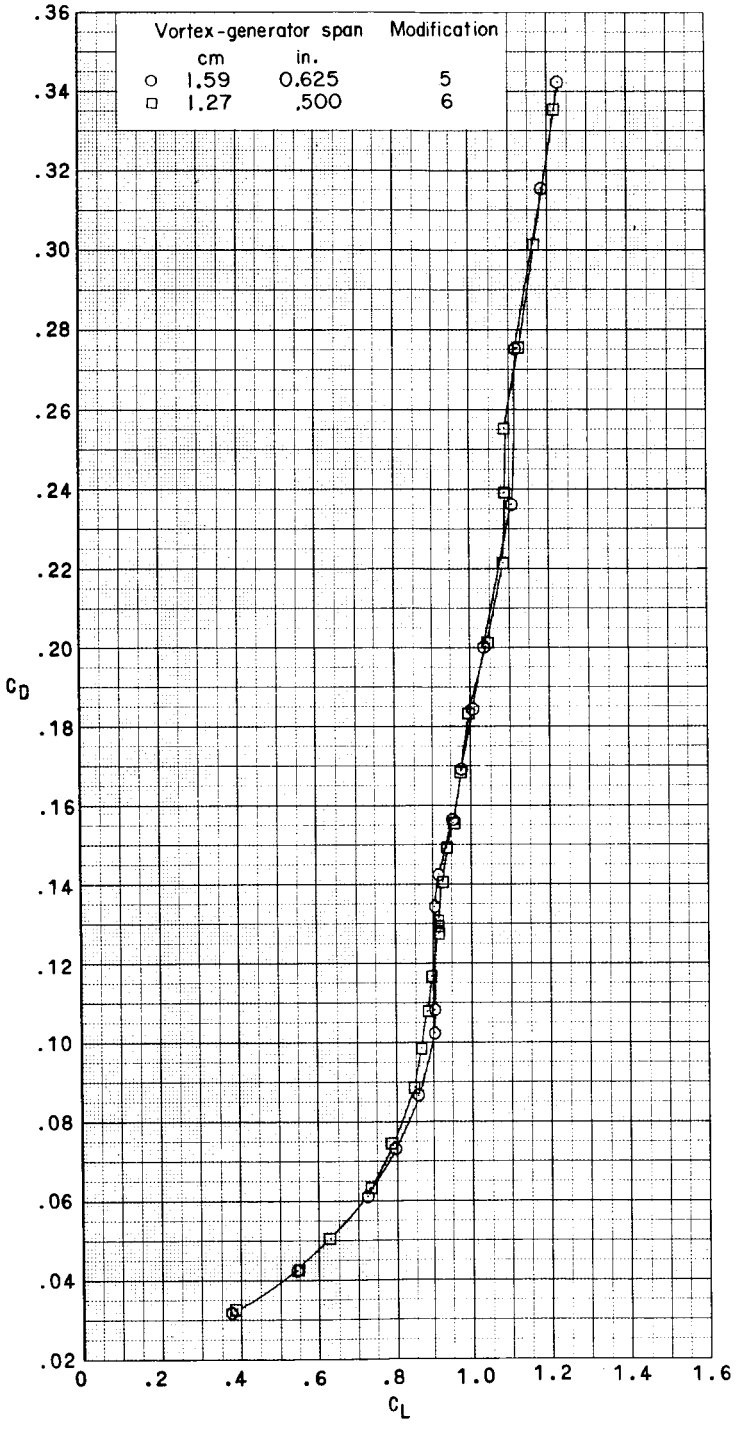


(d) M = 0.90. Concluded.

Figure 12.- Continued.

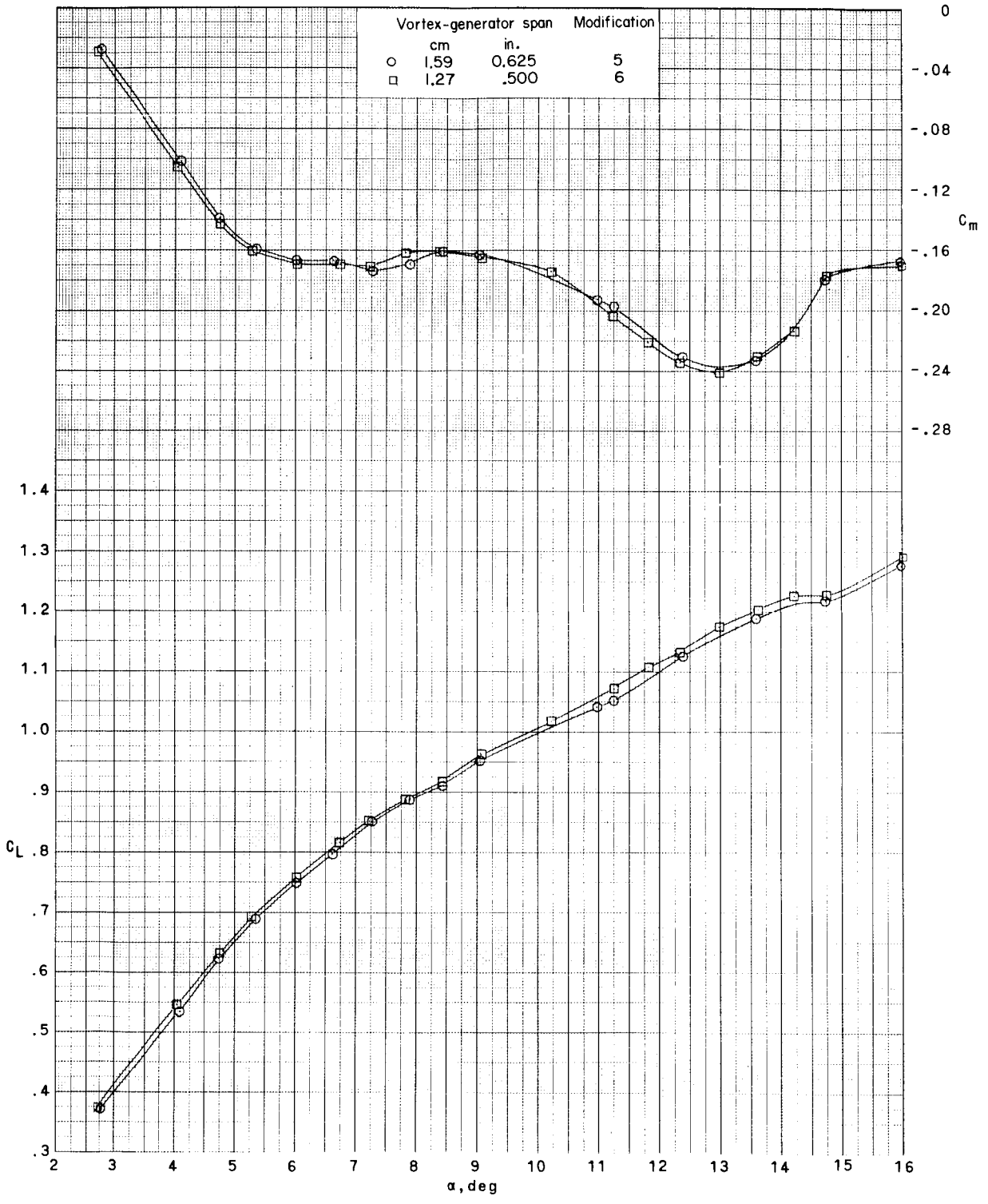


(e) M = 0.95.

Figure 12. - Continued.

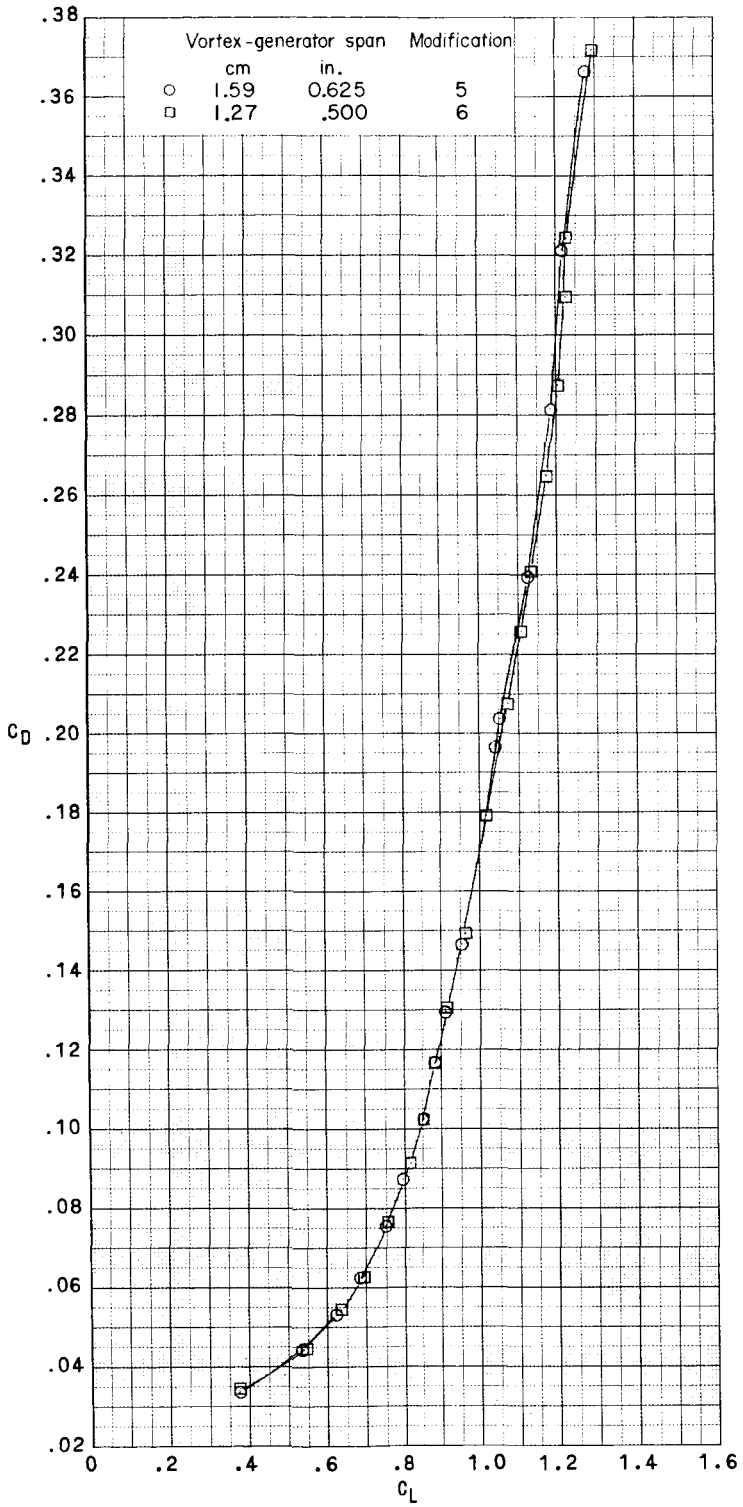


(e) M = 0.95. Concluded.

Figure 12.- Concluded.

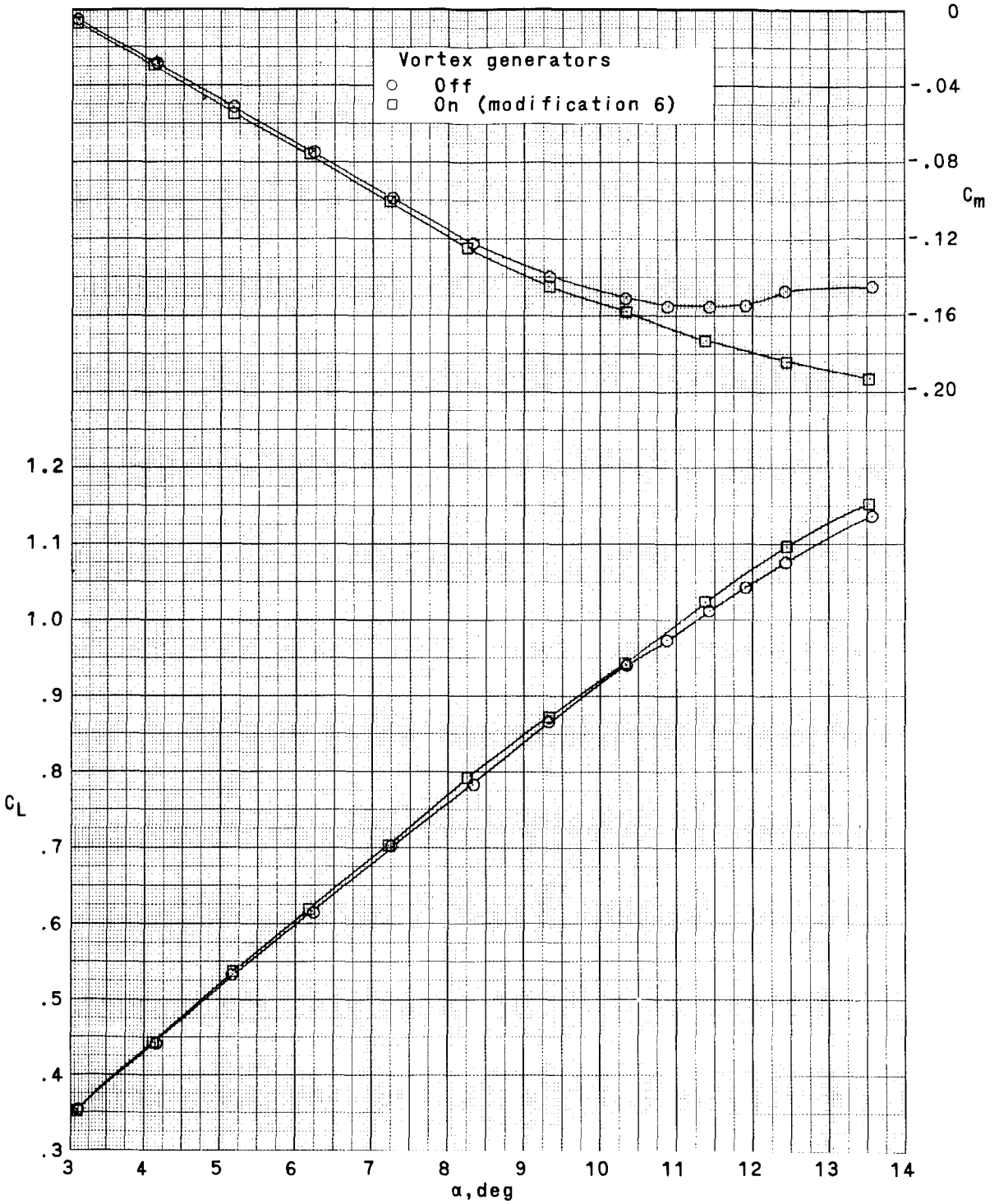


(a) M = 0.25.

Figure 13.- Effect of final vortex-generator configuration (modification 6) on longitudinal aerodynamic characteristics. Aluminum wing.

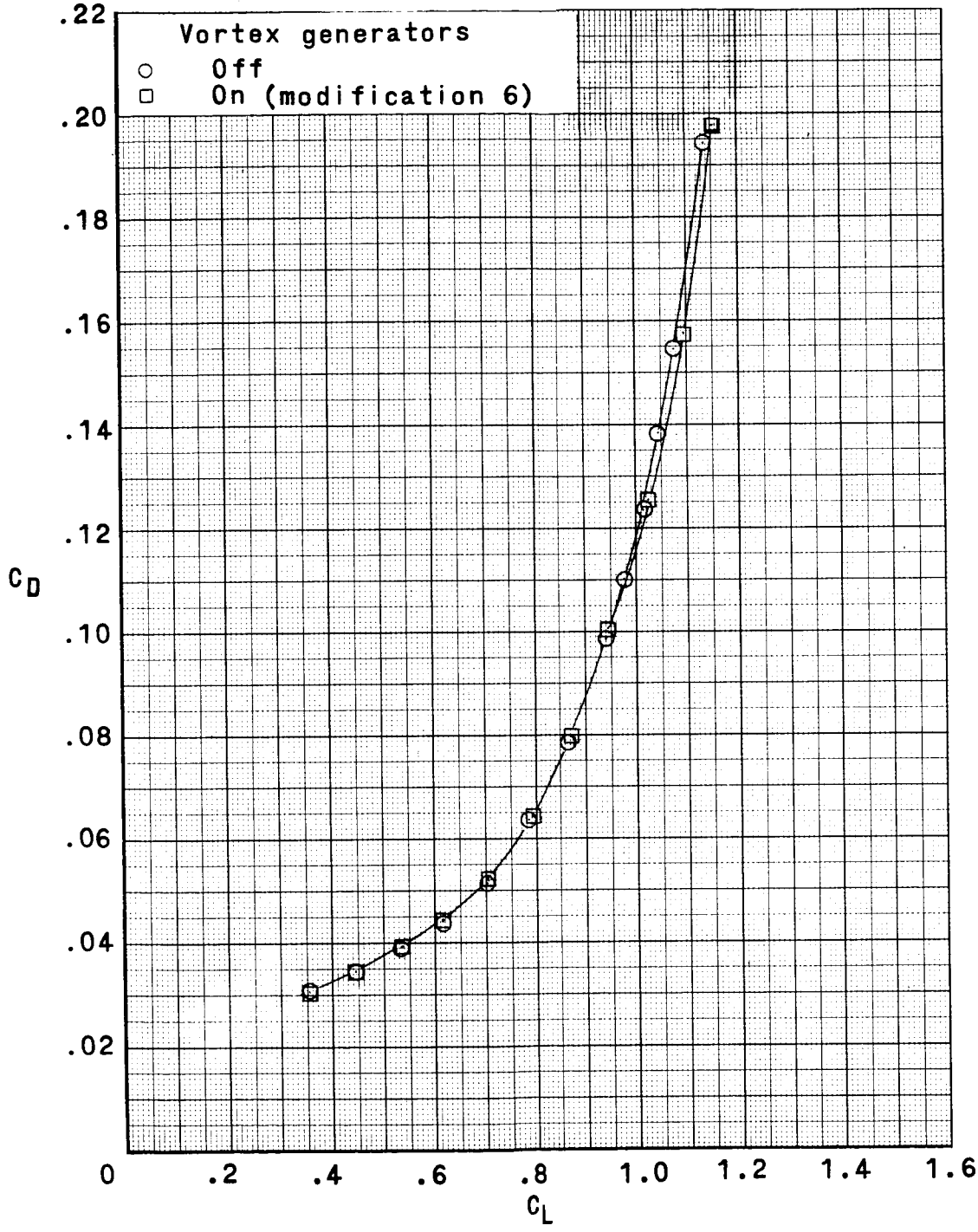


(a) M = 0.25. Concluded.

Figure 13.- Continued.

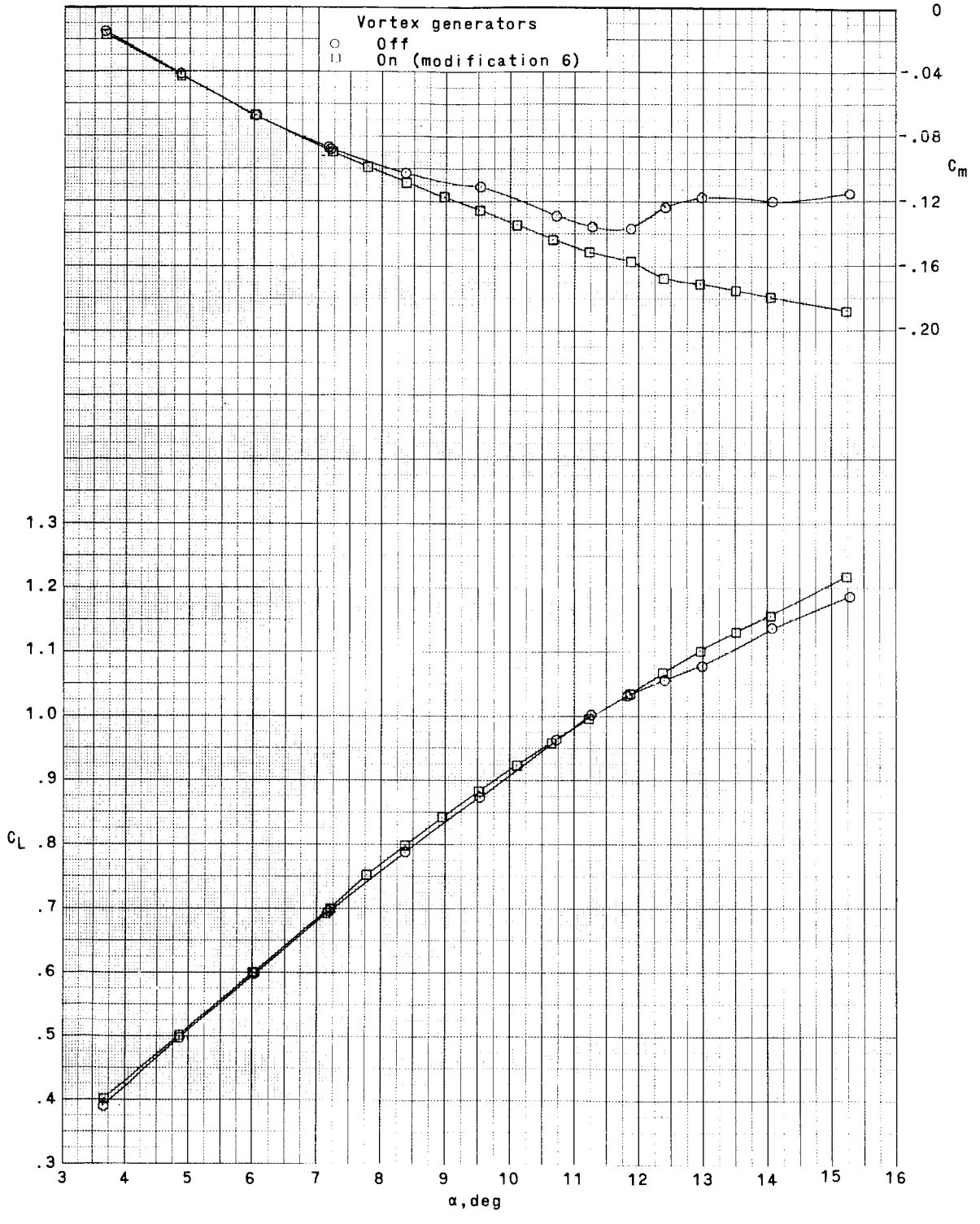


(b) M = 0.50.

Figure 13.- Continued.

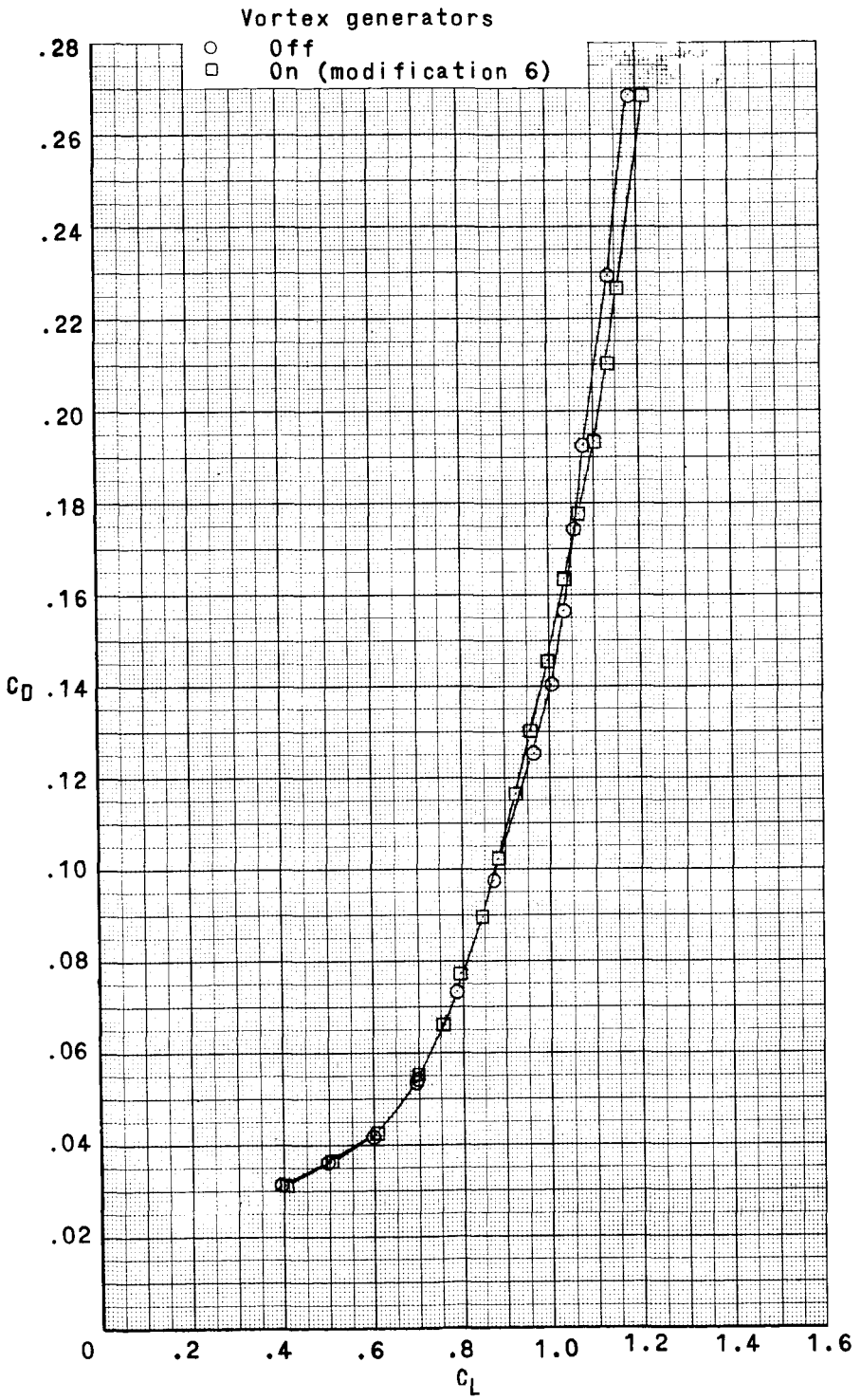


(b) M = 0.50. Concluded.

Figure 13.- Continued.


(c) M = 0.80.

Figure 13.- Continued.

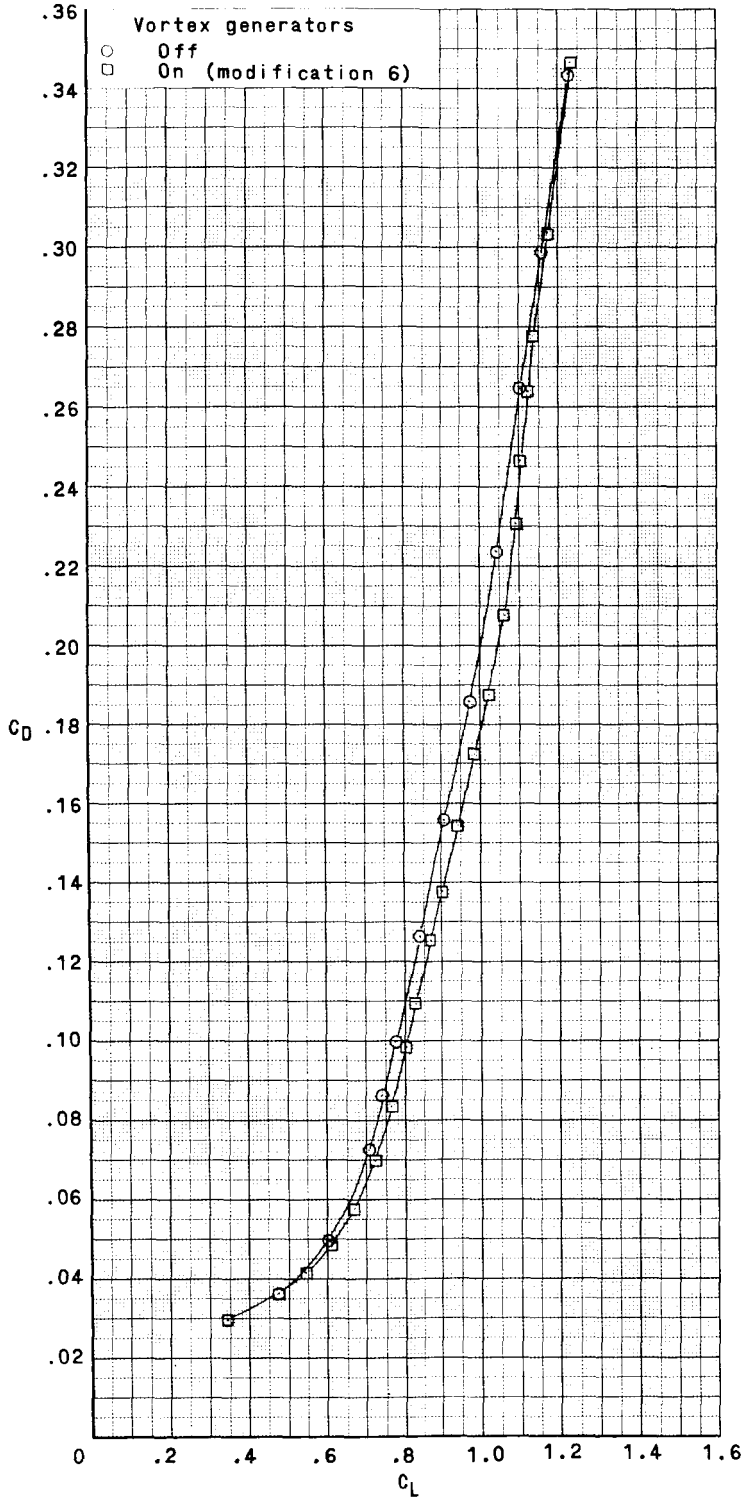


(c) M = 0.80. Concluded.

Figure 13.- Continued.

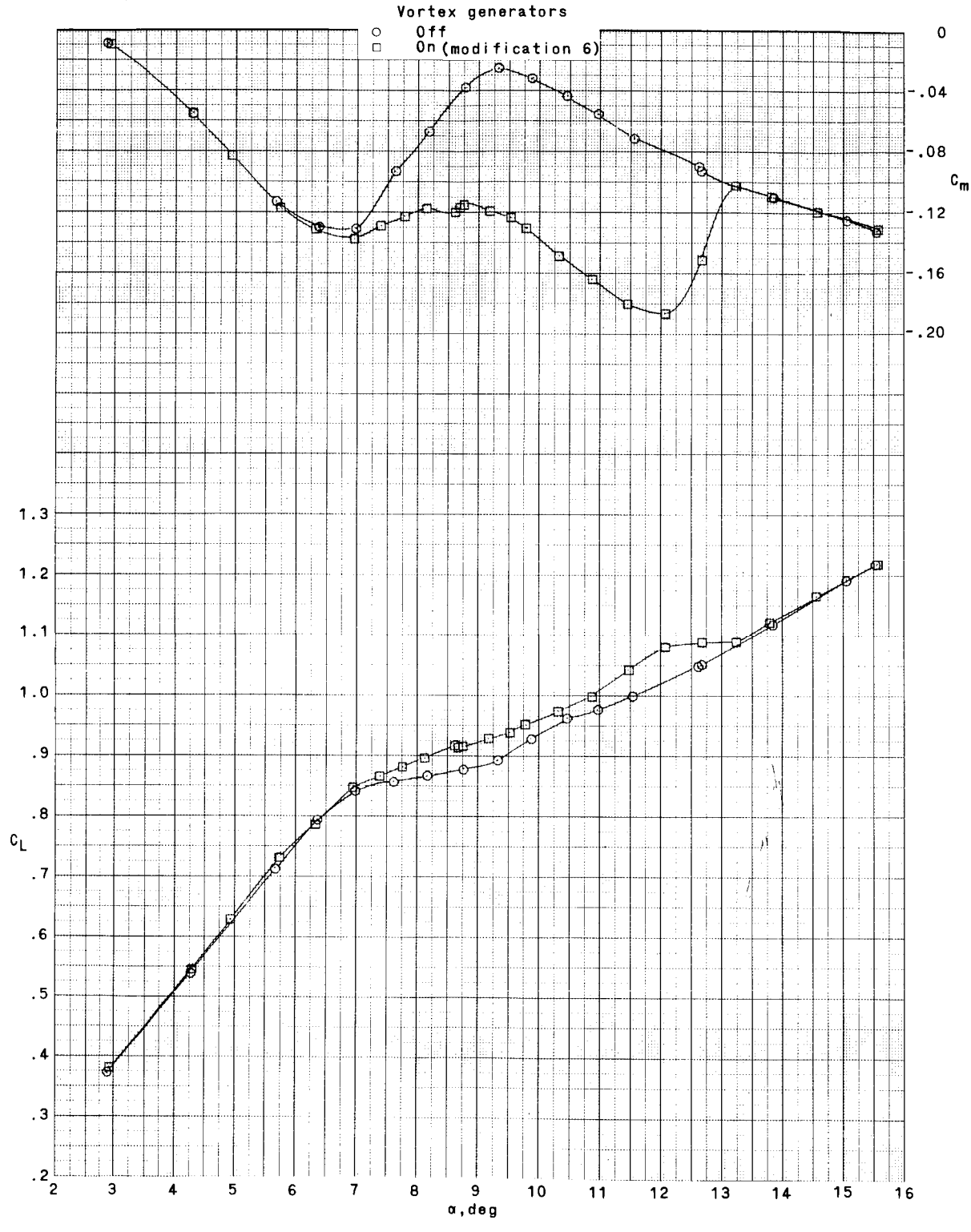


(d) M = 0.90.

Figure 13.- Continued.

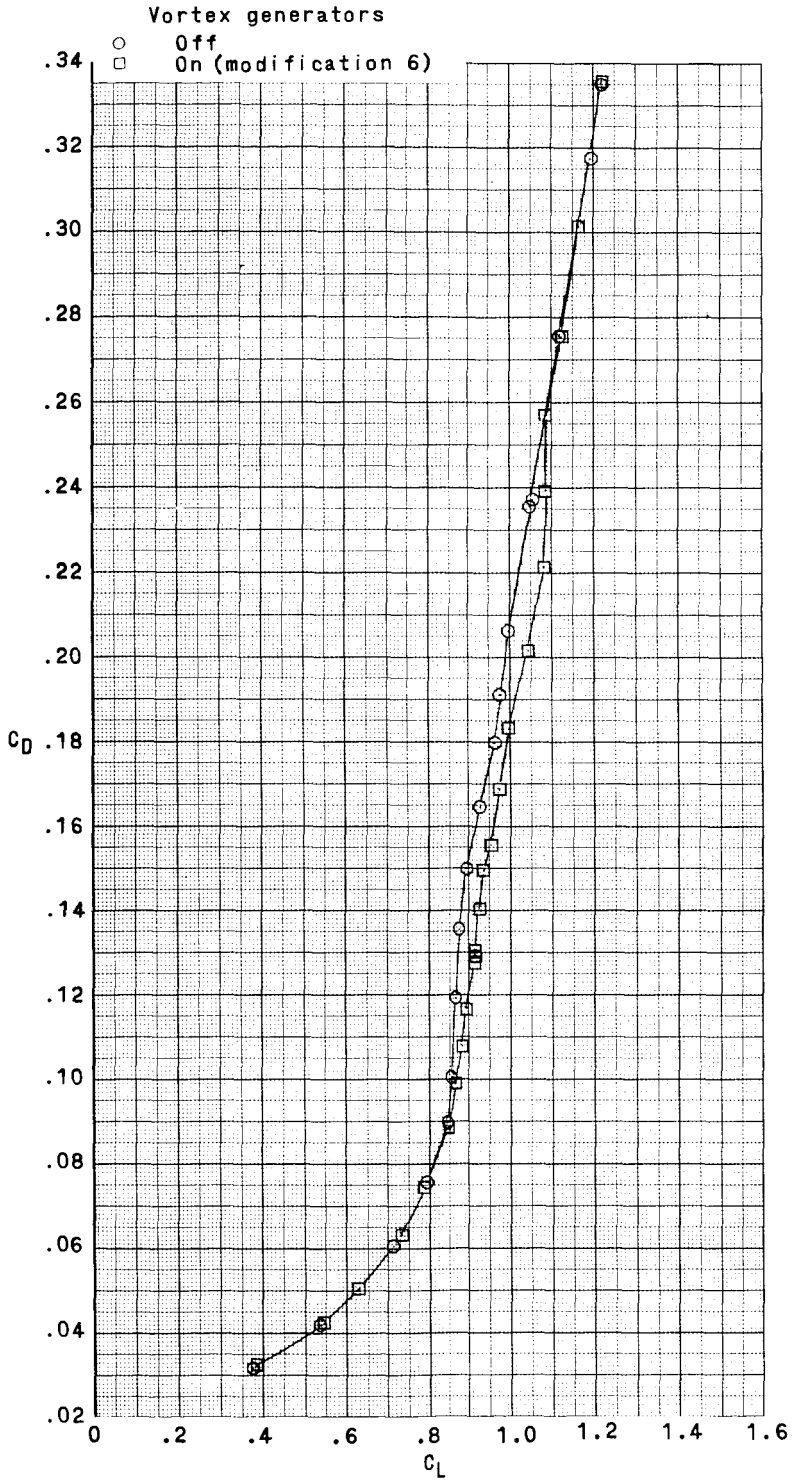


(d) M = 0.90. Concluded.

Figure 13.- Continued.

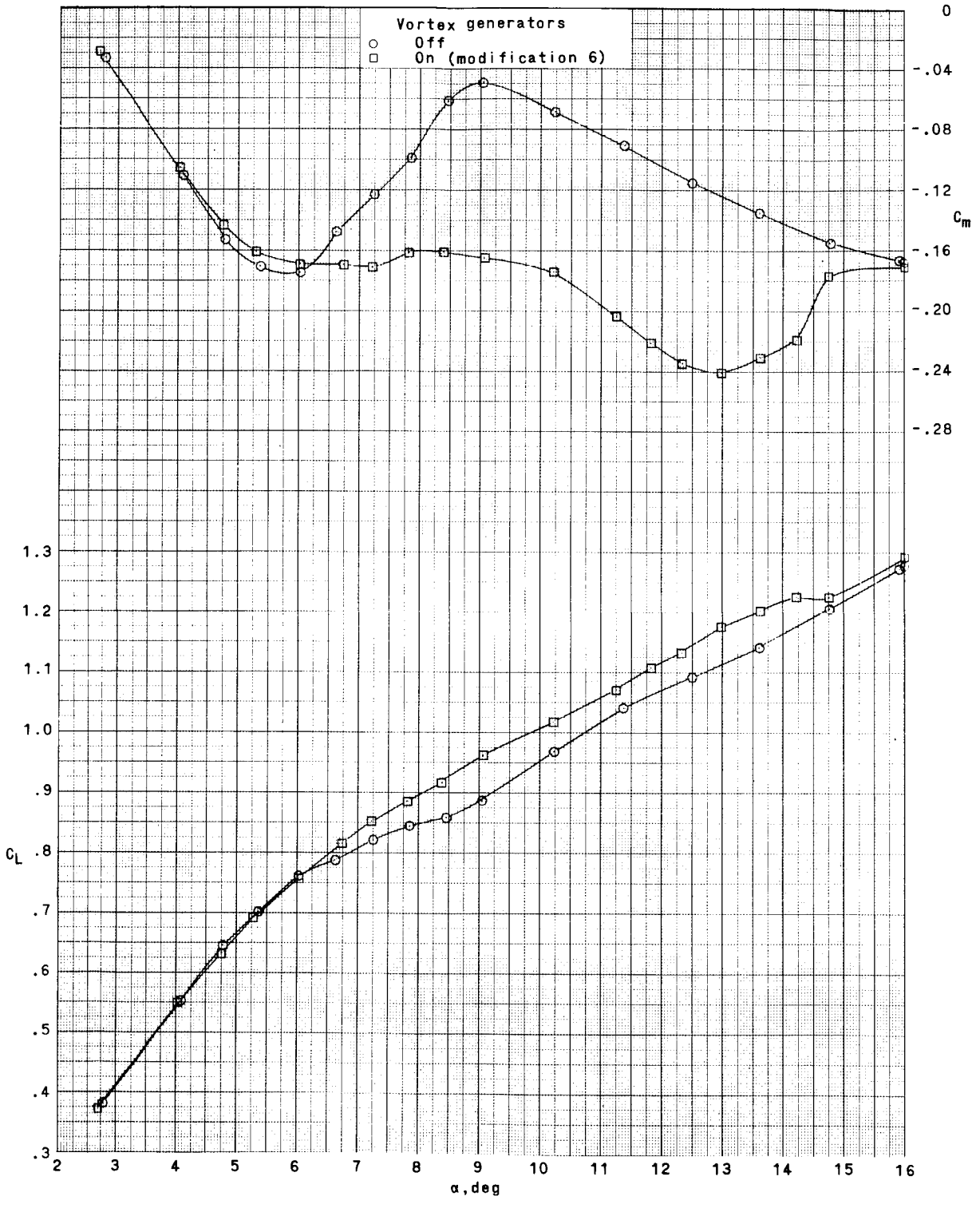


(e) M = 0.95.

Figure 13.- Continued.

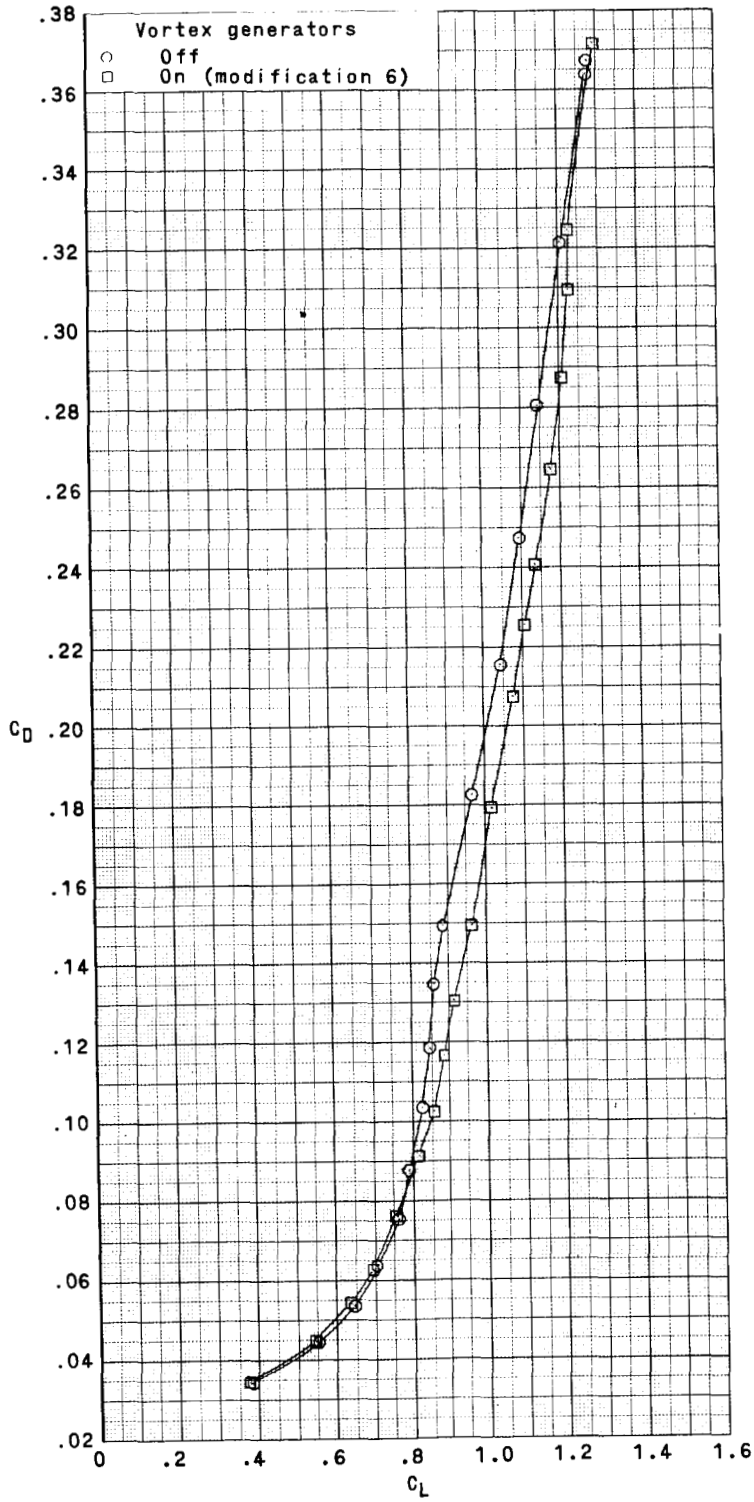


(e) M = 0.95. Concluded.

Figure 13.- Concluded.

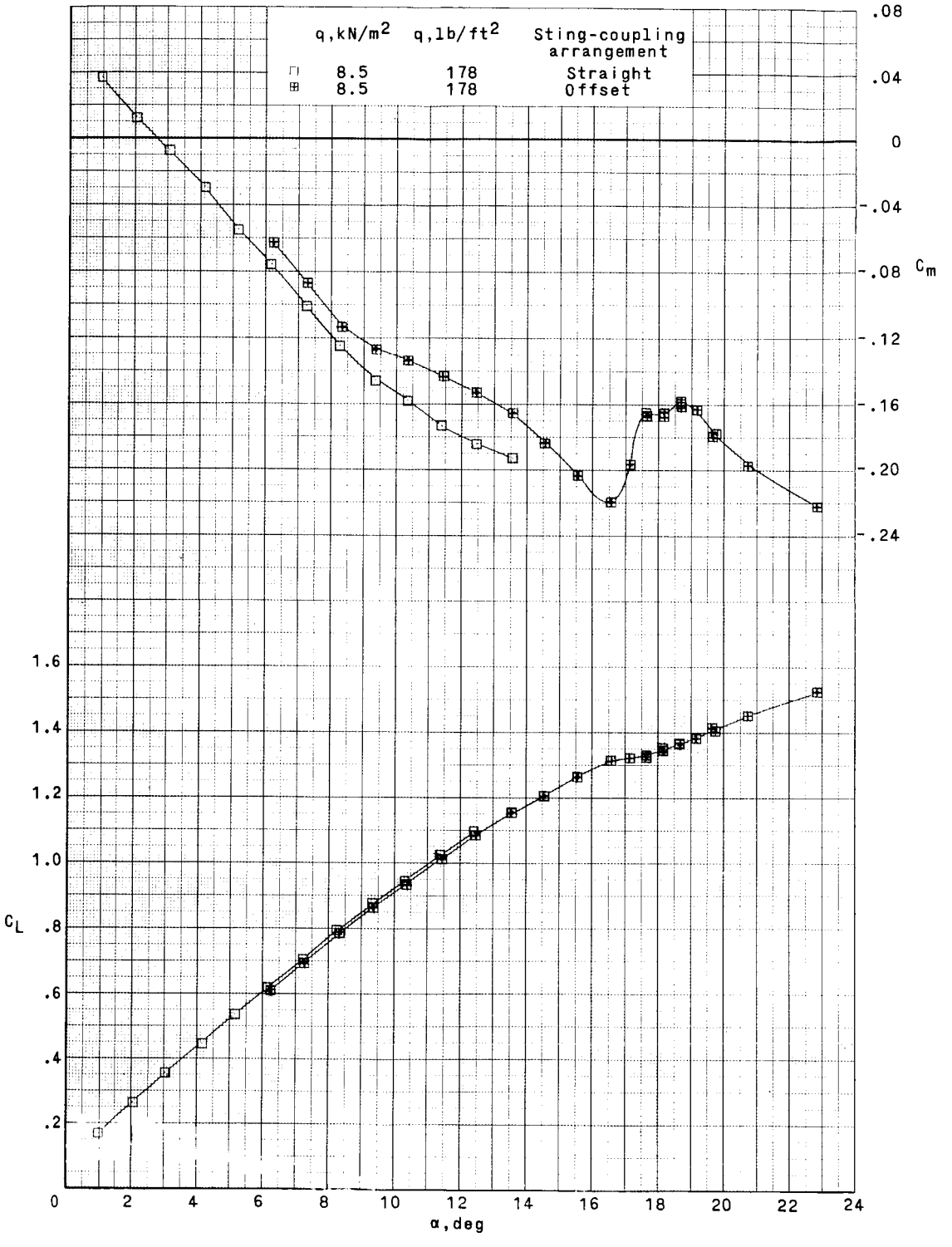


(a) M = 0.25.

Figure 14.- Lift and pitching-moment characteristics of model with final vortex-generator configuration (modification 6) at extended angles of attack. Aluminum wing.

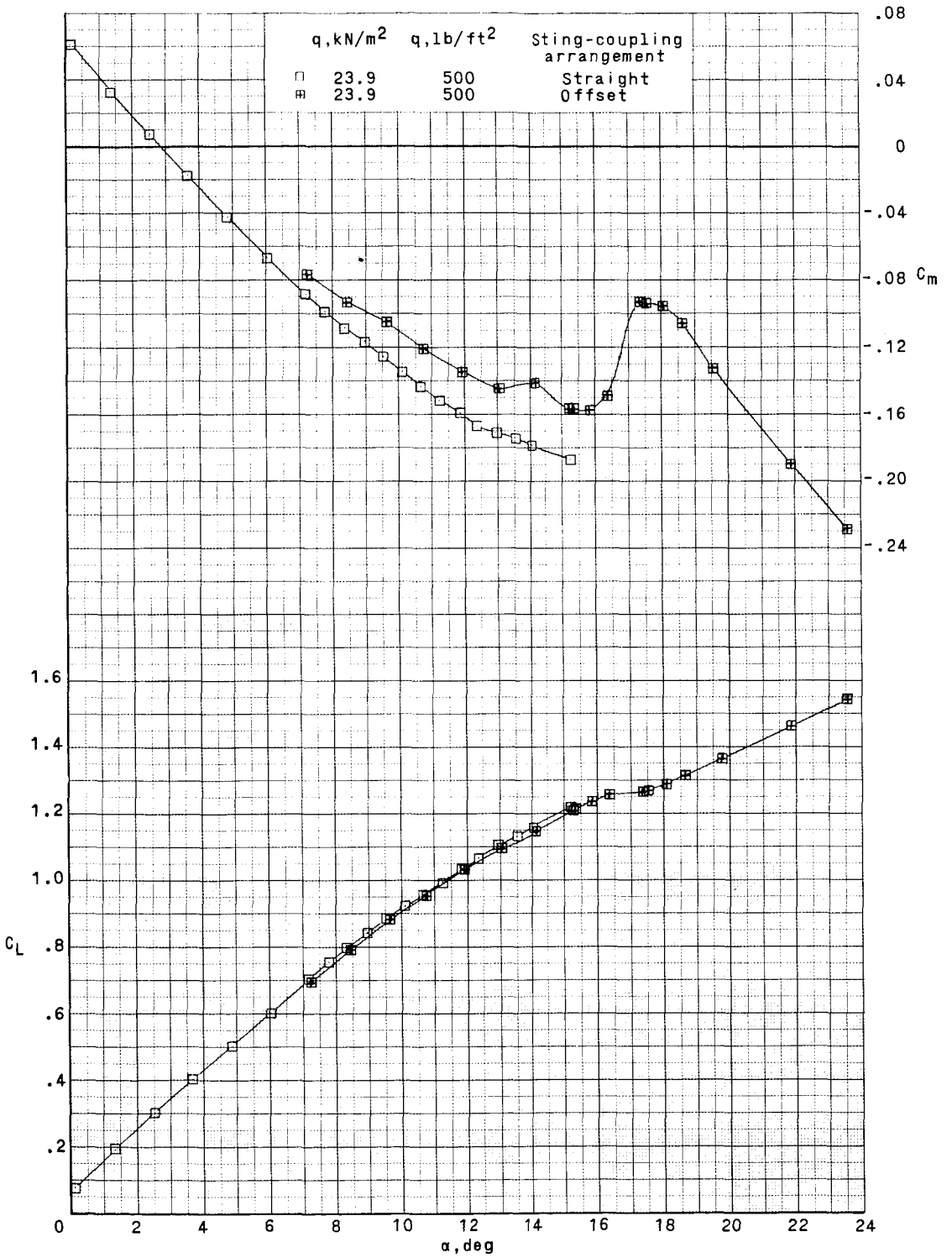


(b) M = 0.50.

Figure 14.- Continued.

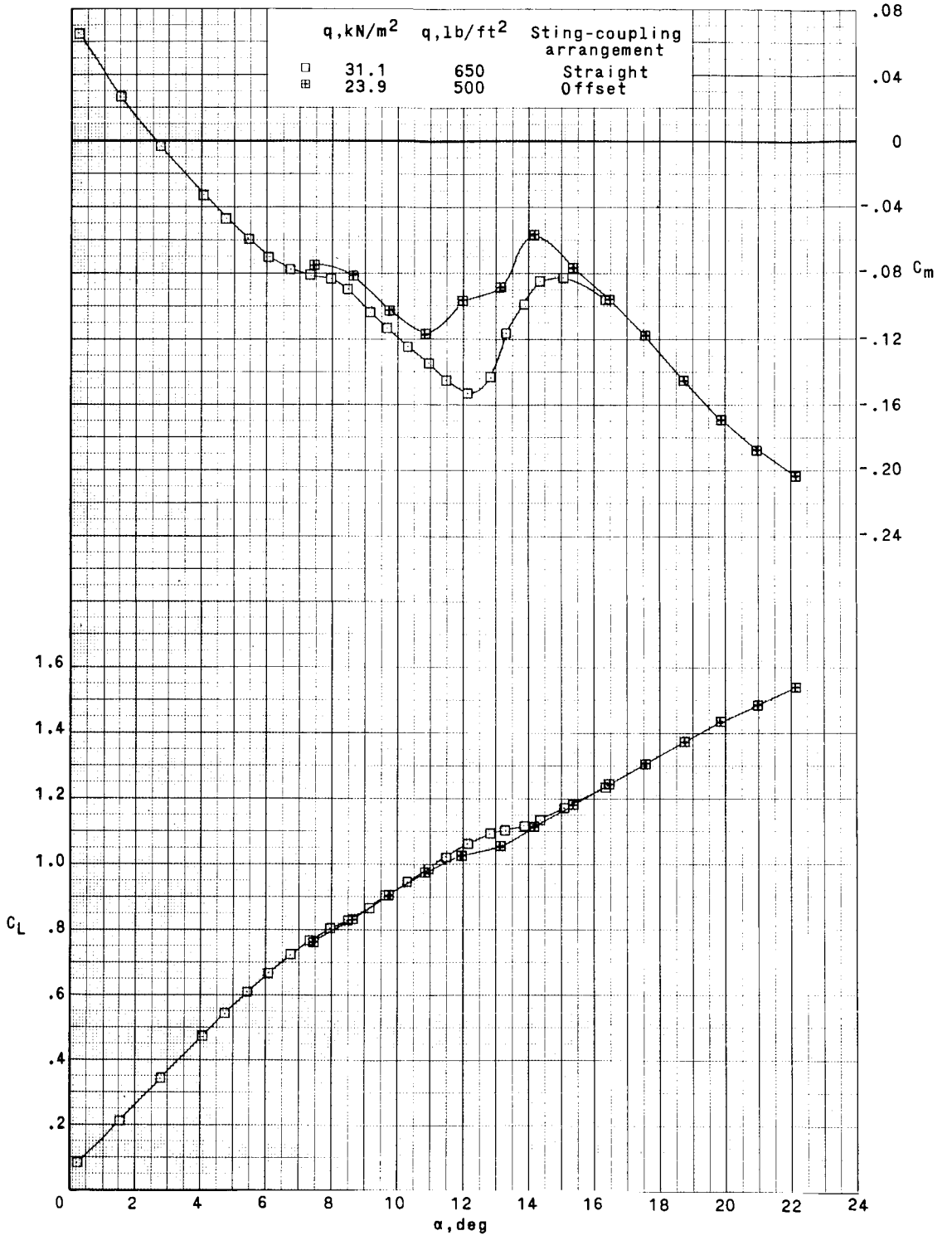


(c) M = 0.80.

Figure 14.- Continued.

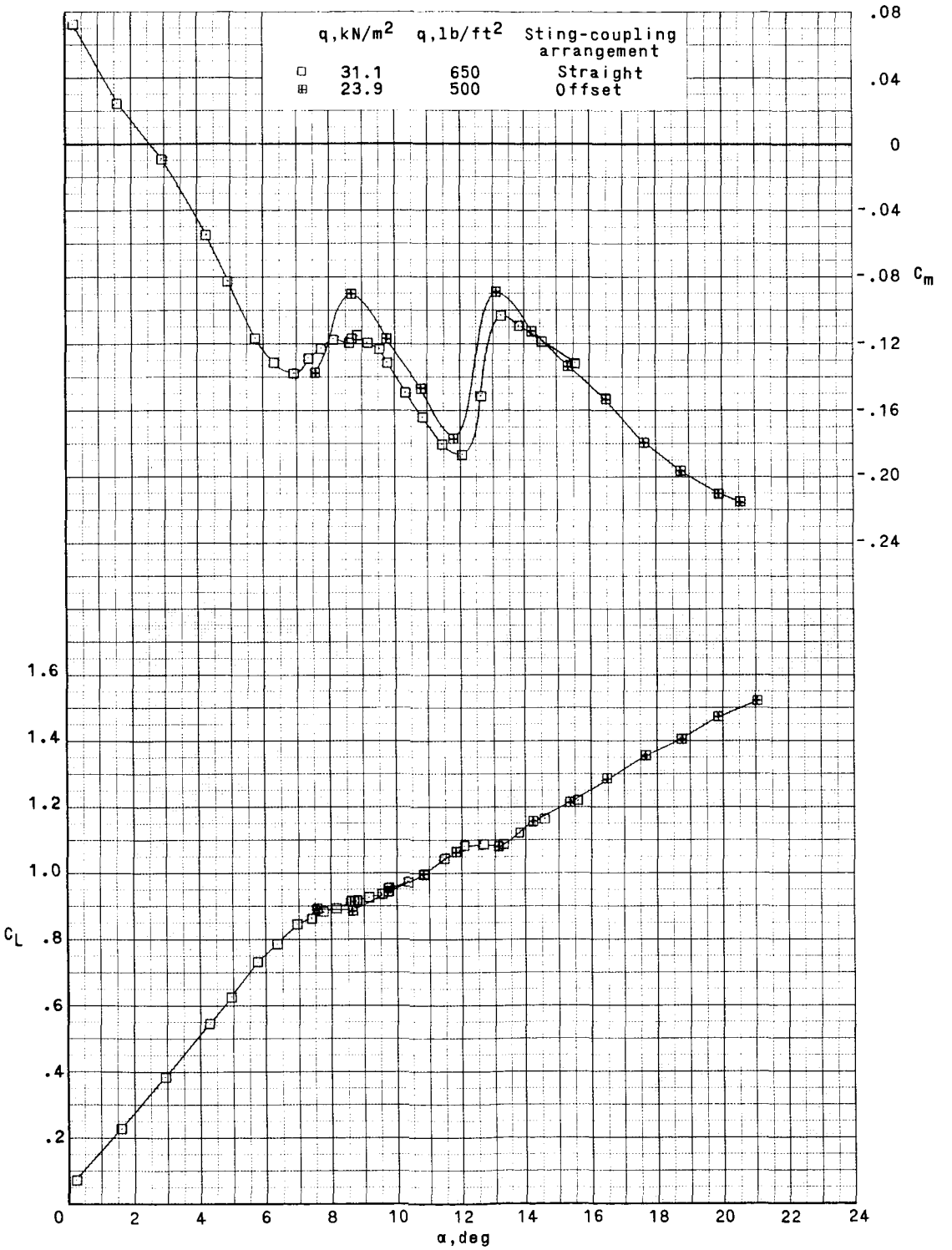


(d) M = 0.90.

Figure 14.- Continued.

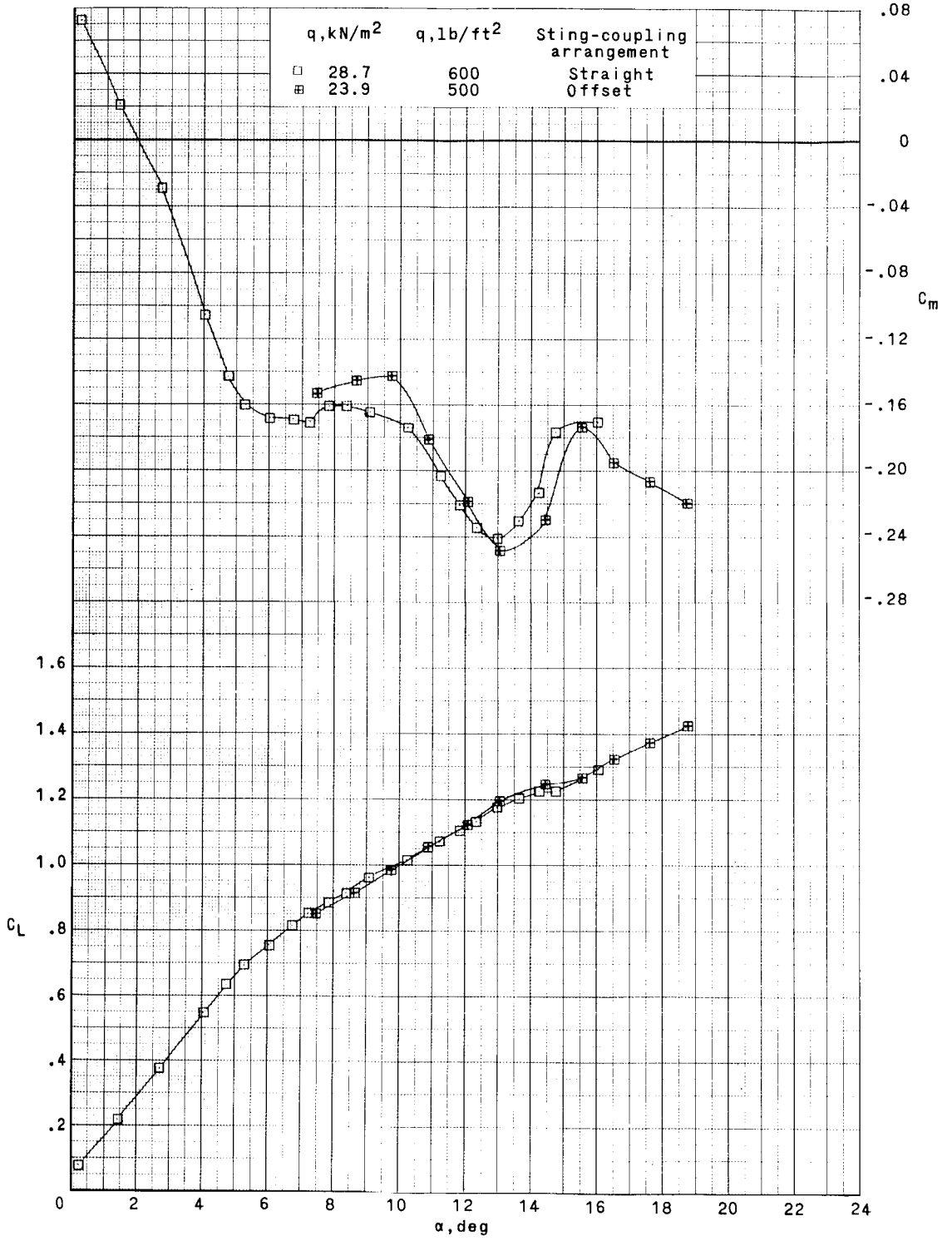


(e) M = 0.95.

Figure 14.- Concluded.

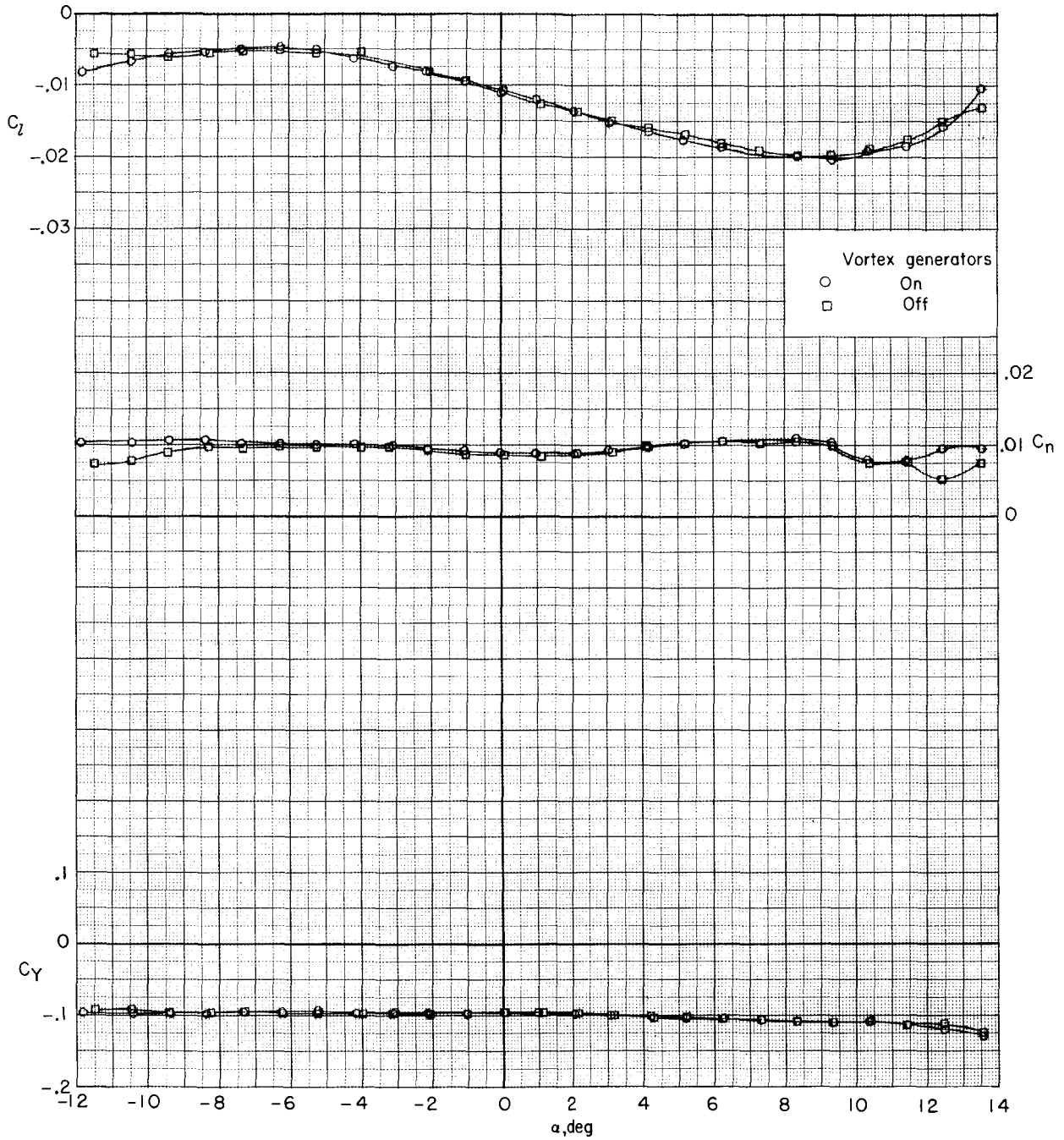


(a) M = 0.25.

Figure 15.- Effect of final vortex-generator configuration (modification 6) on lateral-directional aerodynamic characteristics for $\beta = 5^{\circ}$. Steel wing; aileron hinge fairings on.

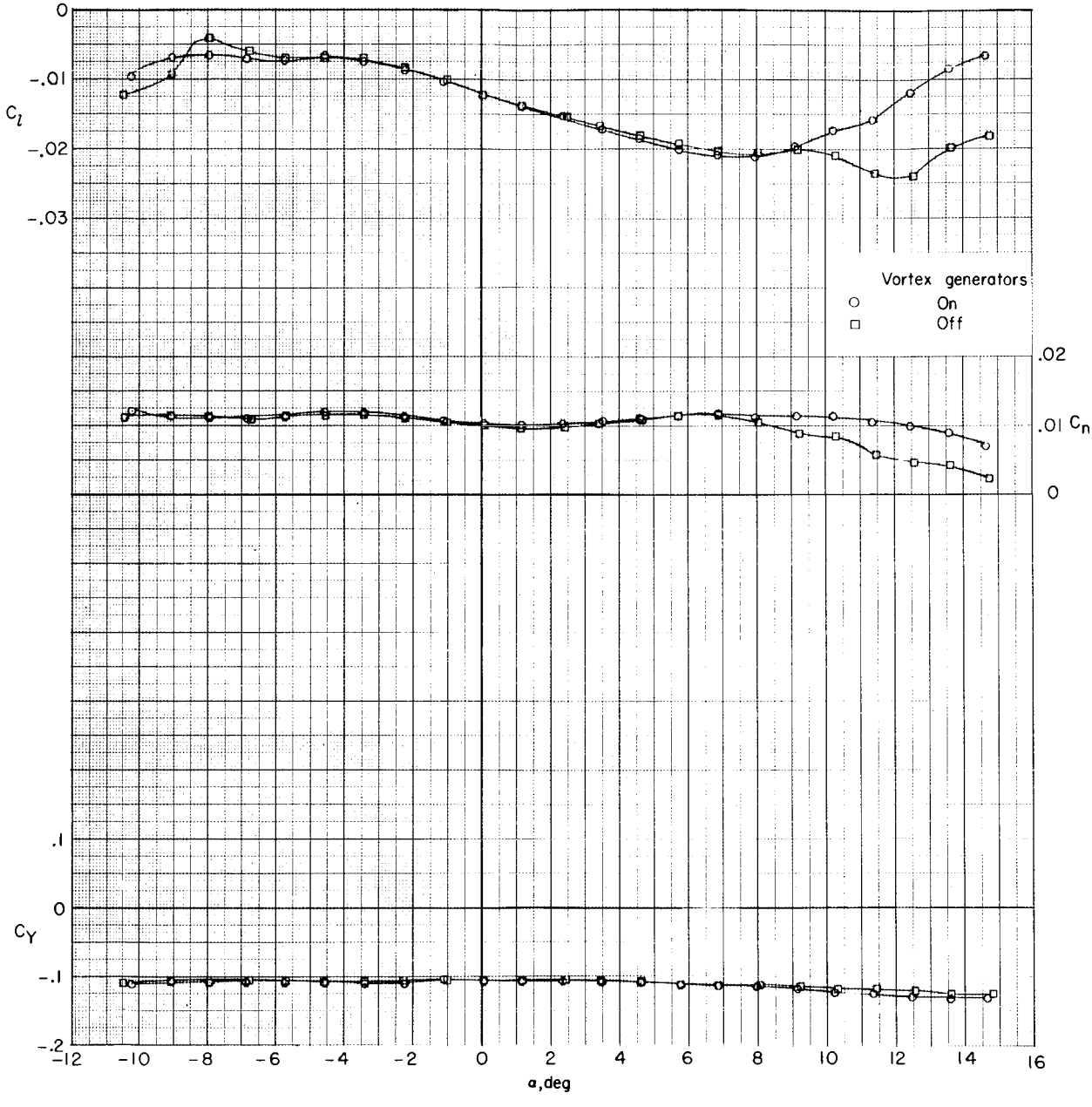


(b) M = 0.50.

Figure 15.- Continued.

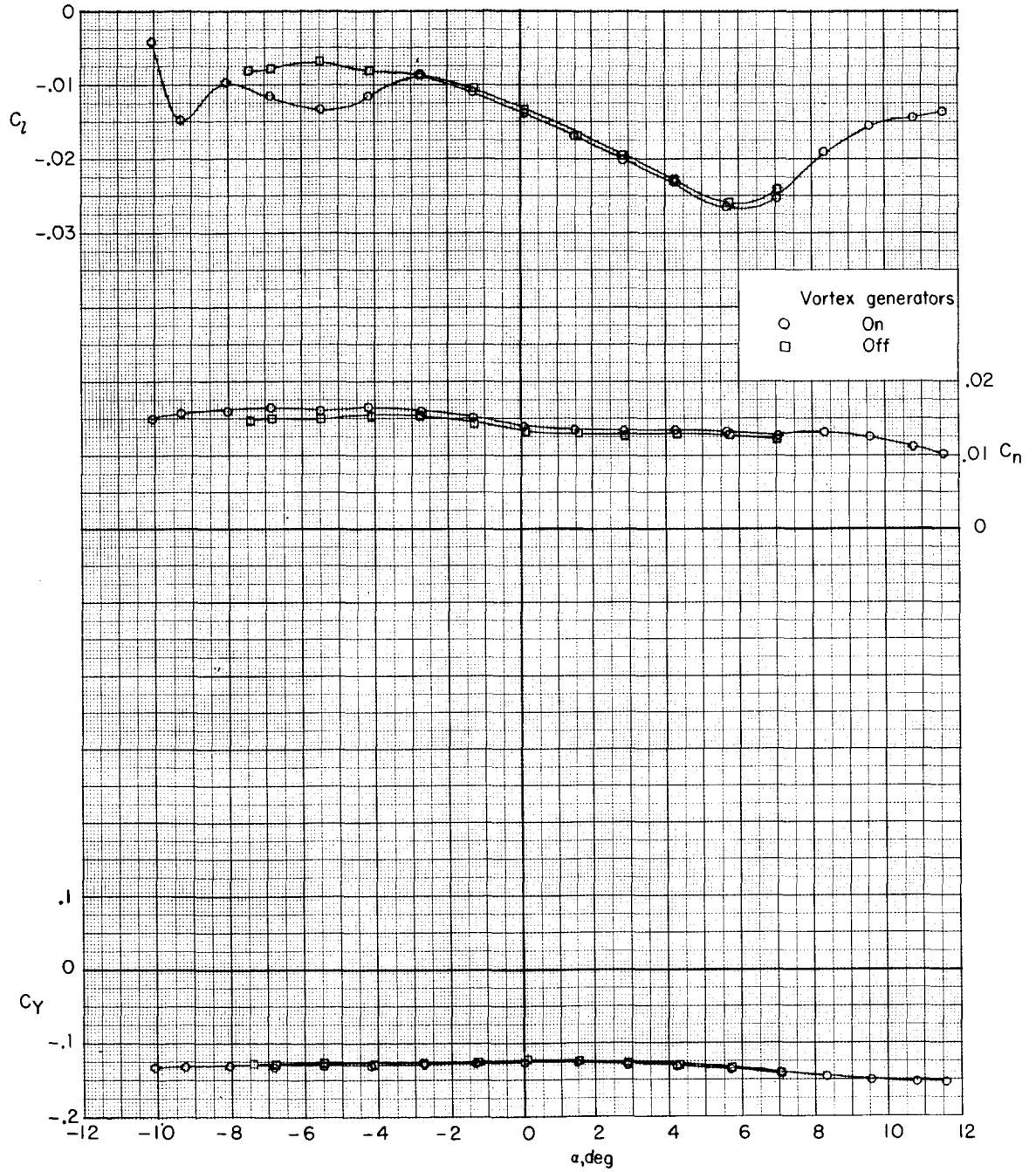


(c) M = 0.80.

Figure 15.- Continued.

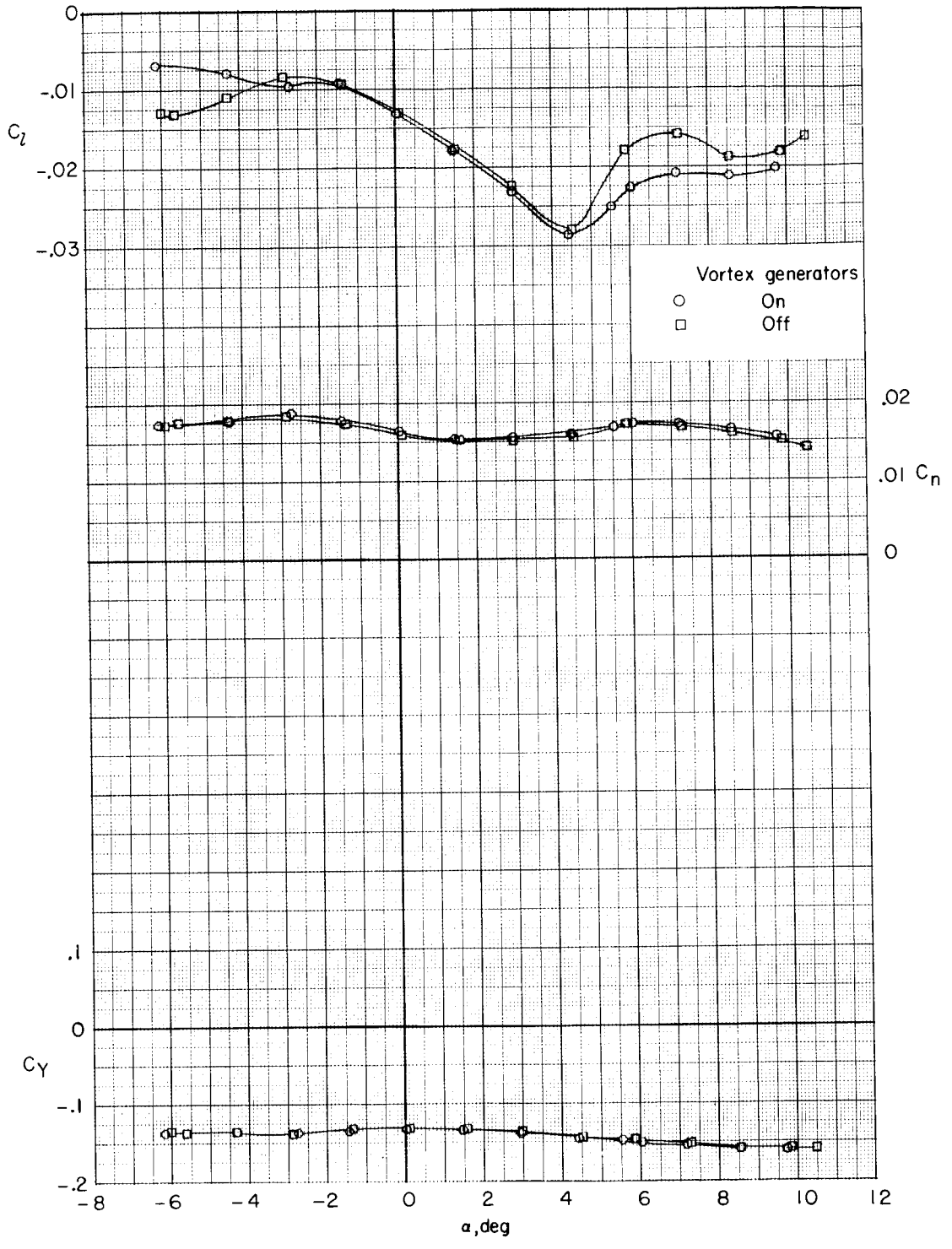


(d) M = 0.90.

Figure 15.- Continued.

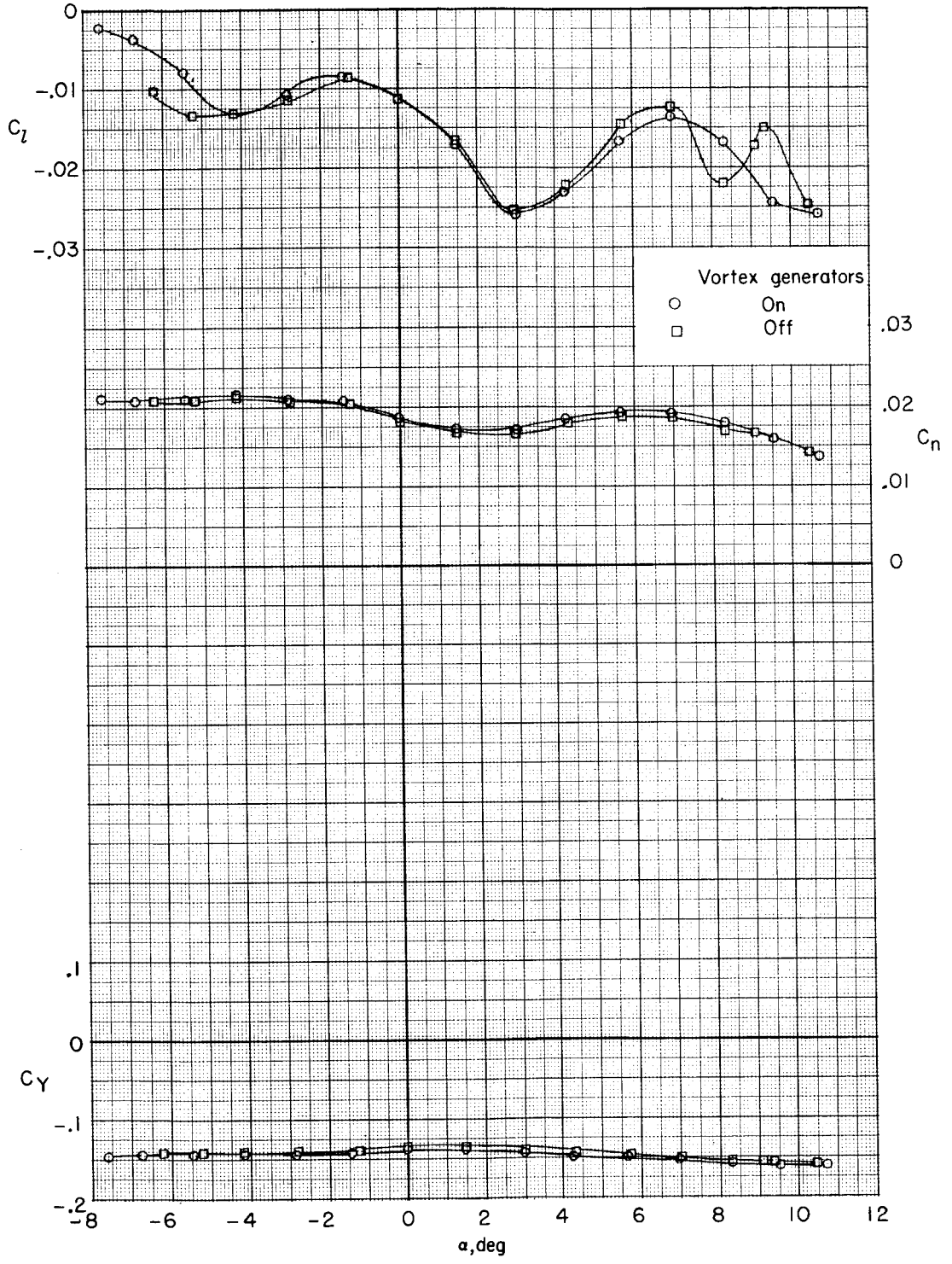


(e) M = 0.95.

Figure 15.- Continued.

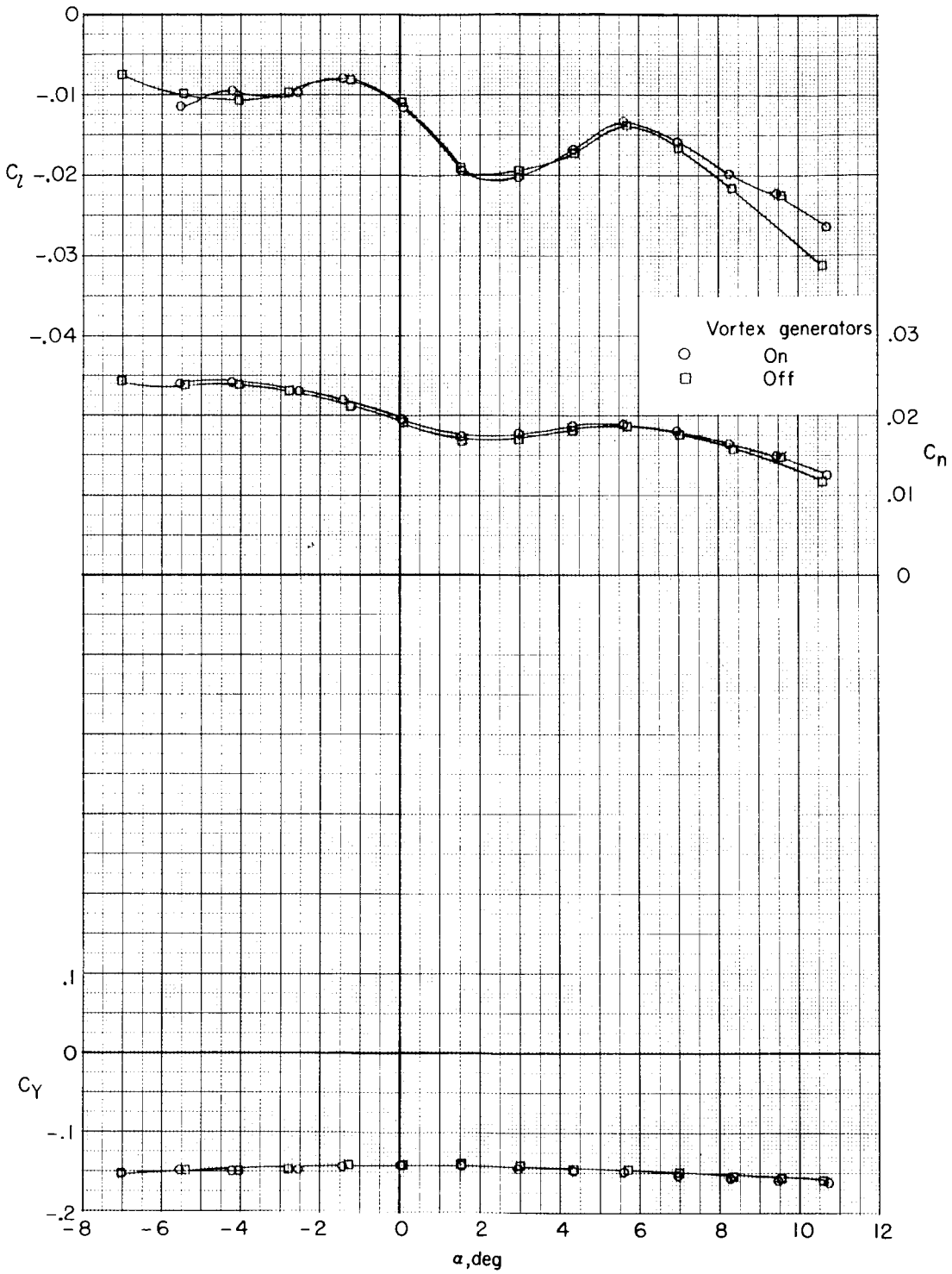


(f) M = 0.98.

Figure 15.- Concluded.

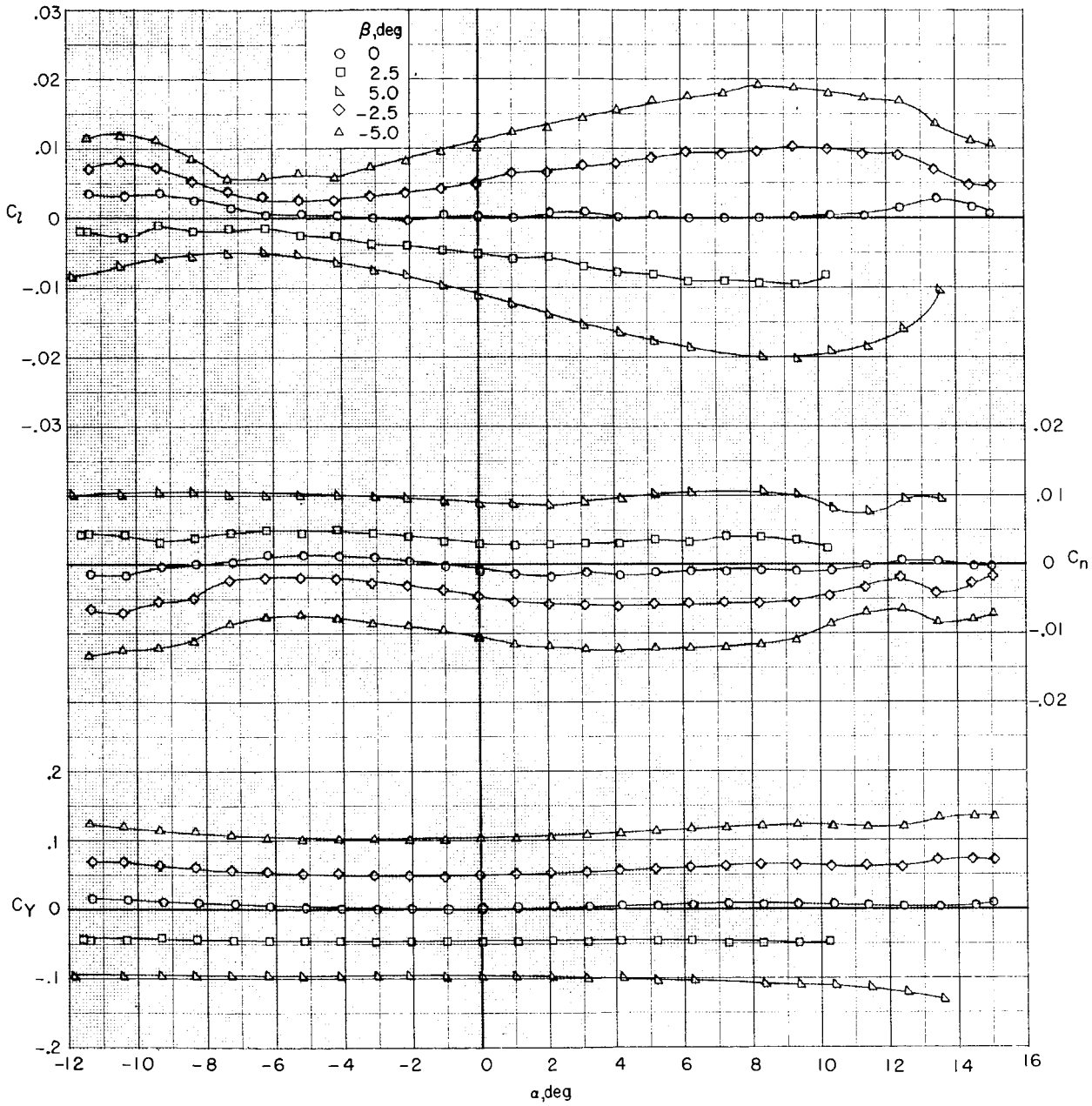


(a) M = 0.25.

Figure 16.- Effect of sideslip angle on lateral-directional aerodynamic characteristics of model with final vortex-generator configuration (modification 6). Steel wing; aileron hinge fairings on.

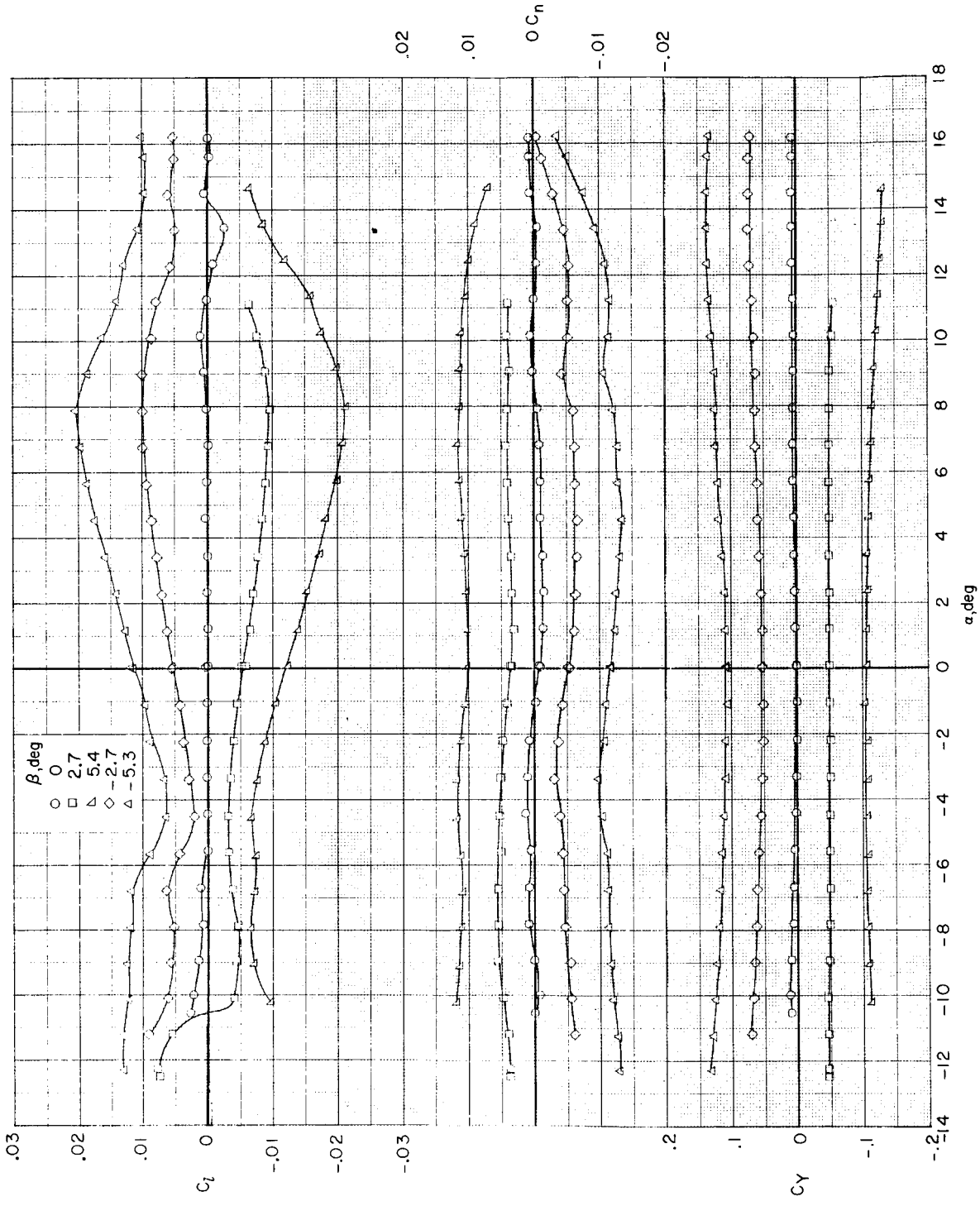


(b) M = 0.50.

Figure 16.- Continued.

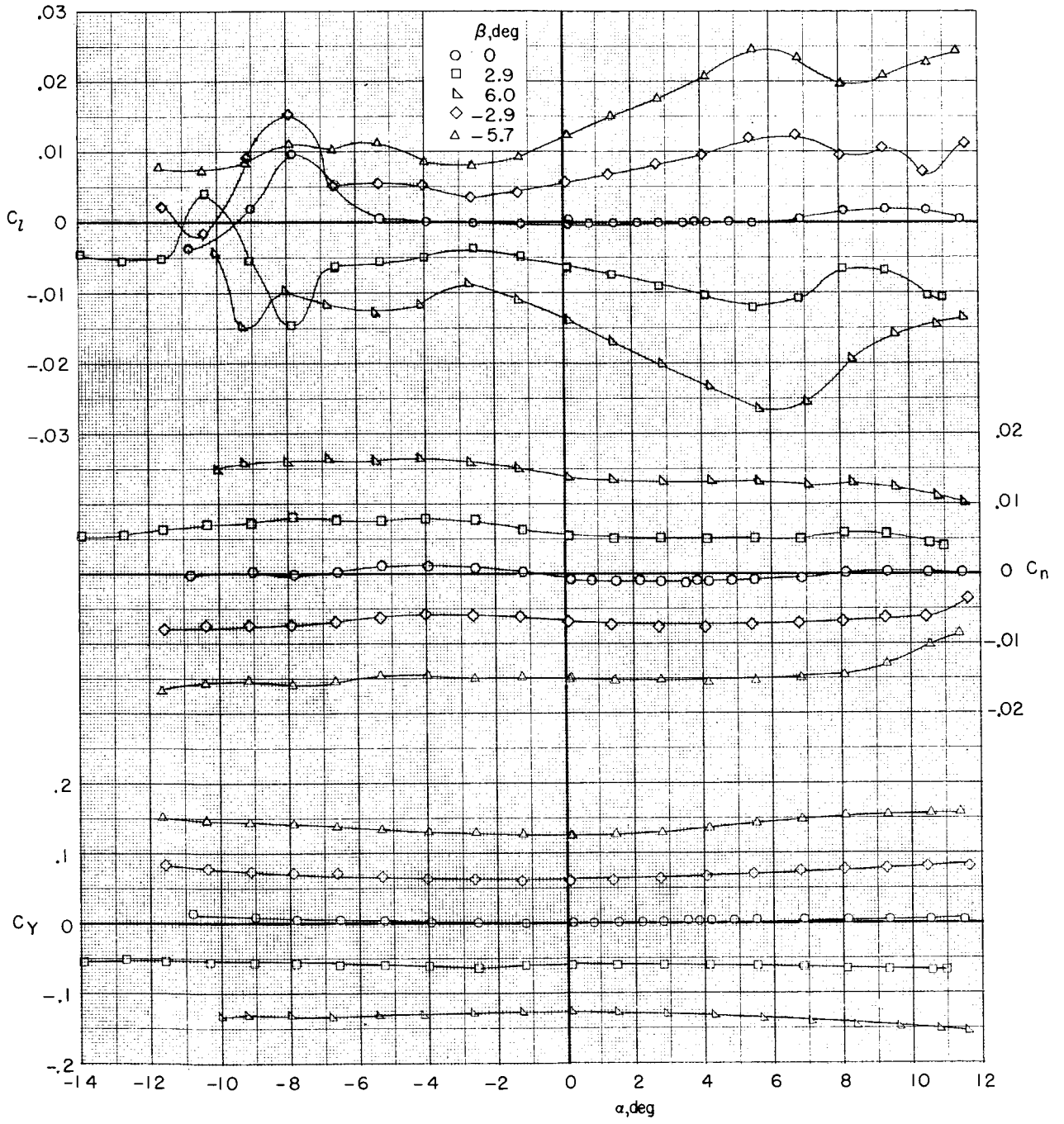


(c) M = 0.80.

Figure 16.- Continued.

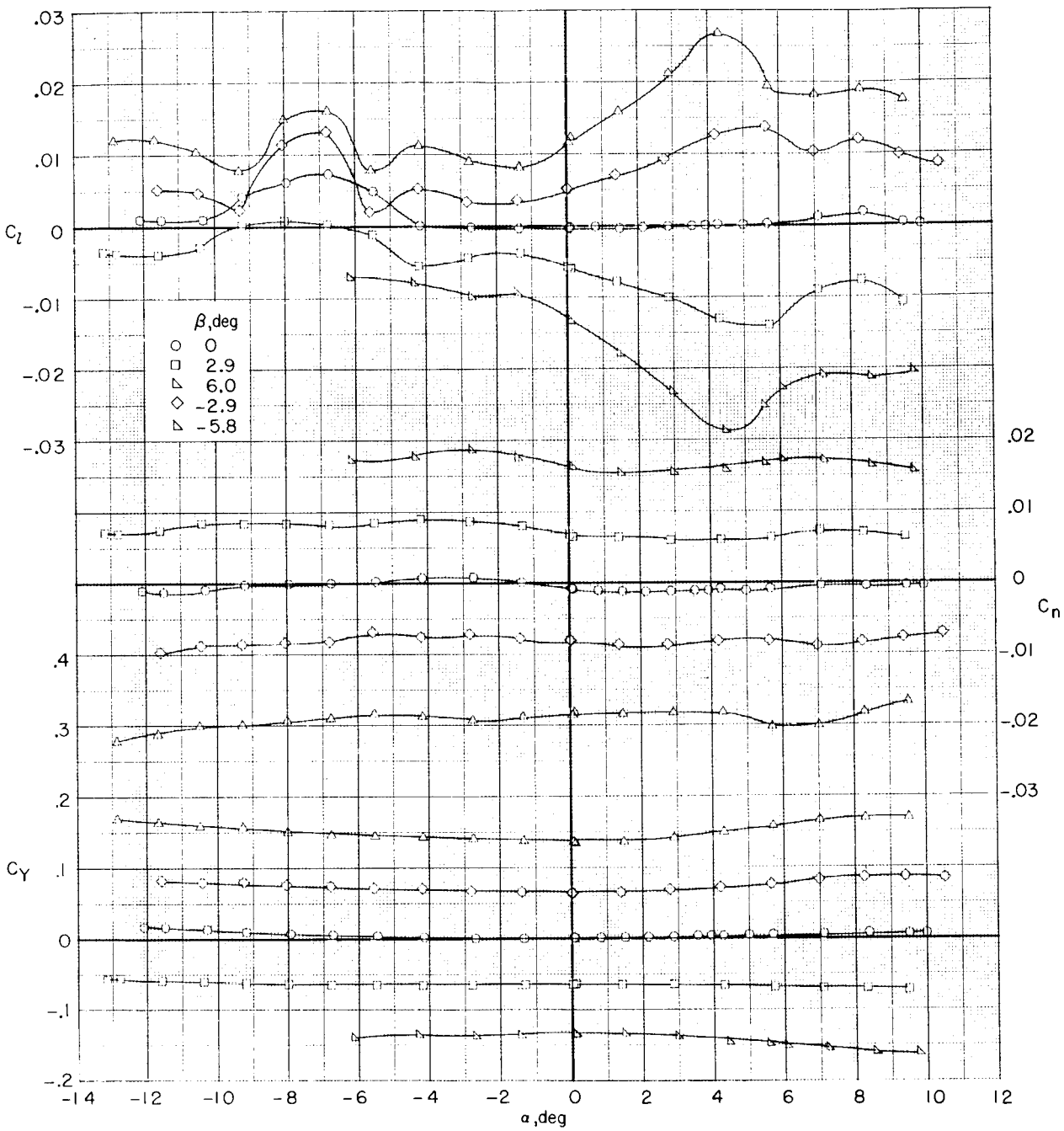


(d) M = 0.90.

Figure 16.- Continued.

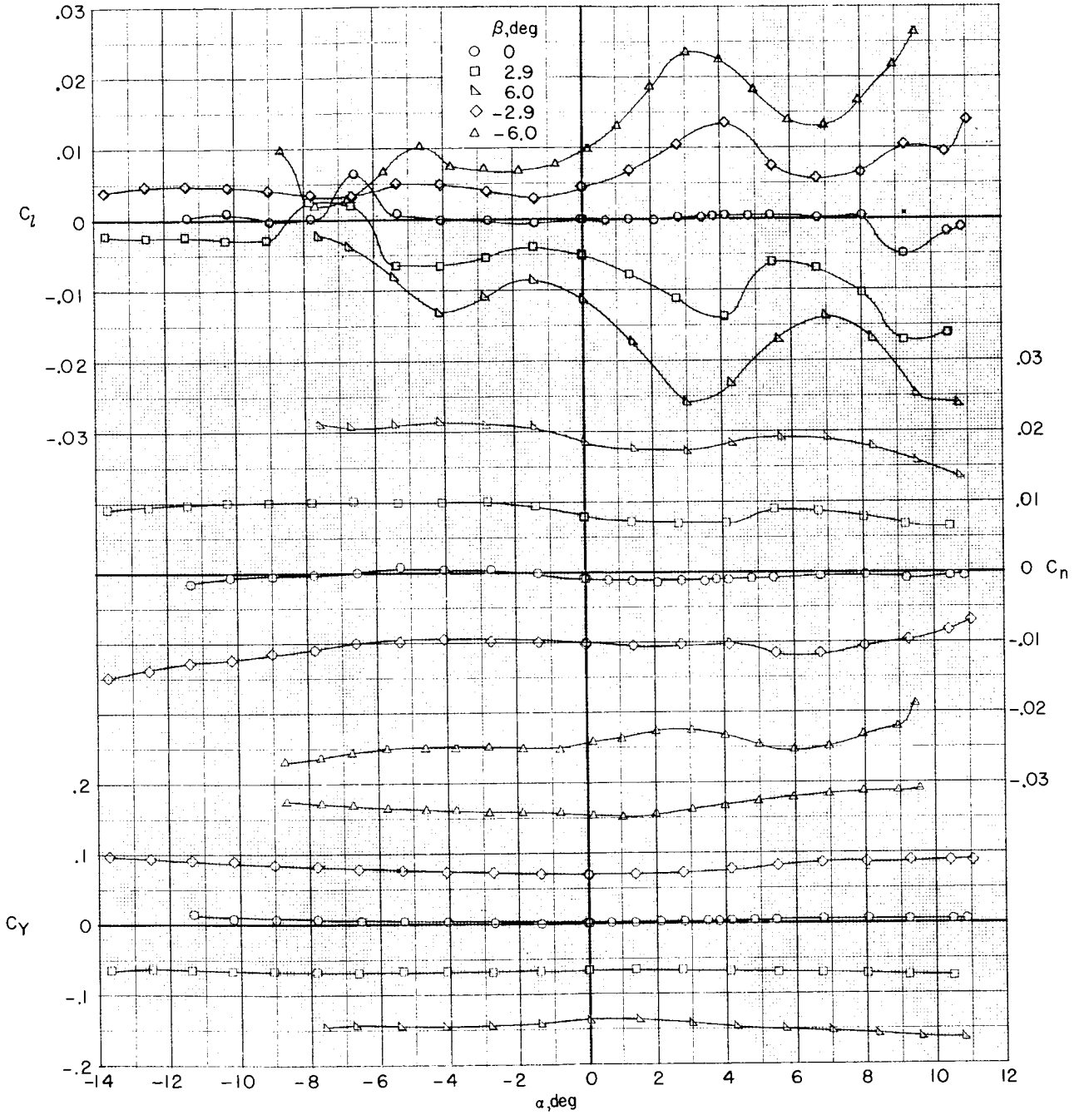


(e) M = 0.95.

Figure 16.- Continued.

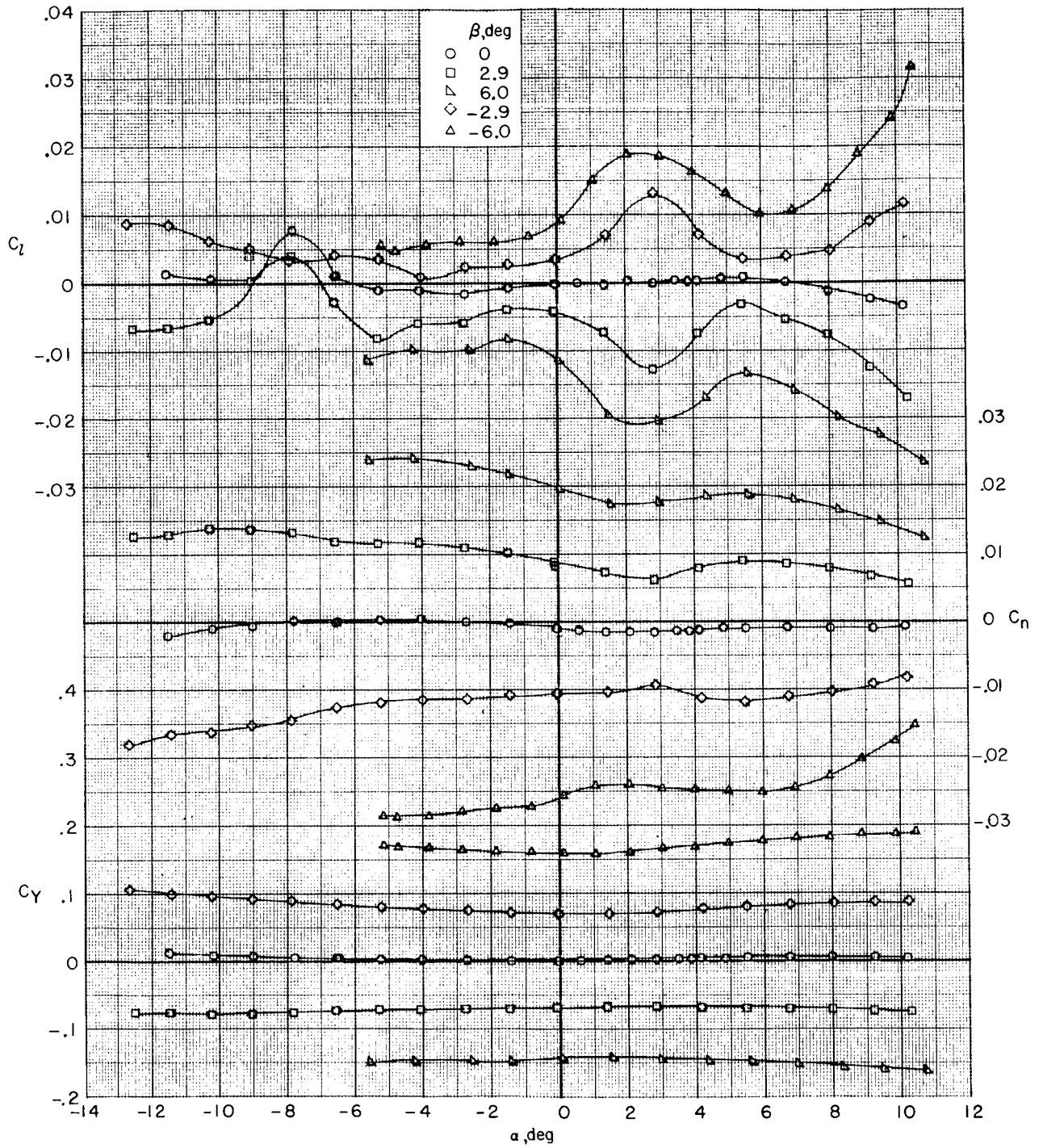


(f) M = 0.98.

Figure 16.- Continued.

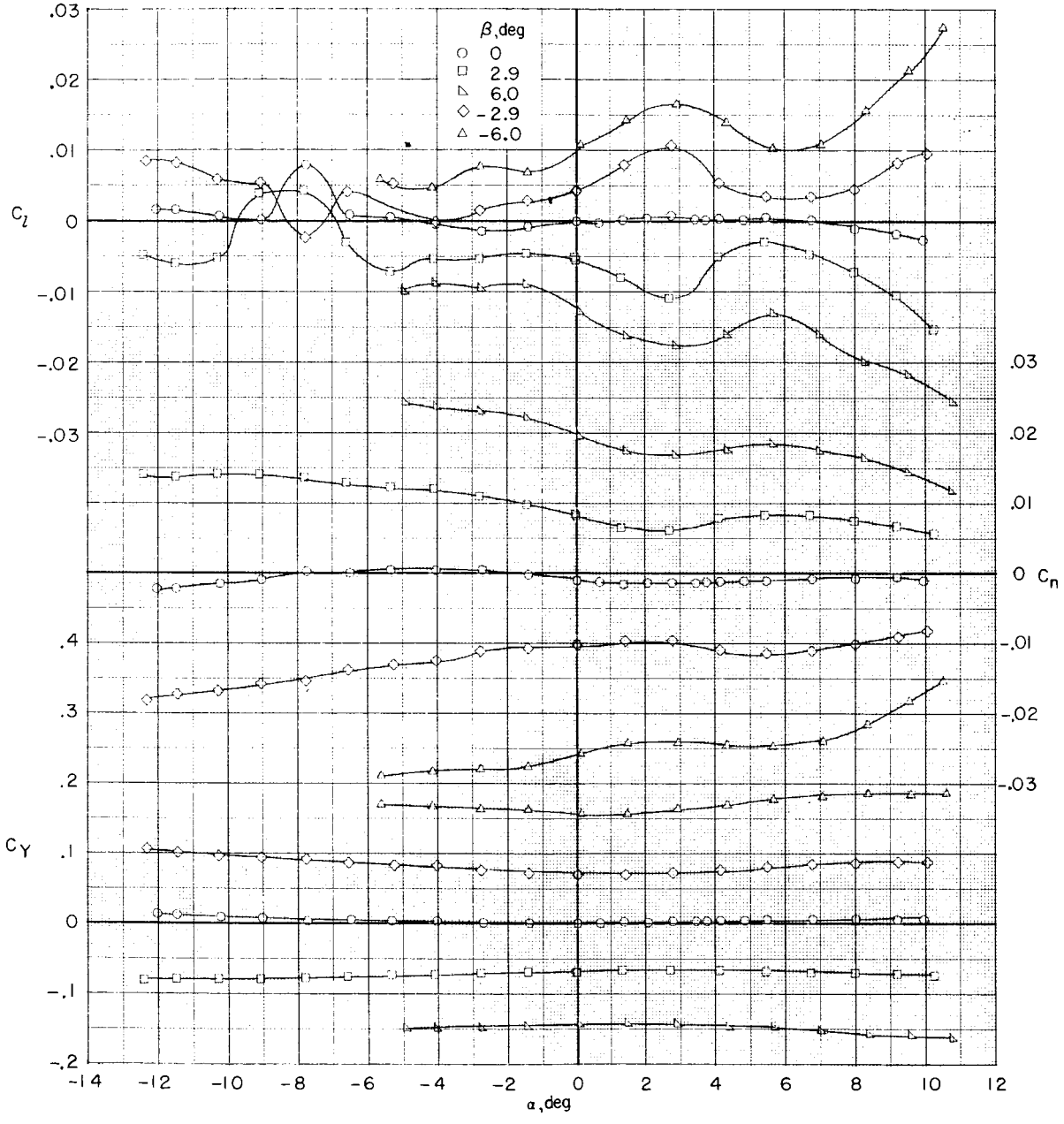


(g) M = 0.99.

Figure 16.- Concluded.

[redacted]

| 1. Report No. NASA TM X-2808 | 2. Government Accession No. | 3. Recipient's Catalog No. |
|---|---|---|
| 4. Title and Subtitle<br>WIND-TUNNEL DEVELOPMENT OF UNDERWING LEADING-EDGE VORTEX GENERATORS ON AN NASA SUPERCRITICAL-WING RESEARCH AIRPLANE CONFIGURATION (U) | | 5. Report Date<br>November 1973<br>6. Performing Organization Code |
| 7. Author(s)<br>Dennis W. Bartlett, Charles D. Harris, and Thomas C. Kelly | | 8. Performing Organization Report No.<br>L-8495 |
| 9. Performing Organization Name and Address<br>NASA Langley Research Center<br>Hampton, Va. 23665 | | 10. Work Unit No.<br>767-73-01-04<br>11. Contract or Grant No. |
| 12. Sponsoring Agency Name and Address<br>National Aeronautics and Space Administration<br>Washington, D.C. 20546 | | 13. Type of Report and Period Covered<br>Technical Memorandum<br>14. Sponsoring Agency Code |

15. Supplementary Notes

16. Abstract

A program for the wind-tunnel development of underwing leading-edge vortex generators on an NASA supercritical-wing research airplane model has been conducted in the Langley 8-foot transonic pressure tunnel at Mach numbers from 0.25 to 0.99. Presented are the effects on the longitudinal aerodynamic characteristics of vortex-generator wing semispan location, distance from wing leading edge, leading-edge sweep angle, toe-in angle, and span. In addition, the effects of the vortex generators on the lateral-directional aerodynamic characteristics of the model are presented for a sideslip angle of $5^{o}$.



17. Key Words (Suggested by Author(s))
Vortex generators
Transonic aerodynamics

| 19. Security Classif. (of this report) | 20. Security Classif. (of this page) | 115 | |
|---|---|---|---|
| [redacted] | Unclassified | | |